Simulación de propiedades

Miriam Marqués Arias

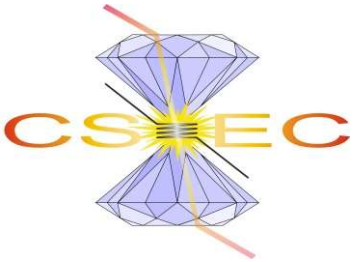

Estructura → Propiedades

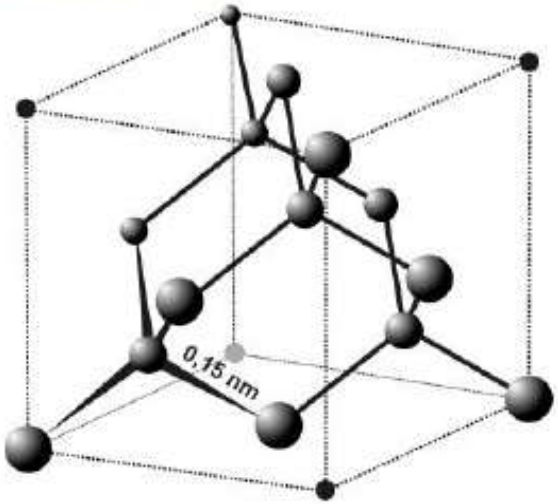

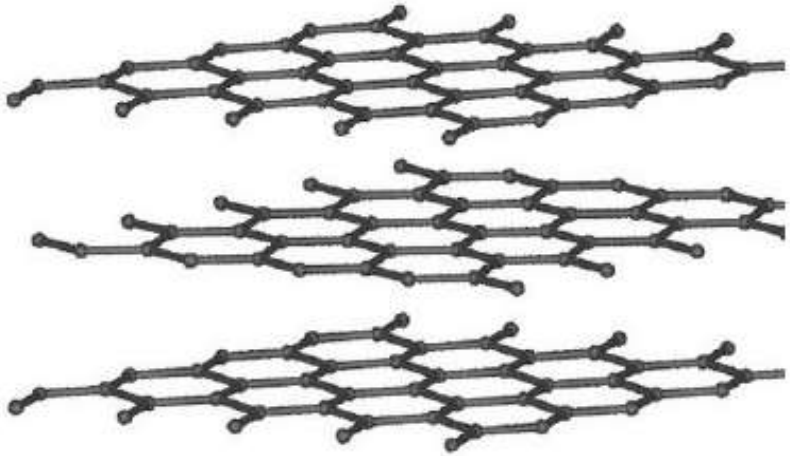

Intervalo de presión en el universo

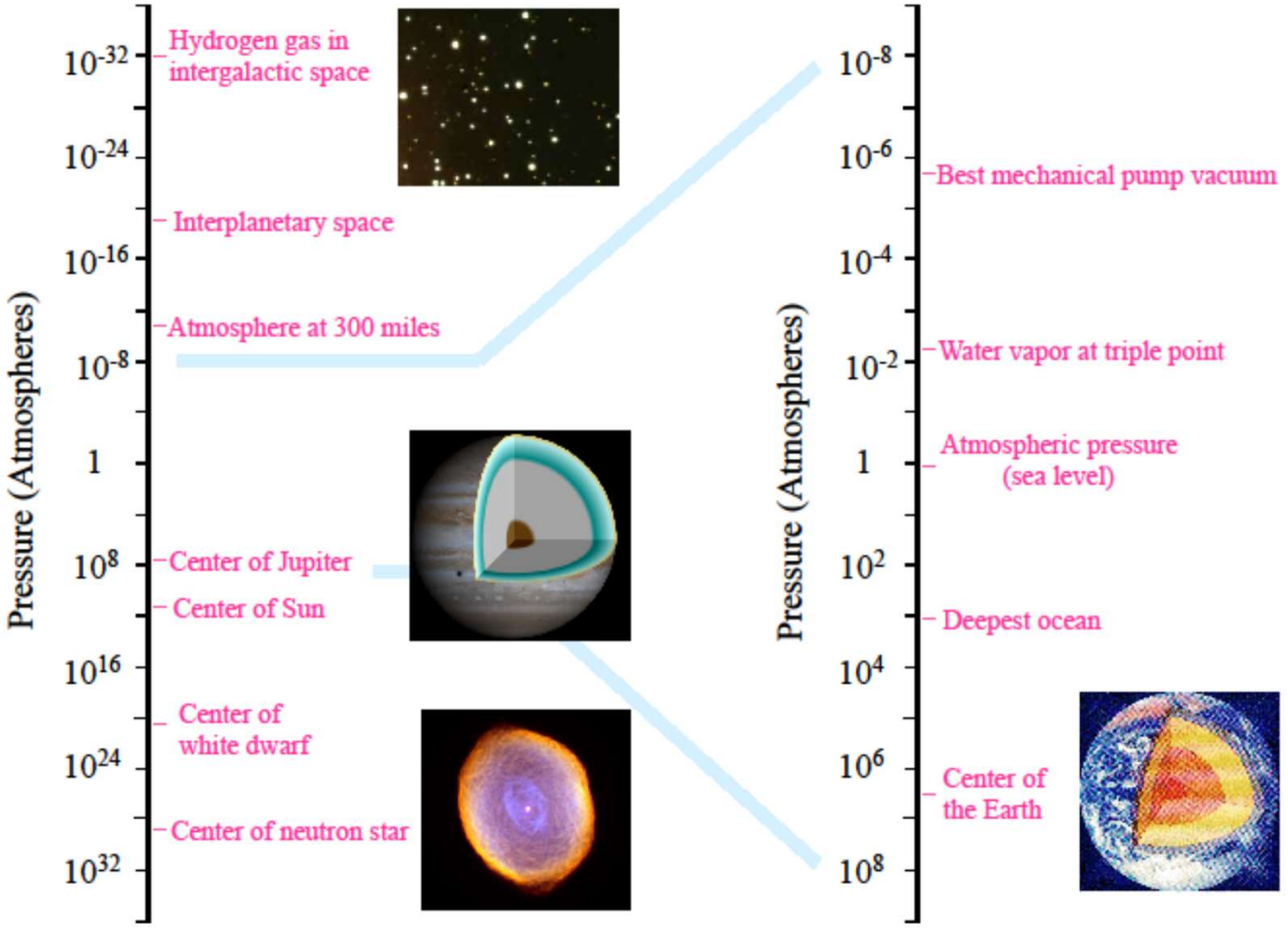

Un nuevo mundo bajo presión

- Líquidos → sorprendentes sólidos, gases → metales exóticos……. por modificación de distancias interatómicas y ángulos de enlace.

- Transiciones de fase a nuevas estructuras cristalinas con propiedades físicas y químicas inesperadas y novedosas

- Elementos se convierten en superconductores, metales se convierten en aislantes

- Las moléculas se rompen

- Nuevas reacciones químicas son posibles (hidruros de elementos de transición)

Transiciones de fase

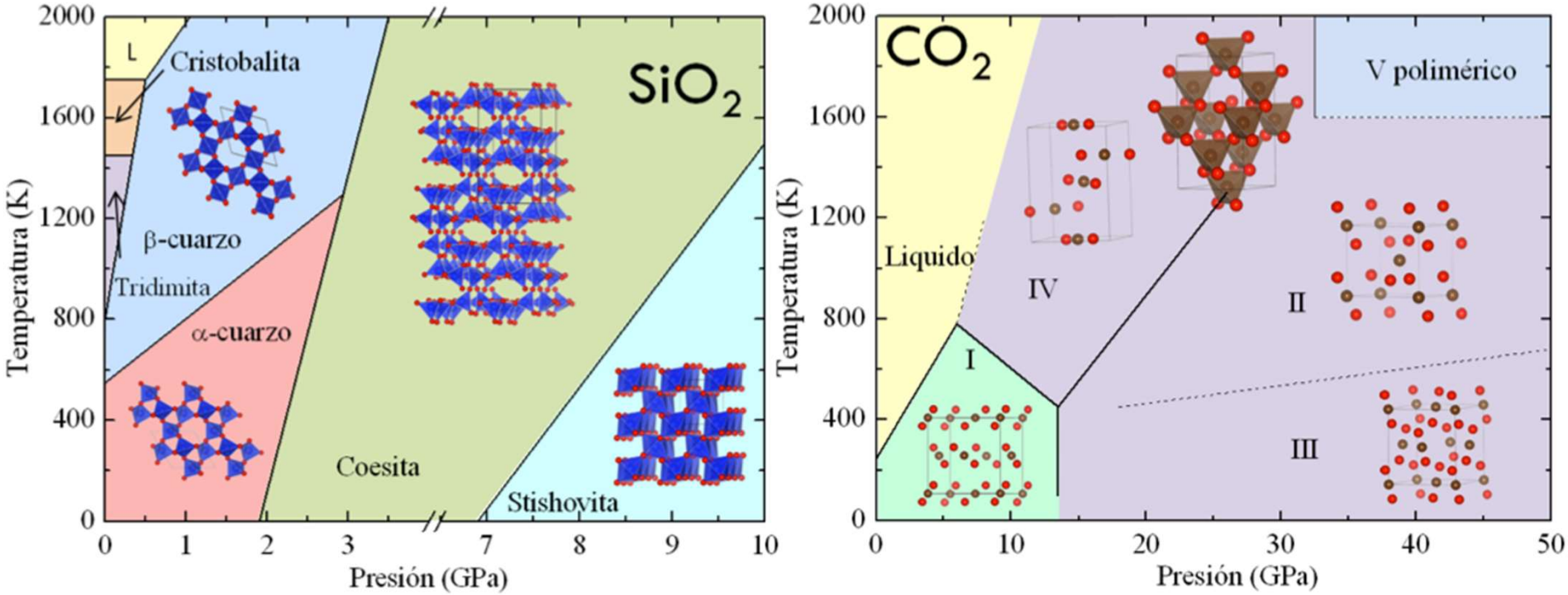

Una nueva tabla periódica

Na: fase hP4

- hP4 : aislante con band gap directo (Eg=2.1 eV)
- Cuencas de ELF: unidades localizadas sin conexión. Puede esto ayudarnos a entender la conductividad?

(W. Kohn, Phys Rev A **133**,171: Theory of the insulating state")

- Qué es un metal?

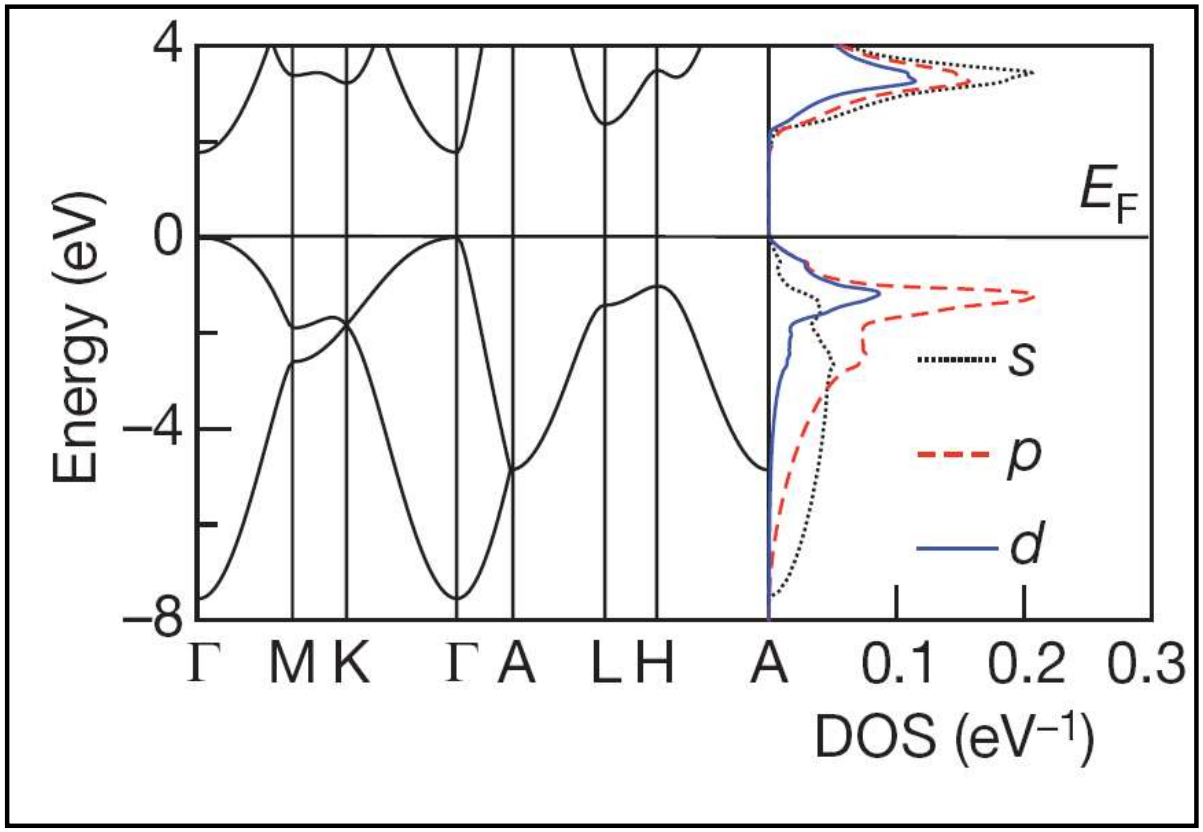

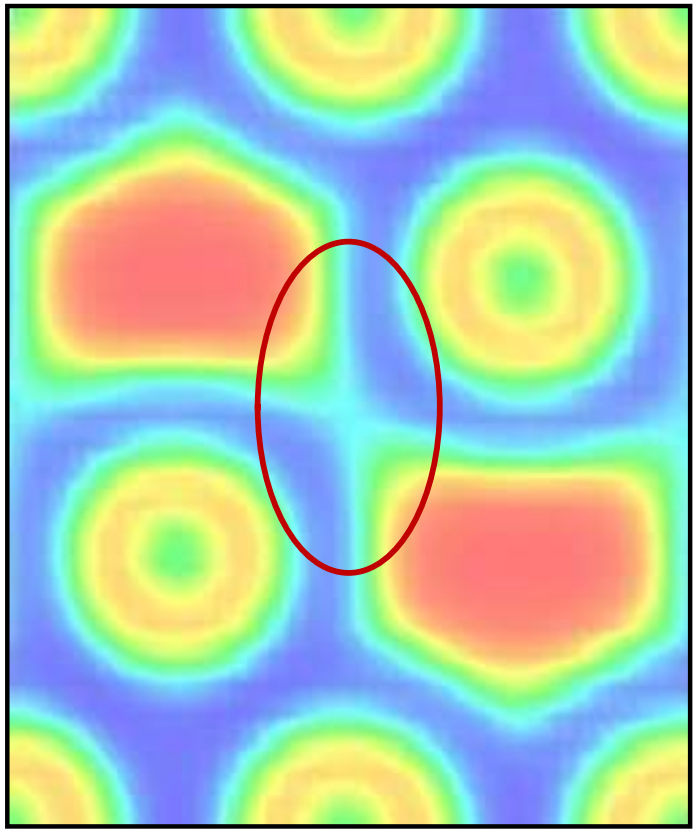

Simulación computacional?

EXPERIMENTO:

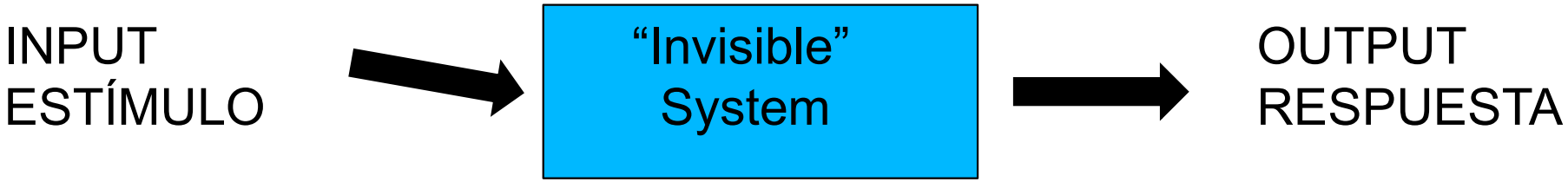

MODELO:

- Descripción simplificada de un sistema real y complejo
- Captura la física esencial responsable del comportamiento del sistema
- Obvia los detalles irrelevantes sin impacto significativo en la respuesta
- El resultado del modelo tiene que estar de acuerdo con los experimentos, si no puede ser demasiado simple
- Los modelos permiten extrapolar la respuesta del sistema en condiciones no accesibles por los experimentos

Simulación computacional?

MODELO:

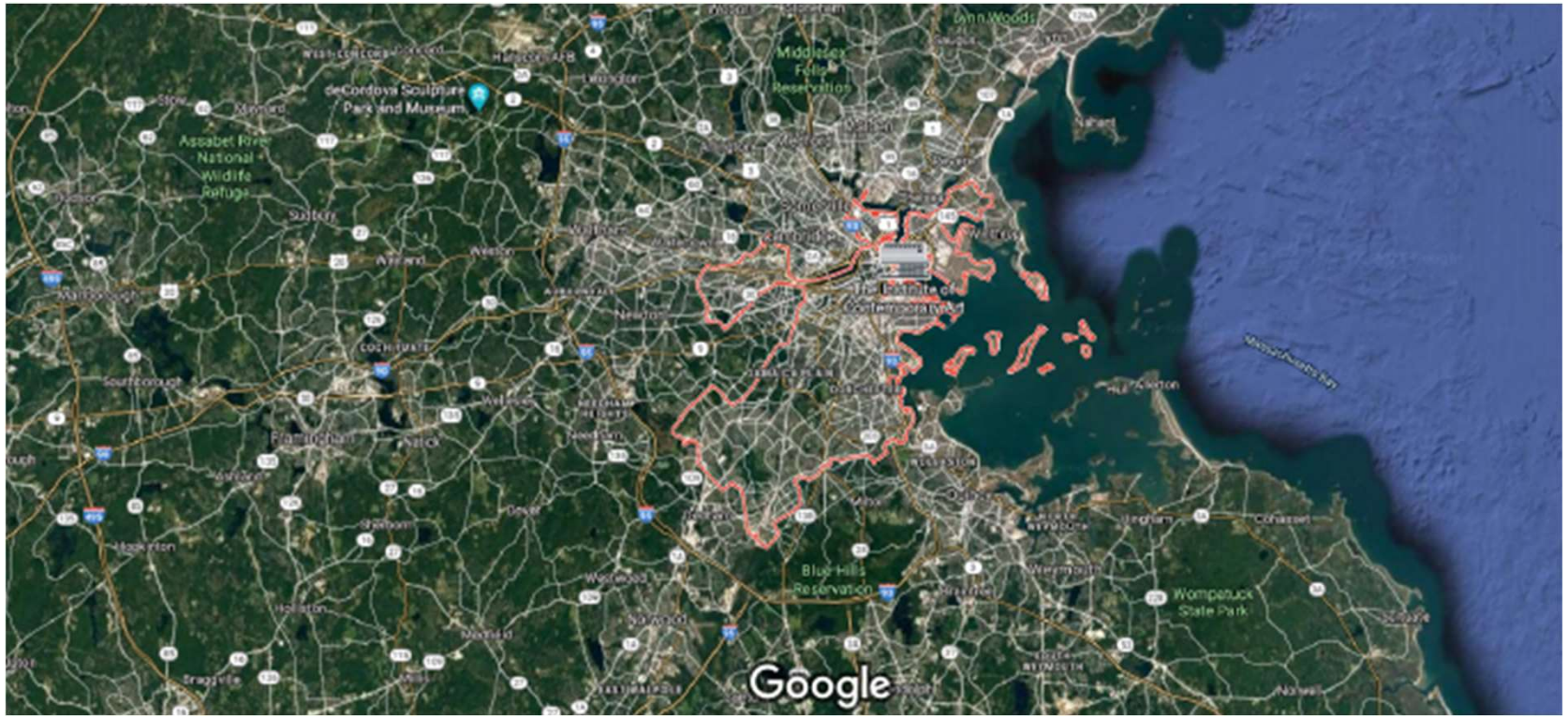

Simulación computacional?

MODELO:

- Distancias, direcciones?
- Conectividad O.K.
- Qué nos interesa?

Simulación computacional?

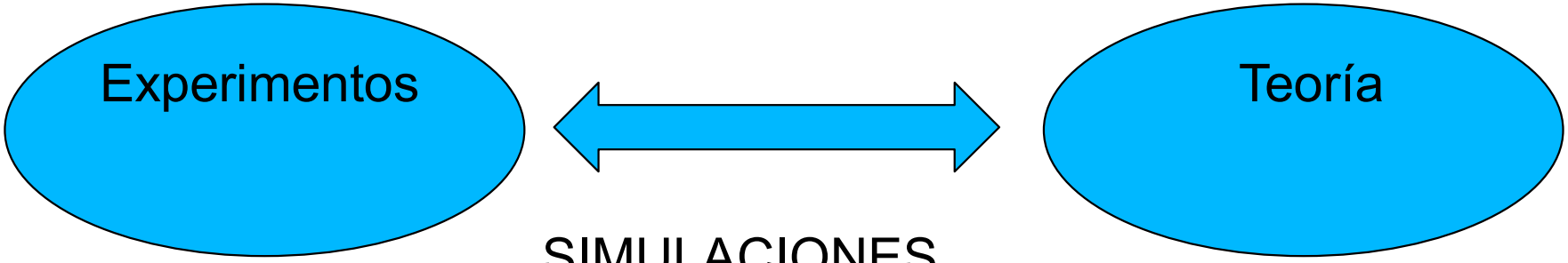

SIMULACIONES
COMPUTACIONALES

- Presentes en nuestra vida diaria (simulaciones en economía, previsión metereológica, simuladores de vuelos…)
- Método general para resolver modelos que no pueden resolverse analíticamente por su complejidad
- Se basan en algoritmos (series de instrucciones)

Simulación computacional?

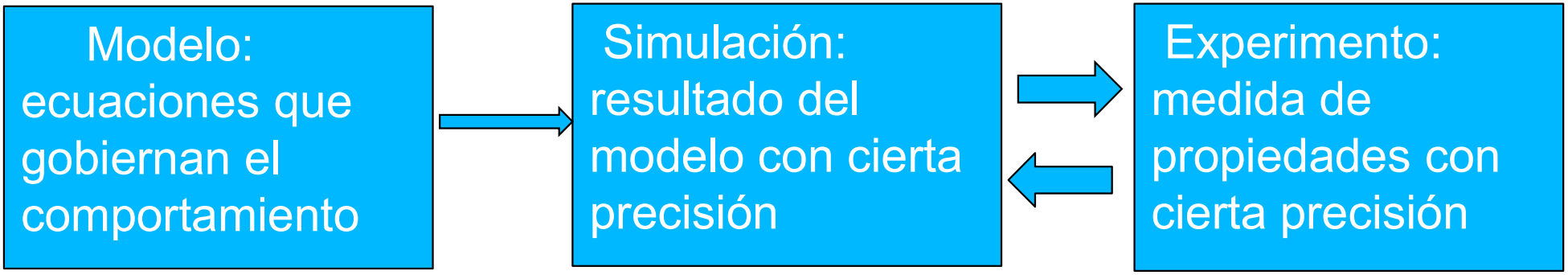

- Experimento computacional: el ordenador sirve para resolver numéricamente las ecuaciones definidas por el modelo
- Permiten testear diferentes modelos
- Necesitamos herramientas para el análisis de los resultados de la simulación
- En materiales: estudian el modo en que los componentes del sistema interaccionan entre ellos, con el entorno y frente a factores externos (presión, temperatura)

Goal: Describe properties of matter from theoretical methods firmly rooted in fundamental equations

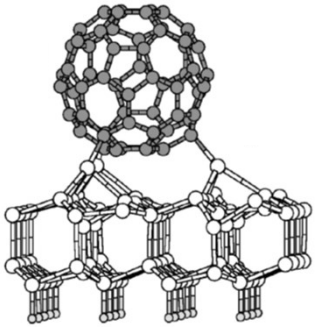

structural

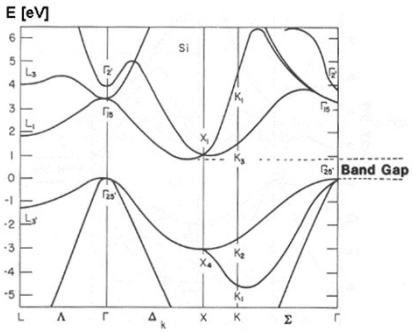

electronic

PROPERTIES

vibrational

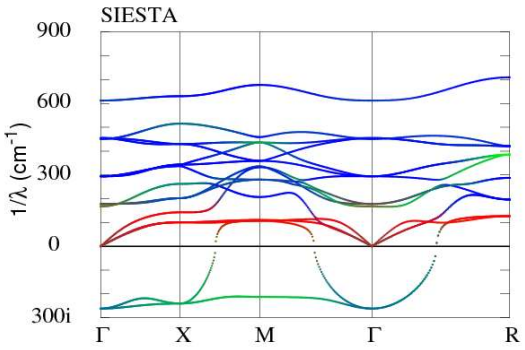

optical

magnetic

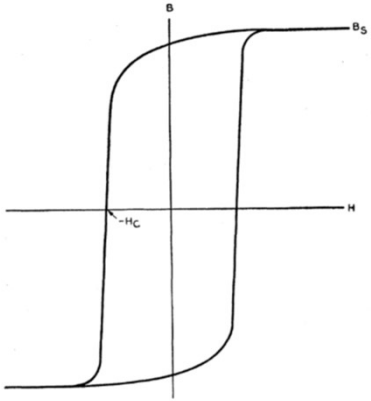

EXPERIMENTS

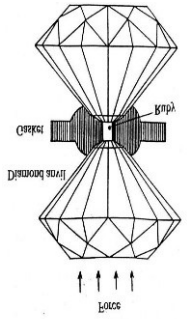

\+ characterization techniques

PROBLEMS:

Small size of the sample

No hydrostaticity

Limited range of pressures

Non recoverable structures

Lack of crystallinity

Pressure sensors

Transition mechanisms

↔

SIMULATIONS

ideal samples

any conditions

It allows:

- Complement experiments
- Interpret and predict

PROBLEMS:

approximations

experiment-theory comparison

Ab initio simulations

- Quantum nightmare: Solving Schrödinger equation $\hat{H}\Psi = E\Psi$
- The Hamiltonian can be expressed as: $\hat{H} = \hat{T}_e + \hat{T}_n + \hat{U} + \hat{V}_{en} + \hat{V}_{nn}$
  where the kinetic contributions of the electrons and nuclei are:

$$\hat{T}_e = -\sum_{i=1}^{N} \frac{\nabla_i^2}{2}, \qquad \hat{T}_n = -\sum_{A=1}^{M} \frac{\nabla_A^2}{2M_A}$$

  and the electron-electron, nucleus-electron and nucleus-nucleus interactions are:

$$\hat{U} = \sum_i^N \sum_{j\neq i}^N \frac{1}{2|\vec{r}_i - \vec{r}_j|}, \quad \hat{V}_{en} = -\sum_{A=1}^M \sum_{i=1}^N \frac{Z_A}{|\vec{r}_i - \vec{R}_A|}, \quad \hat{V}_{nn} = \sum_{A=1}^M \sum_{B\neq A}^M \frac{Z_B Z_A}{2|\vec{R}_B - \vec{R}_A|}.$$

  N: number of electrons, M: number of nuclei, M_A, Z_A and $\vec{R}_A$: mass, charge and position of the A nucleus, $\vec{r}_i$: position of i electron.

- The Born-Oppenheimer approximation (M $\gg$ m)

$$\Psi(\vec{r}, \vec{R}) = \Phi_{\text{nucl}}(\vec{R})\psi_{elec}(\vec{r}; \vec{R}), \quad \hat{H}_{elec} = \hat{T}_e + \hat{V}_{en} + \hat{V}_{ee} + \hat{V}_{nn}$$

$$\hat{H}_{elec}\psi_{elec} = \epsilon\psi_{elec}, \quad \hat{H}_{\text{nucl}}\Phi_{\text{nucl}} = E\Phi_{\text{nucl}}, \quad \hat{H}_{\text{nucl}} = \hat{T}_n + \epsilon.$$

Density functional theory

- Basic variable: electron density $\rho(\vec{r})$
- The ground-state total energy is an unique functional of the electron density.
- But the functional is not know $\Rightarrow$ Kohn-Sham formalism ($\rho(\vec{r}) = \sum_{i=1}^{N} [\psi_i(\vec{r})]^2$)

$$E[\rho] = T_s[\rho] + \int \rho(\vec{r}) v(\vec{r}) d\vec{r} + \frac{1}{2} \int d\vec{r} d\vec{r}' \frac{\rho(\vec{r})\rho(\vec{r}')}{|\vec{r} - \vec{r}'|} + E_{xc}[\rho].$$

- $E_{\rm xc}$ is not known $\rightarrow$ Approximations:
  - Local Density Approximation (LDA)
    - $E_{\rm xc}^{LDA} = \int \varepsilon_{\rm xc}(\rho(\vec{r}))\rho(\vec{r}) d^3\vec{r}$
  - Generalised Gradient Approximation (GGA)
- Kohn-Sham equations:

  $\hat{h}_{\rm KS}\psi_i = \varepsilon_i \psi_i, \quad \hat{h}_{\rm KS} = -\frac{1}{2}\nabla_i^2 + v_{\rm eff}(\vec{r}), \quad < \psi_i | \psi_j >= \delta_{ij}.$

  Many-electron problem $\Rightarrow$ noninteracting electrons moving in an effective potential

In a crystal?

- Crystals contain $\approx 10^{23}$ atoms. IMPOSSIBLE?
- NO!!!!!! Use symmetry $\rightarrow$ UNIT CELL
- Bloch theorem: The one-particle effective Hamiltonian $\hat{H}$ in a periodic lattice ($V(r+R) = V(r)$) commutes with the lattice-translation operator $\hat{T}_R$, allowing us to choose the common eigenstates according to the prescriptions of Bloch theorem:
  - $[\hat{H}, \hat{T}_R] = 0 \rightarrow \psi_{nk}(r) = u_{nk}(r)e^{ikr}$
- n, k are the quantum numbers (band index and crystal momentum), u is periodic.
- From two requirements: a translation can't change the charge density, and two translations must be equivalent to one that is the sum of the two.
- Changes the problem of calculating and infinite number of electronic wave functions to one of calculating a finite number of electronic wave functions in a infinite number of k points.

Periodic crystals

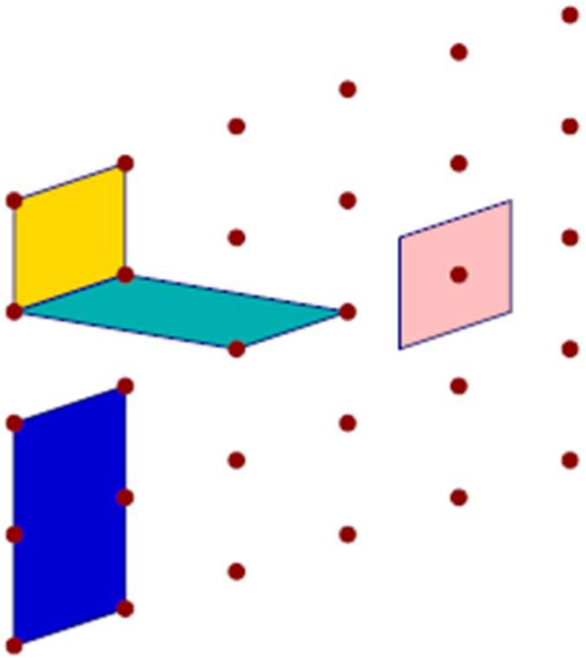

Unit cell: The $\{\vec{a}, \vec{b}, \vec{c}\}$ vectors define a parallelepipedon that reproduces the whole lattice network by means of primitive translations. There is an inifinite number of ways for selecting a unit cell.

Primitive cell: Any primitive cell contains exactly one lattice point and encloses the minimal volume that reproduces the whole crystal by translations alone.

Centered cell: n primitive cells can be glued together to form a centered cell containing n lattice points.

The use of a primitive cell means that the lattice is formed by primitive translations alone.

The use of a centered cell means that the lattice contains fractional translations in addition to the primitive ones.

Centered cells are used for convenience: showing better the symmetry of the crystal, evidencing the relationship of two structures, etc.

Periodic crystals

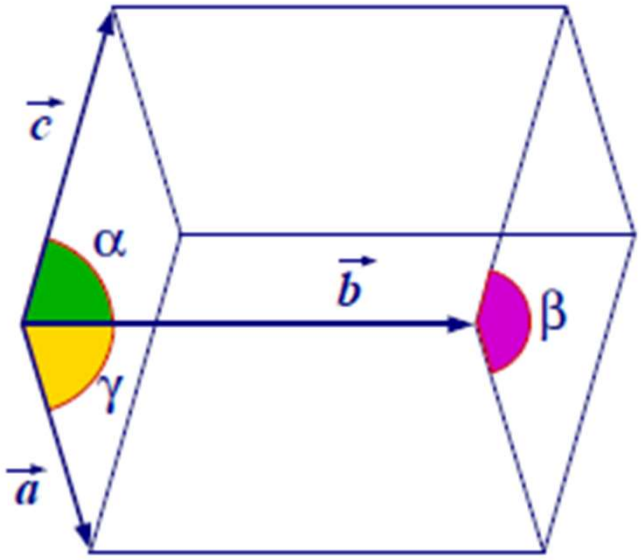

Crystal geometry

Cell parameters: $(a, b, c, \alpha, \beta, \gamma)$.

Director cosines:

$$\cos\alpha = (\vec{b}\cdot\vec{c})/bc,$$
$$\cos\beta = (\vec{c}\cdot\vec{a})/ca,$$
$$\cos\gamma = (\vec{a}\cdot\vec{b})/ab.$$

Cell volume: $V = \vec{a}\cdot(\vec{b}\times\vec{c}) = \vec{b}\cdot(\vec{c}\times\vec{a}) = \vec{c}\cdot(\vec{a}\times\vec{b})$.

Crystallographic coordinates: Any arbitrary point in the crystal is described by a vector:

$$\vec{r}_i = x_i\vec{a} + y_i\vec{b} + z_i\vec{c} = \begin{pmatrix}\vec{a} & \vec{b} & \vec{c}\end{pmatrix}\begin{pmatrix}x_i\\ y_i\\ z_i\end{pmatrix} = \underset{\sim}{a}\,\underline{x}_i, \qquad \underline{x}_i \in \mathbb{R}^3.$$

Periodic crystals

The 7 crystal systems appear as a consequence of imposing symmetry conditions upon the lattice vectors. The consideration of primitive or centered cells on the crystal systems produces 14 different cell types known as **Bravais lattices**.

System	Symmetry	Cell parameters	Bravais latt.
Cubic	Four $C_3(3)$ axes	$a = b = c,\ \alpha = \beta = \gamma = 90^\circ$	P, I, F
Hexagonal	a $C_6(6)$ or $S_3(\bar{6})$ axis	$a = b,\ \alpha = \beta = 90^\circ,\ \gamma = 120^\circ$	P
Trigonal (H)	a $C_3(3)$ or $S_6(\bar{3})$ axis	$a = b,\ \alpha = \beta = 90^\circ,\ \gamma = 120^\circ$	R
Trigonal (R)	a $C_3(3)$ or $S_6(\bar{3})$ axis	$a = b = c,\ \alpha = \beta = \gamma$	R
Tetragonal	a $C_4(4)$ or $S_4(\bar{4})$ axis	$a = b,\ \alpha = \beta = \gamma = 90^\circ$	P, I
Orthorhombic	three $\perp$ $C_2(2)$ or $S_2(\bar{2})$ axes	$\alpha = \beta = \gamma = 90^\circ$	P, I, F. C
Monoclinic	a $C_2(2)$ or $S_2(\bar{2})$ axis	$\alpha = \beta = 90^\circ$ or $\alpha = \gamma = 90^\circ$	P, B or C
Triclinic	$E(1)$ or $i(\bar{1})$	none	P

Trigonal or rhombohedral: The true R cell is primitive, but the R cell with hexagonal axes contains three lattice points and it is centered on $(2/3, 1/3, 1/3)$ (*obverse*) or $(1/3, 2/3, 1/3)$ (*reverse*).

Calcite: fluorite structure

Cubic, $Fm\bar{3}m$ (225), a = 5.4626 Å, $Z = 4$.

Ca	4a	$(0, 0, 0)$
F	8c	$(1/4, 1/4, 1/4)$

From the International Tables of Crystalography:

Wyckoff	Sim.	Equiv. positions
4a	$m3m$	$(0, 0, 0)$
8c	$\bar{4}3m$	$(1/4, 1/4, 1/4)$, $(1/4, 1/4, 3/4)$

Centering vectors
$(0, 0, 0)$, $(1/2, 1/2, 0)$, $(1/2, 0, 1/2)$, $(0, 1/2, 1/2)$

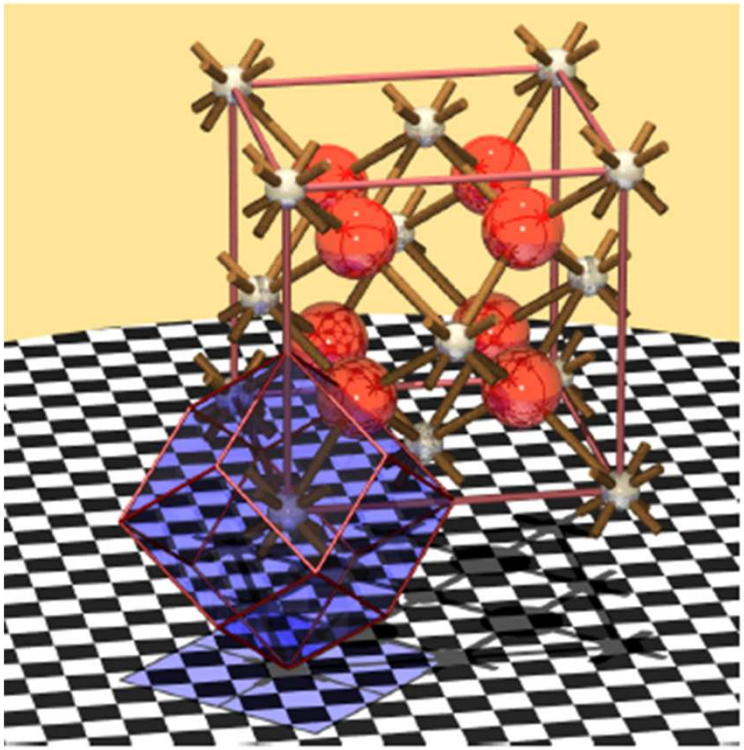

Primitive cell

	F:	I:	C:
$\vec{a}_P$	$(\vec{a}+\vec{b})/2$	$(\vec{a}+\vec{b}-\vec{c})/2$	$(\vec{a}-\vec{b})/2$
$\vec{b}_P$	$(\vec{b}+\vec{c})/2$	$(-\vec{a}+\vec{b}+\vec{c})/2$	$(\vec{a}+\vec{b})/2$
$\vec{c}_P$	$(\vec{c}+\vec{a})/2$	$(\vec{a}-\vec{b}+\vec{c})/2$	$\vec{c}$

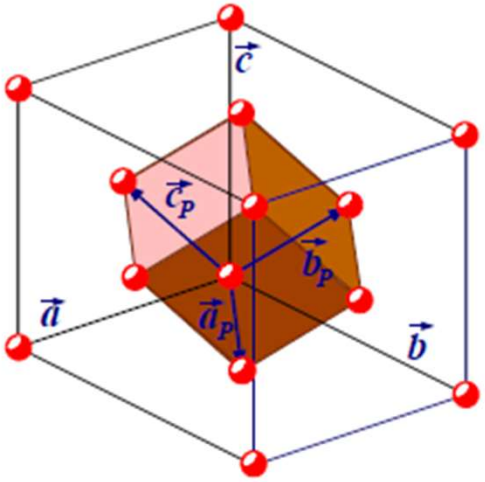

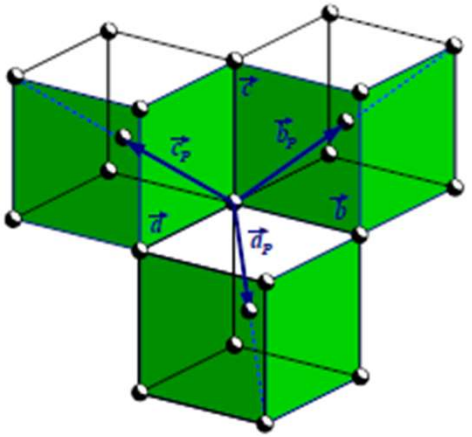

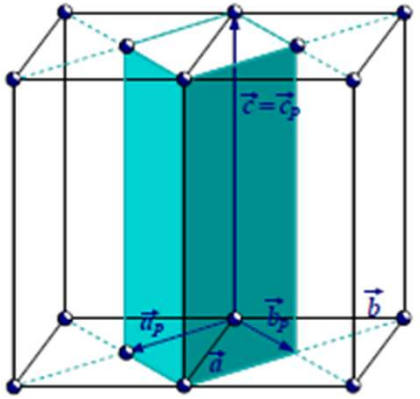

Basis sets: Plane waves

- u is expanded in planewaves, whose wave vectors are the reciprocal lattice vectors of the crystal, $u_{nk}(r) = \sum_G C_{nk}^G e^{iGr}$
- $\vec{b_i}\vec{a_j} = 2\pi\delta_{ij}$, $\psi_{nk}(r) = \sum_G C_{nk}^G e^{i(k+G)r}$

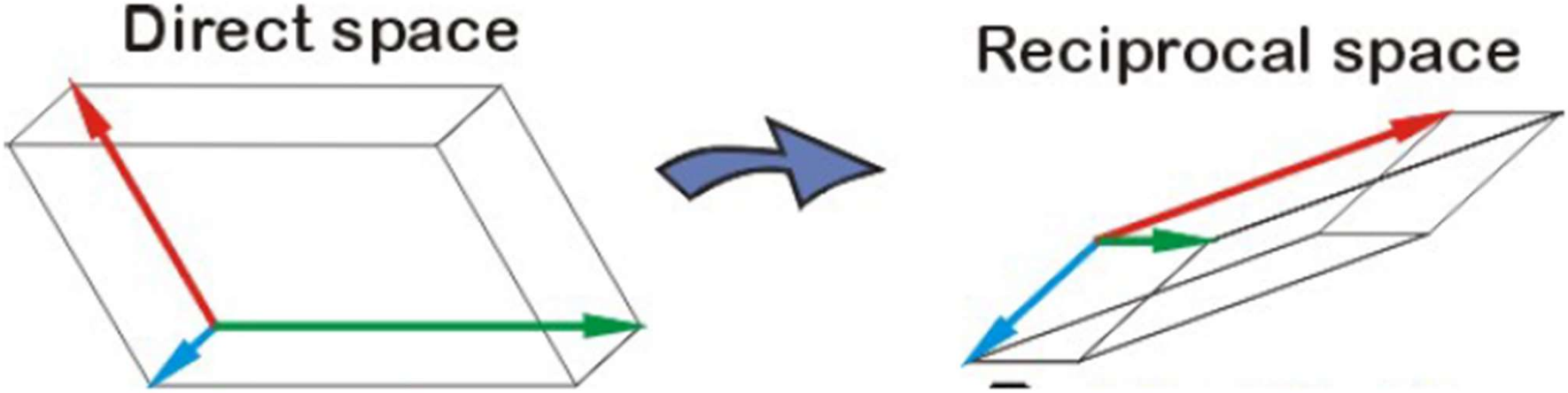

- $\vec{R} = n_1\vec{a_1} + n_2\vec{a_2} + n_3\vec{a_3}$, $\vec{G} = h\vec{b_1} + k\vec{b_2} + l\vec{b_3}$
- $\vec{b_1} = 2\pi\frac{\vec{a_2}\mathrm{x}\vec{a_3}}{\vec{a_1}\bullet\vec{a_2}\mathrm{x}\vec{a_3}}$, $\vec{b_2} = 2\pi\frac{\vec{a_3}\mathrm{x}\vec{a_1}}{\vec{a_1}\bullet\vec{a_2}\mathrm{x}\vec{a_3}}$, $\vec{b_3} = 2\pi\frac{\vec{a_1}\mathrm{x}\vec{a_2}}{\vec{a_1}\bullet\vec{a_2}\mathrm{x}\vec{a_3}}$
- $V_{cell} = |\vec{a_1}, \vec{a_2}, \vec{a_3}|$, $V_{BZ} = |\vec{b_1}, \vec{b_2}, \vec{b_3}| = (2\pi)^3/V_{cell}$

Brillouin zones

- A Brillouin zone is defined as a Wigner-Seitz primitive cell in the reciprocal lattice.
- Draw vectors to all the nearest reciprocal lattice vectors, then bisect them.
- The 1^{st} BZ is the smallest volume entirely enclosed by the planes that are perpendicular bisectors of the reciprocal lattice vectors dranw from the origin.

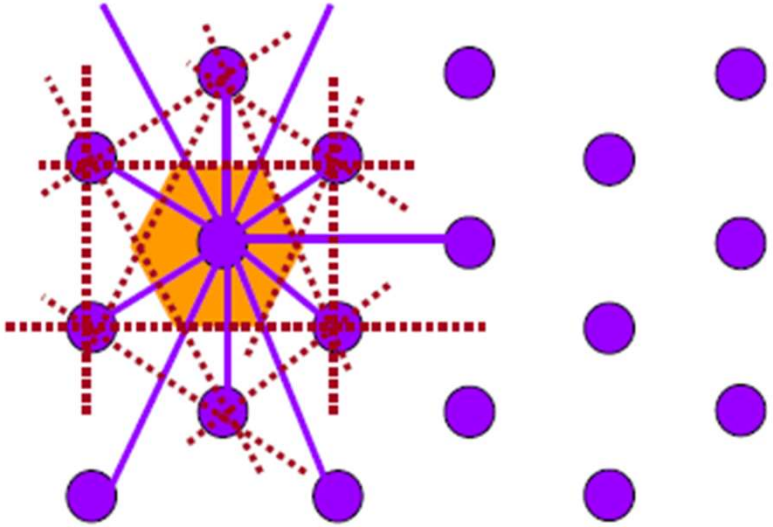

Cutoff: finite basis set

- Computationally, a complete expansion in terms of infinitely many plane waves is not possible.
- Each basis function $e^{i\vec{G}\vec{r}}$ represents a plane-wave travelling in space, perpendicular to the vector $\vec{G}$ and with a Kinetic energy $-\frac{\delta^2}{2} \rightarrow \frac{(G^2)}{2}$.
- There are an infinite number of allowed $\vec{G}$ but the coefficients $c_{n\vec{k}}^{\vec{G}}$ for the lowest eigenvectors decrease exponentially with the kinetic energy $\frac{(k+G)^2}{2}$.
- Selection of plane waves determined by a cutoff energy value, E_{cut}.
- PW sphere: $\frac{(\vec{k}+\vec{G})^2}{2} < E_{cut}$
- N_{pw} is a discontinuous function of the PW kinetic energy cutoff. $N_{pw} \approx \frac{1}{2\pi^2} V E_{cut}^{\frac{3}{2}}$.
- And is variational.

Advantages of plane waves

- Independent of atomic positions: there are no Pulay terms in the forces.
- Systematic improvement of completeness/resolution (E_{cut}).
- Orthogonal, no BSSE, periodic.
- Allows for easy evaluation of gradients and Laplacian.
- The information contained in $\psi(\vec{G})$ and $\psi(\vec{r})$ are equivalent and easily transformed using fast Fourier transforms (FFT's).
- Kinetic energy in reciprocal space, potential in real space.

Pseudopotentials

- The very large $\vec{G}$ components describe the region of the space where the wavefunction is varying very quickly. This happens when the potential is very attractive- the strongest potentials are those near the nuclei.
- Electrons in the inner shells do not contribute to valence bonding- so they are frozen in the state they have in an isolated atom.
- Releasing the frozen core does not add any linear term to the energy (von Barth and Gelatt, 1980).
- The physical properties of solids depend mainly on the valence electrons.
- We can replace the Coulomb potential near each nucleus with a modified, weaker potential. This modified potential is called a pseudopotential
- Now, the wavefunctions do not vary as quickly near the nucleus, so we can use a smaller E_{cut}.

Pseudopotentials

- The core electrons spend all their time near the nucleus. They repel the outer electrons, so the outer electrons feel a weaker potential from the nucleus, but otherwise they don't affect the chemical properties....
- We do not treat the core electrons explicitly any more.
- Instead of the strong nuclei Coulombi potential, we consider a softer core (nuclear + core electrons) potential.
- Valence electrons will feel this PP.

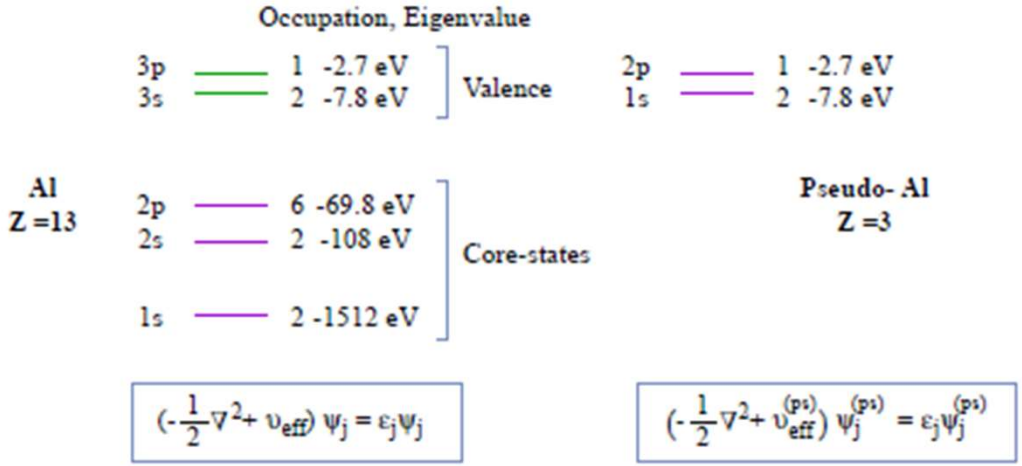

Pseudopotentials

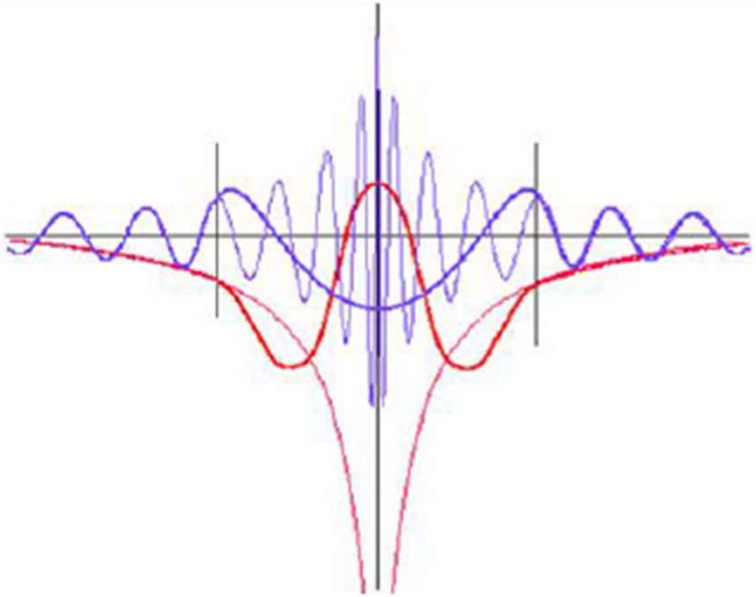

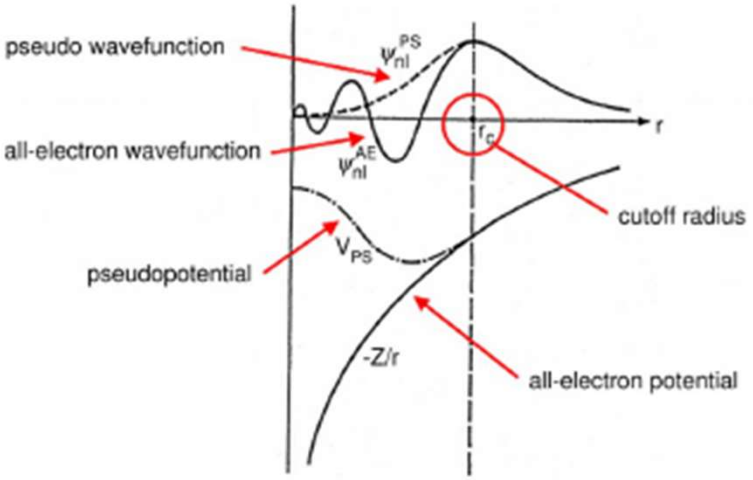

- The valence states will thus be different around r=0.
- Beyond a certain radius (r_{core}), valence states should be identical to all-electron results.

Brillouin zone integration

- Properties like the electron density, total energy... can be evaluated by integration over $\vec{k}$ inside the BZ. Thus, the summation over infinite number of translations becomes an integral over the first Brillouin zone. $\int_R^{\infty} \rightarrow \int_{\vec{k} \in BZ} d\vec{k}$.
- In practise, the integral is replaced by a weighted sum of discrete points. Thus, for the i^{th} band of a function $f_i(\vec{k})$
- $\frac{1}{V_{BZ}} \int_{BZ} d\vec{k} f_i(\vec{k}) \rightarrow \overline{f_i} = \frac{1}{N_{\vec{k}}} \sum_{\vec{k}} f_i(\vec{k})$

Example :

a 2D square lattice

25 $\vec{k}$-points in the BZ

$\bar{f}_i = f_i(\vec{k}_1) + \ldots + f_i(\vec{k}_{25})$

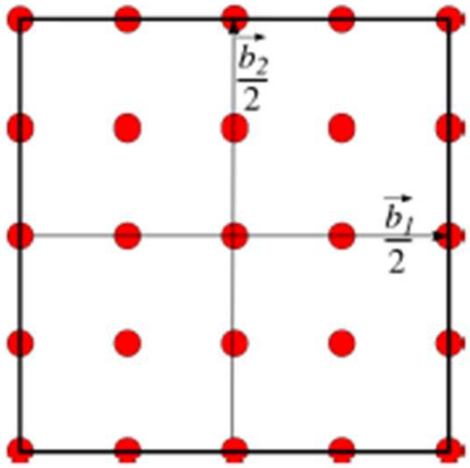

Brillouin zone integration

- Properties like the electron density, total energy... can be evaluated by integration over $\vec{k}$ inside the BZ. Thus, the summation over infinite number of translations becomes an integral over the first Brillouin zone. $\int_R^{\infty} \rightarrow \int_{\vec{k} \in BZ} d\vec{k}$.
- In practise, the integral is replaced by a weighted sum of discrete points. Thus, for the i^{th} band of a function $f_i(\vec{k})$
- $\frac{1}{V_{BZ}} \int_{BZ} d\vec{k} f_i(\vec{k}) \rightarrow \overline{f_i} = \frac{1}{N_{\vec{k}}} \sum_{\vec{k}} f_i(\vec{k})$

Example :

a 2D square lattice

25 $\vec{k}$-points in the BZ

$\bar{f}_i = f_i(\vec{k}_1) + \ldots + f_i(\vec{k}_{25})$

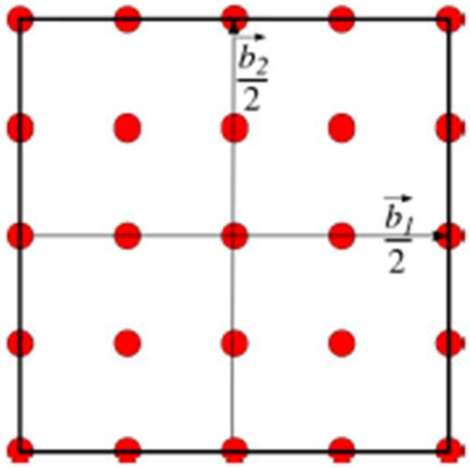

Monkhorst-Pack grid

A uniform mesh of $\vec{k}$-points can be generated by Monkhorst-Pack procedure

$$\vec{k}_{n_1,n_2,n_3} = \sum_{1}^{3} \frac{2n_i - N_i - 1}{2N_i} \vec{G}_i$$

where N_i is the number of $\vec{k}$-points in each direction and $n_i = 1, \ldots, N_i$.

Example : 4×4×1 MP grid for 2D square lattice

$$\vec{G}_1 = \vec{b}_1 = \frac{\pi}{a}\hat{k}_x, \quad \vec{G}_2 = \vec{b}_2 = \frac{\pi}{a}\hat{k}_y, \quad \vec{G}_3 = 0$$

$$\vec{k}_{1,1} = \left(\tfrac{-3}{8}, \tfrac{-3}{8}\right) \qquad \vec{k}_{1,3} = \left(\tfrac{-3}{8}, \tfrac{1}{8}\right)$$

$$\vec{k}_{1,2} = \left(\tfrac{-3}{8}, \tfrac{-1}{8}\right) \qquad \vec{k}_{1,4} = \left(\tfrac{-3}{8}, \tfrac{3}{8}\right)$$

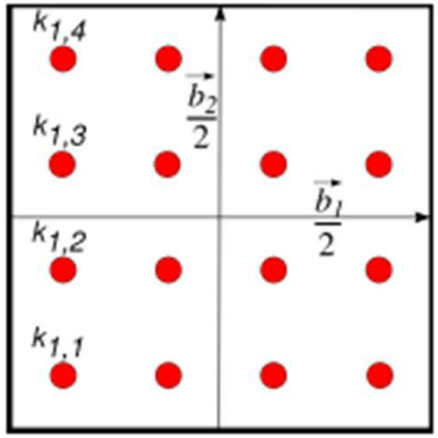

Integrations in the IBZ

- Generate a uniform mesh in reciprocal space
- Shift the mesh if required
- Employ all symmetry operations of the Bravais lattice to each of the $\vec{k}$-points
- Select the $\vec{k}$-points which fall into the IBZ
- Calculate weights, $\omega_{\vec{k}}$, for each of the selected $\vec{k}$-points

$$\omega_{\vec{k}} = \frac{\text{number of symmetry connected } \vec{k}\text{-points}}{\text{total number of } \vec{k}\text{-points in the BZ}}$$

- IBZ integration is then given by

$$\bar{f}_i = \sum_{\vec{k}}^{\text{IBZ}} \omega_{\vec{k}} f_i(\vec{k})$$

Smearing methods

Fermi level : the energy of the highest occupied band.

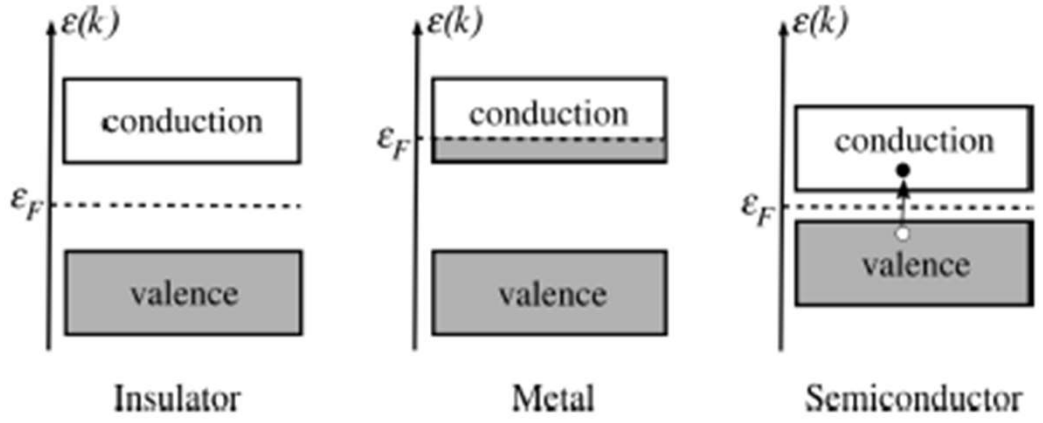

IBZ integration over the filled states : $\bar{f}_i = \sum_{\vec{k}}^{\mathrm{IBZ}} \omega_{\vec{k}} f_i(\vec{k}) \theta(\varepsilon_i(\vec{k}) - \varepsilon_F)$

For insulators and semiconductors, DOS goes to zero smoothly before the gap.

For metals, the resolution of the step function at the Fermi level is very difficult in plane waves.

Trick is to replace sharp $\theta(\varepsilon_i(\vec{k}) - \varepsilon_F)$ function with a smoother $f(\{\varepsilon_i(\vec{k})\})$ function allowing partial occupancies at the Fermi level.

Electronic structure codes

code	basis	webpage	price	source
abinit	pw+ps	www.abinit.org	GNU	yes
CPMD	pw+ps	www.cpmd.org	0	yes
crystal09	CGTO	www.crystal.unito.it	1000 Eur.	no
elk	FPLAPW	elk.sourceforge.org	GNU	yes
gpaw!	PAW	wiki.fysik.dtu.dk/gpaw	GNU	yes
QE (pwscf)	pw+ps	www.quantum-espresso.org	GNU	yes
siesta	Loc+ps	www.icmab.es/siesta	0	yes
vasp	pw+ps	cms.mpi.univie.ac.at/marsweb	yes	yes
wien2k	FPLAPW	www.wien2k.at	yes	yes

Total energy & derivatives

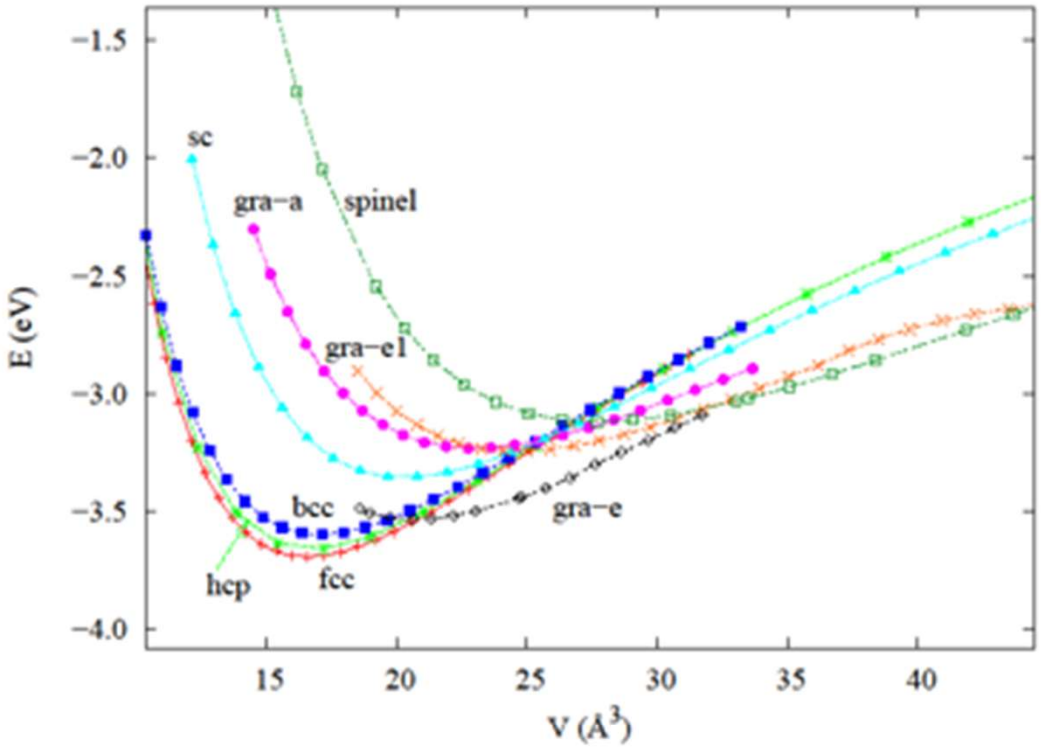

Thermodynamics

- $(E_i, V_i) \longrightarrow (P_i, V_i) \longrightarrow B(p), B'(p), x_{opt}(p), G(p)$
- Phase equilibrium: $G_\alpha = G_\beta$ $p = p_t$

Total energy & derivatives

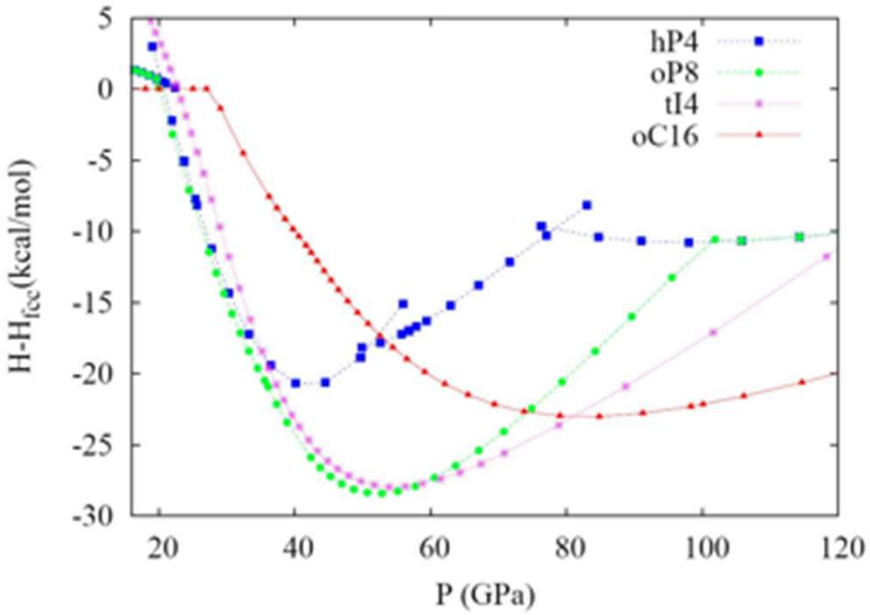

Relative stability

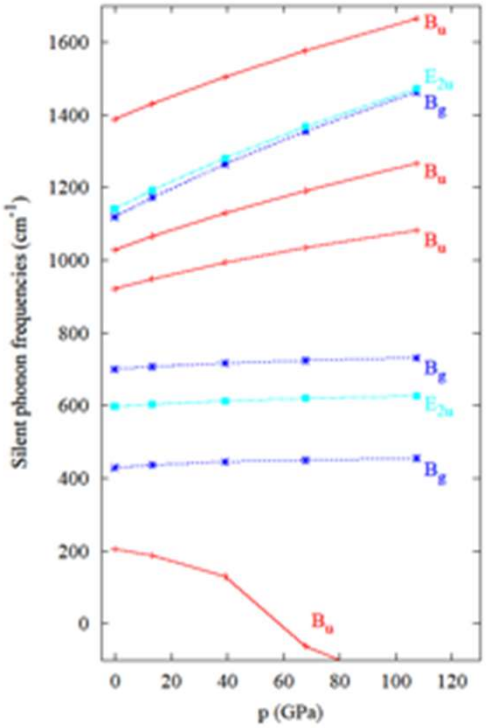

Crystal vibrations

Structure searching

"One of the continuing scandals in the physical sciences is that it remains in general impossible to predict the structure of even the simplest crystalline solids from a knowledge of their chemical composition" (Maddox, Nature 1988)

What structure will a collection of atoms adopt?

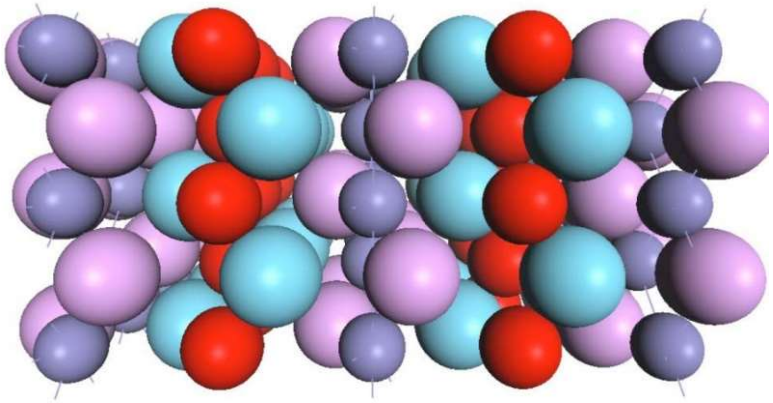

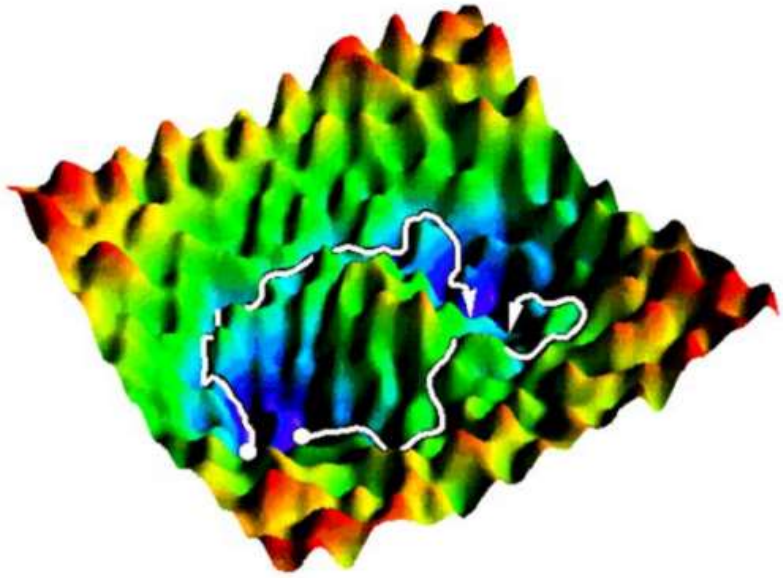

Potential energy surfaces

Crystal structure prediction: minimization of Gibbs free energy

G= U + pV –TS. Normally, H= U +pV is minimized.

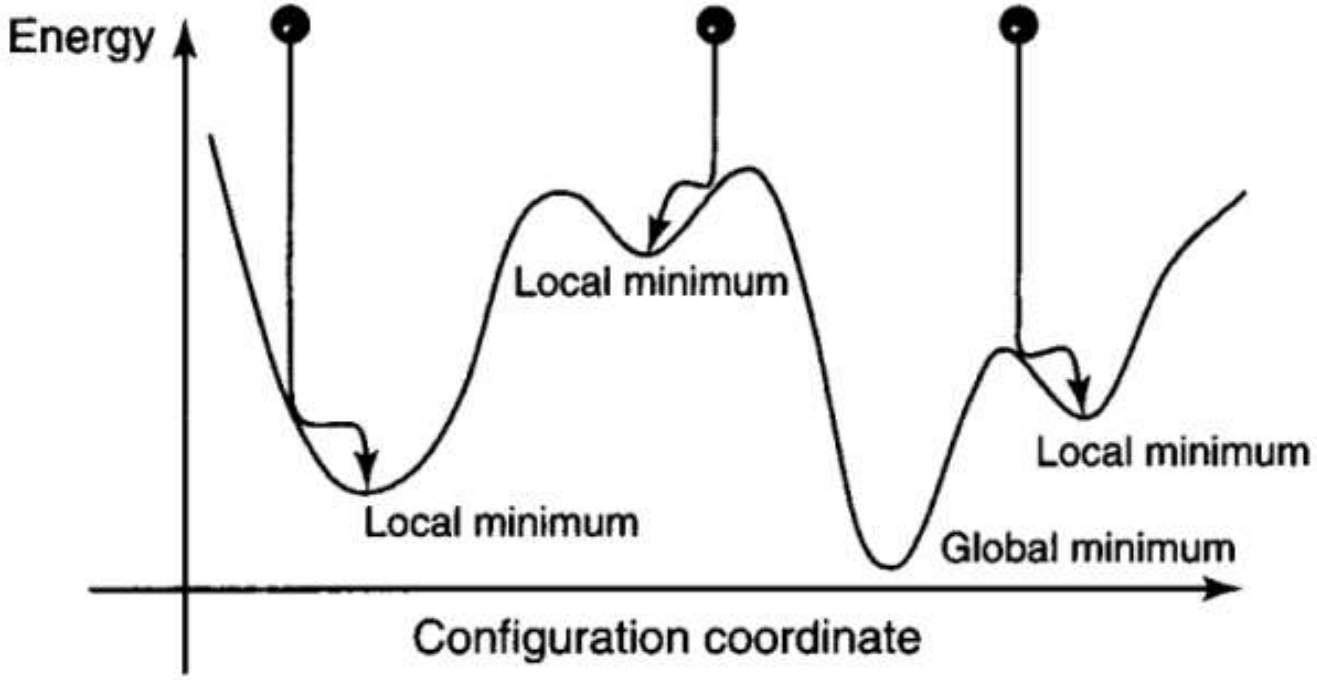

d= 3N+3 (N= number of atoms).

Potential energy surface = a fractal?

- A big region of the PES contains almost no minima: it corresponds to very high-energy structures with unphysical short distances and fragmented units.
- Going from one minimum to another minimum of lower energy is more likely when the barrier between basins is small.
- Basins with lower-energy minima tend to have larger hyper-areas than higher-energy minima.
- Very low-energy minima usually correspond to symmetrical structures.

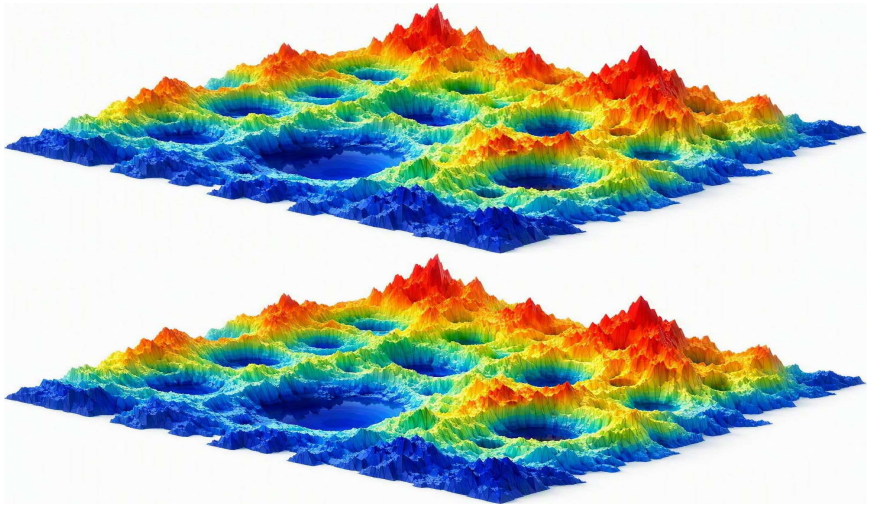

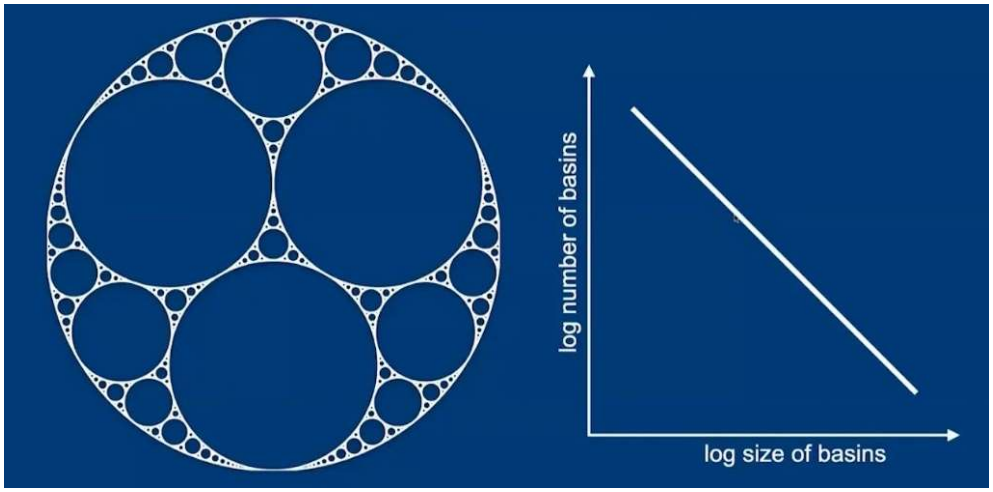

Semilocal methods

- They need a good initial starting guess.
- Exploration on the neighbourhood of this low-energy structure and subsequently found structures.

- Simulated annealing
- Minima hopping
- Basin hopping
- Metadynamics

Simulated annealing

- Mimics the metallurgy process to reduce defects & obtain large single crystals. Heating & cooling in a controled way.
- When a metal melts, atoms in a disorded state in which atomic diffusion and kinetic barriers crossing are allowed.
- An abrupt decrease of T leads to crystals with defects.
- But ,if cooling is slow, atoms arrange in the global minimum.

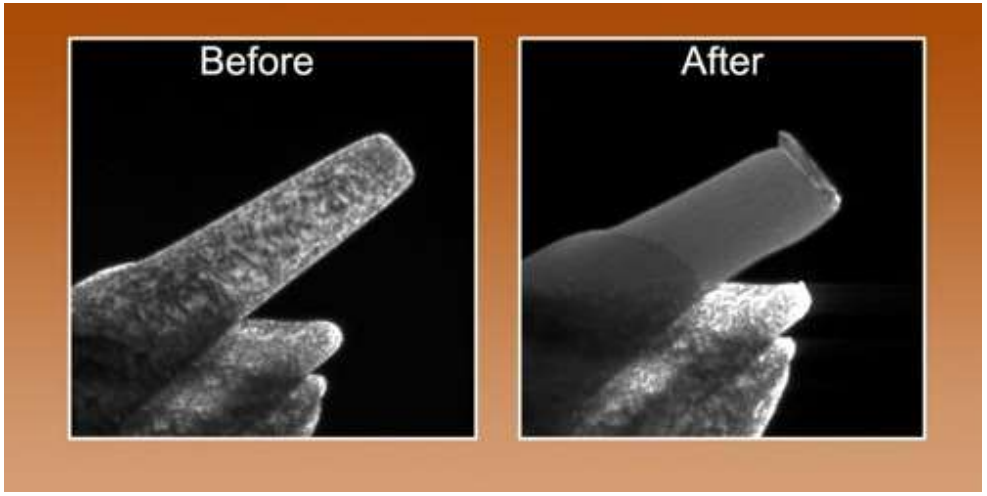

Simulated annealing

- A candidate structure is continuosly perturbed through random atomic displacements, atomic mutations, changes of lattice parameters using a Monte Carlo scheme.

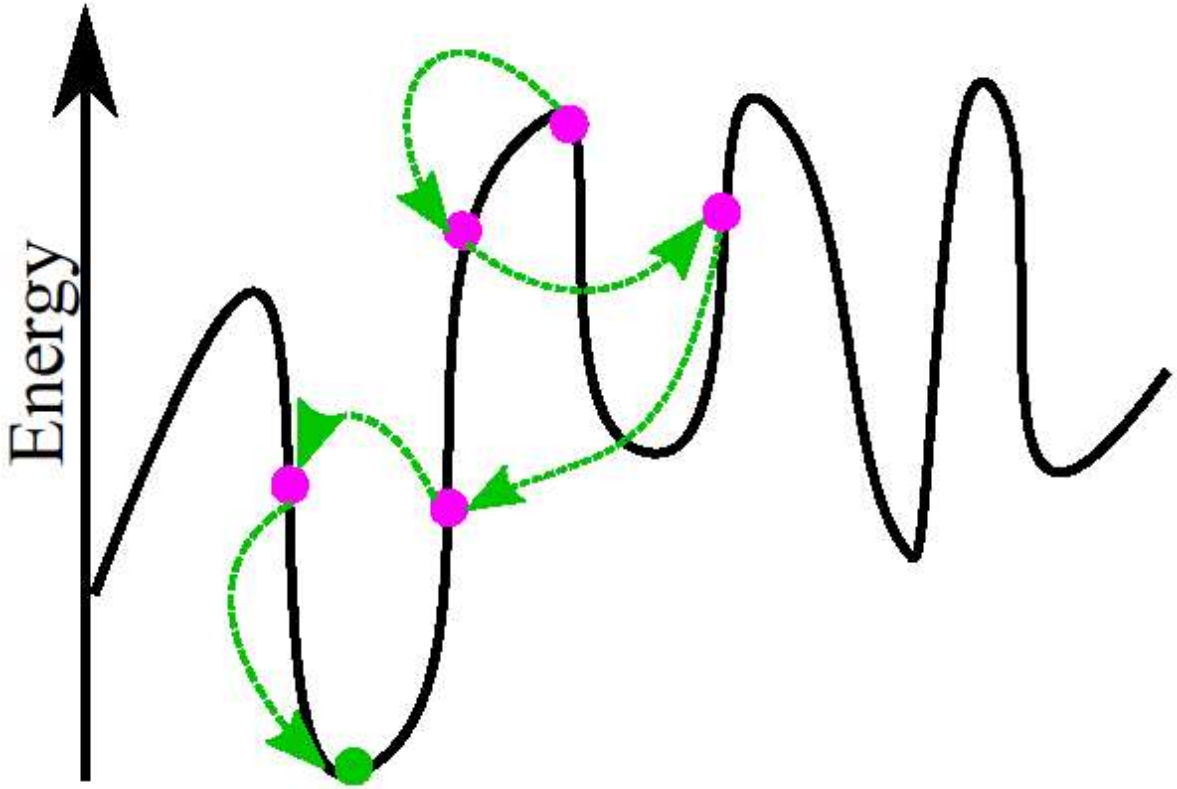

Simulated annealing

- Move accepted if, $E_f < E_i$ or $\varepsilon < P$, $P=\exp(-\Delta E/K_B T)$.
- Simulation starts at high T (most of new configurations accepted, kinetic barriers overcomed easily).
- Then, temperature is reduced, fewer high-energy configurations accepted….an hopefully, the global minimum will be found.

PROBLEMS:

- system stuck in a local minimum or the wrong funnel……. especially if there are surrounded by high energy barriers.

EFFICIENCY depends strongly on:

- Type & magnitude of moves. Large enough to jump local minima, but small to enable learning.
- Temperature annealing process.

Basin hopping

- It starts at a random configuration, relaxed to its local minimum.
- After a random move, the new configuration is also relaxed to its local minimum.

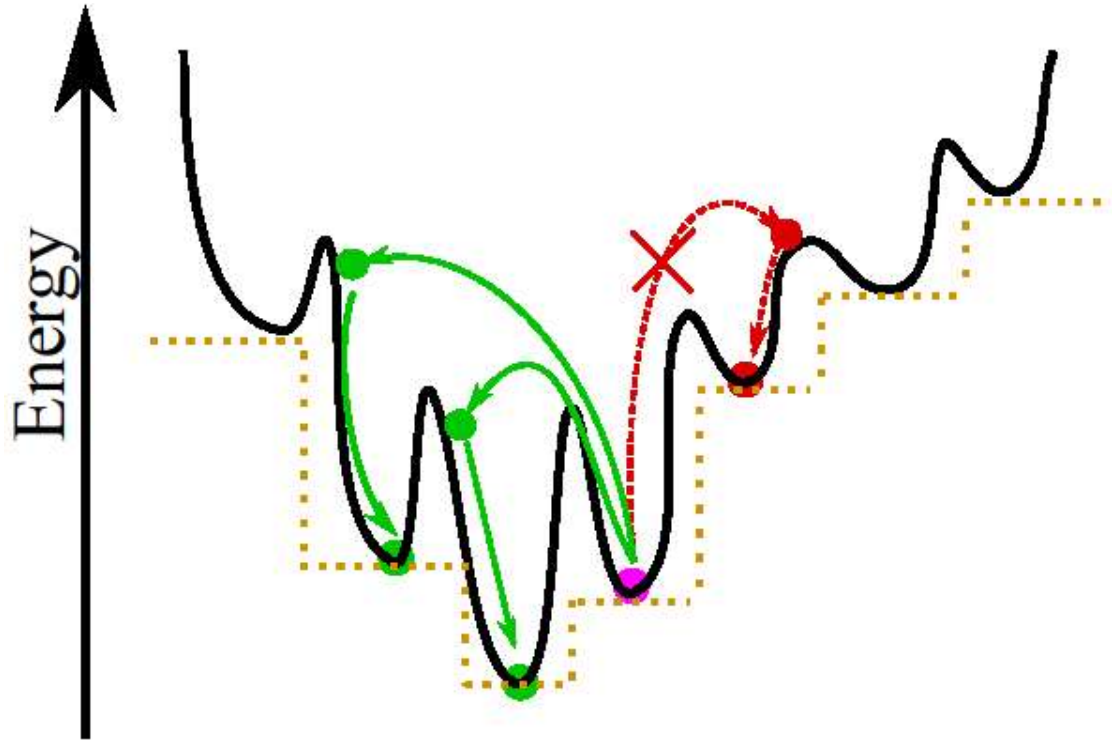

Basin hopping

- Metropolis criterion, $E_f < E_i$ or $\varepsilon < P$, $P=\exp(-\Delta E/K_B T)$ on the minimized energies.
- Temperature can be maintained or constantly reduced.
- Original PES transforms into a staircase function representing the energies of the local minima.
- Barriers between local minima are smaller and jumping easier.

EFFICIENCY depends strongly on:

- Type & magnitude of moves.
- Choice of temperature.

Minima hopping

- It uses molecular dynamics to overcome barriers.
- It starts at a local minimum. The MD simulation is stopped when U reaches another minimum.

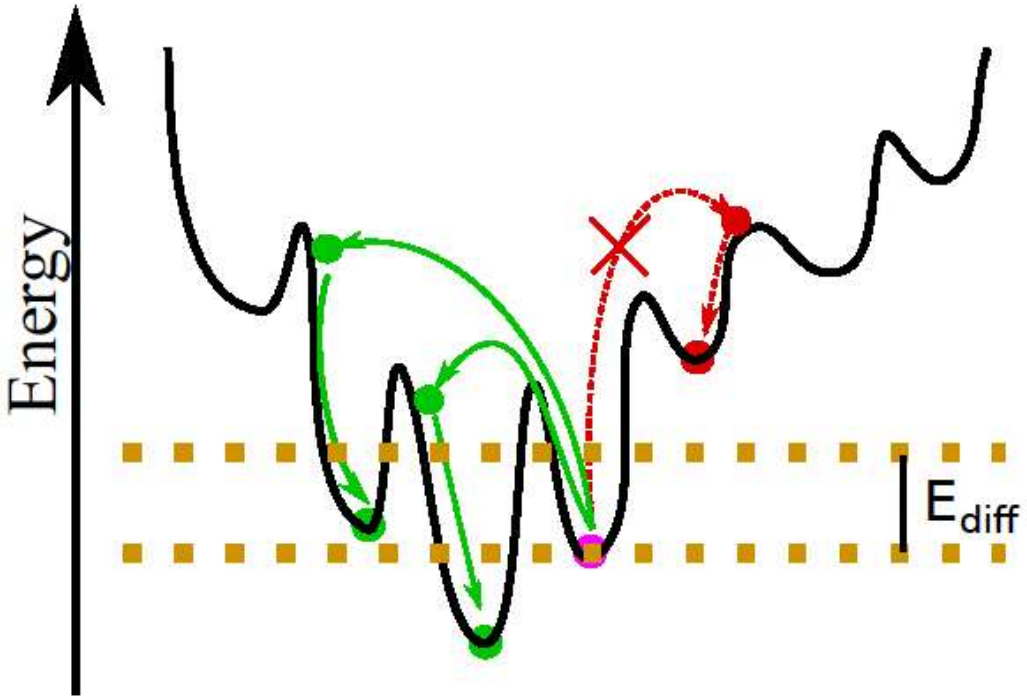

Minima hopping

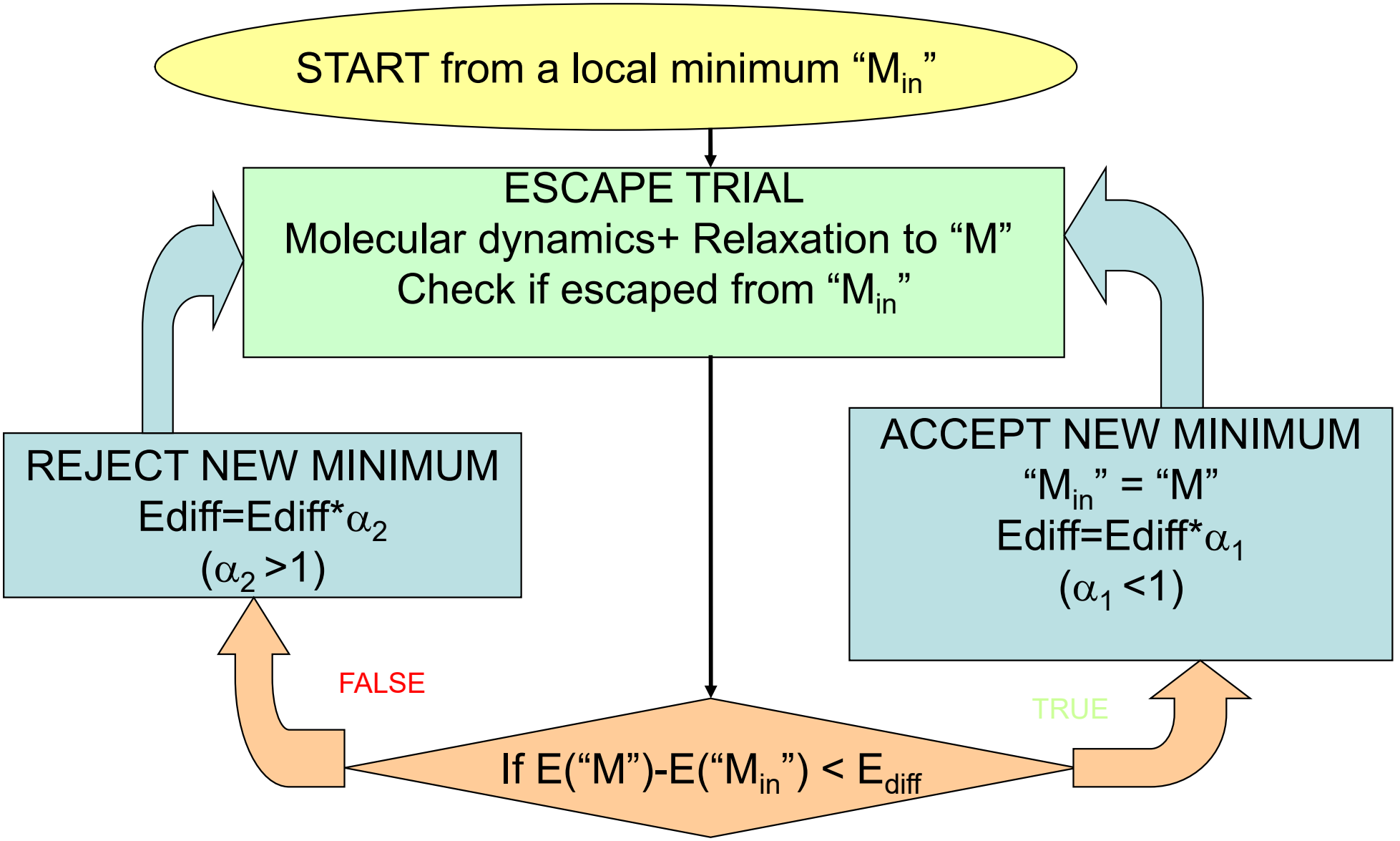

Minima hopping

- It exploits the Bell-Evans-Polayani principle, it moves from one minimum to another by crossing low barriers which significantly increases the probability of hopping into a low energy local minimum.

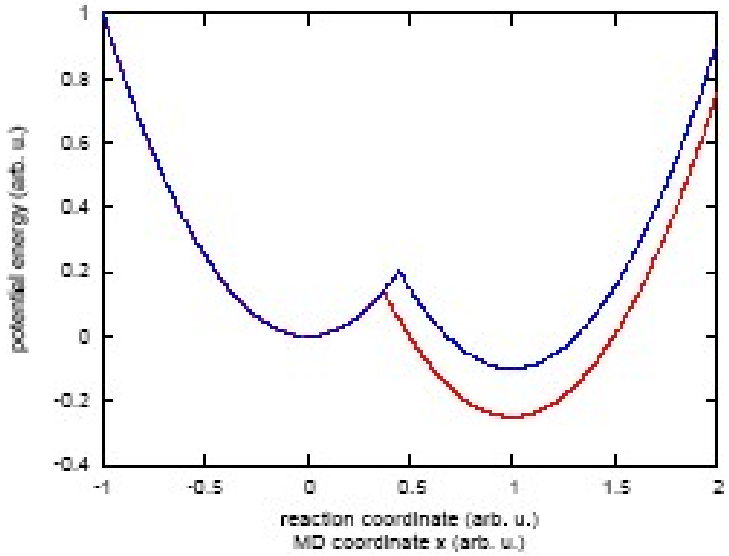

•Exothermic reactions have a low activation energy.

•Reactant and product are neighboring minima and chemical reactions are transition of barriers connecting them.

•Low E_{kin} in MD for hops into low neighboring minima

Minima hopping

Inner Loop

- Perform MD escape trials followed by local geometry relaxation.
- E_{kin} continuously adjusted.

Outer Loop

- Accepting or rejecting. Dynamic Ediff: 50 % accepted
- Eventually accept high energy structures.

EFFICIENCY depends on $E_{kin.}$

- Too high → visiting lots of undesirable minima
- Too low → big number of MD simulations to escape the current basin of attraction

Metadynamics

- Ideally, standard NPT MD simulations allow to simulate phase transitions (structure prediction & kinetics).
- But, they face a time scale problem, only transitions with activation barriers < $k_B T$ are observable with reasonable t_s.
- Solid-solid phase transitions generally first-order → high barriers & slow.
- Periodic boundary conditions → NO heterogenous nucleation; transition proceeds in a collective & concerted way with large barrier.
- It can lead to unrealistic kinetics & skipping of phases.

Metadynamics

- Solution to decrease barrier: adding a suitable potential to the original Gibbs energy landscape.
- Search for the lowest-energy path connecting 2 minima in the space of a suitable order parameter (supercell box m.).

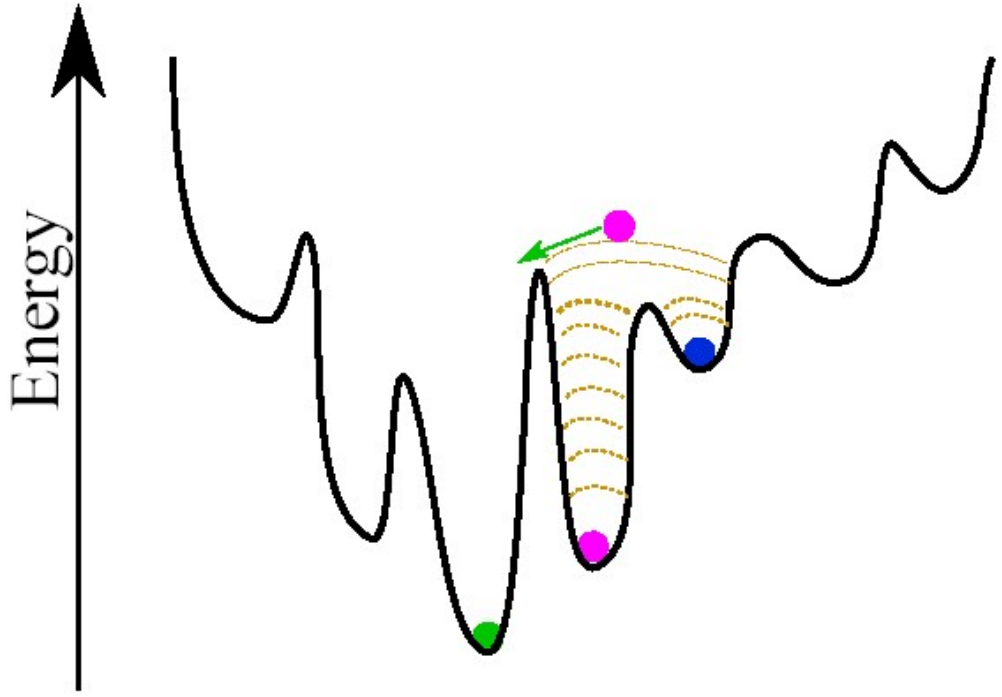

Metadynamics

- G modified by a history-dependent term: sum of Gaussians placed at visited points to discourage dynamics from visiting them again.
- Basin of atraction filled with Gaussians that increase G. When G becomes high enough to overcome the barrier, the system enters a new basin of atraction of a new structure.

EFFICIENCY depends on:

- Width & amplitude of Gaussians.
- Too large may lead to wrong phase transitions
- But too small, may require too many metadynamics steps.

Global methods

- They do not need a good initial starting guess.
- Initial randomly generated structures

- Random structure searches
- Evolutionary algorithms
- Particle swarm optimization technique

Random searching (AIRSS)

- The simplest approach if nothing is known about the system
- Exploration of the whole PES by calculating the Gibbs free energy of a set of random structures.

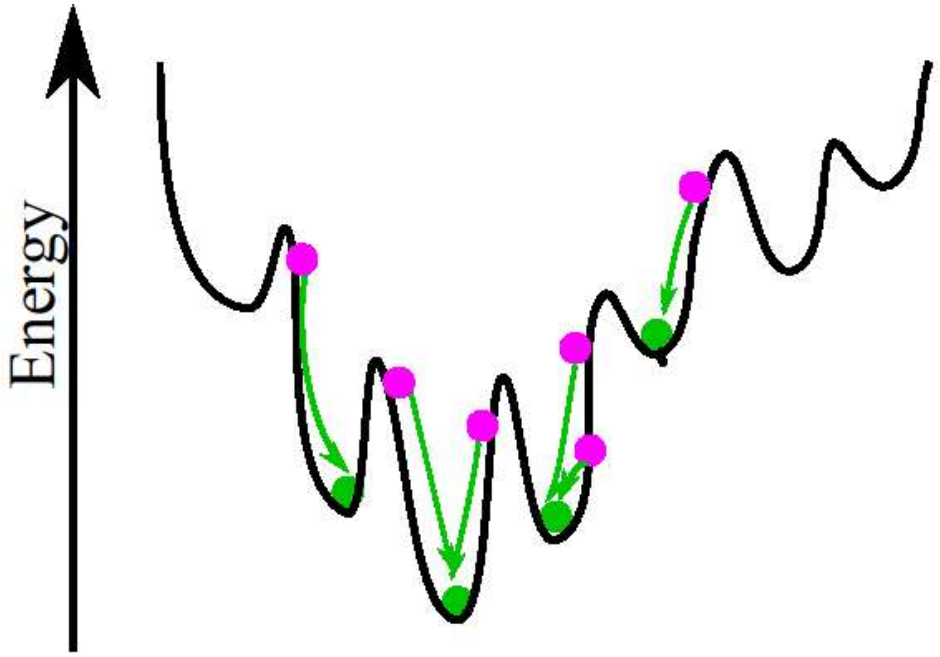

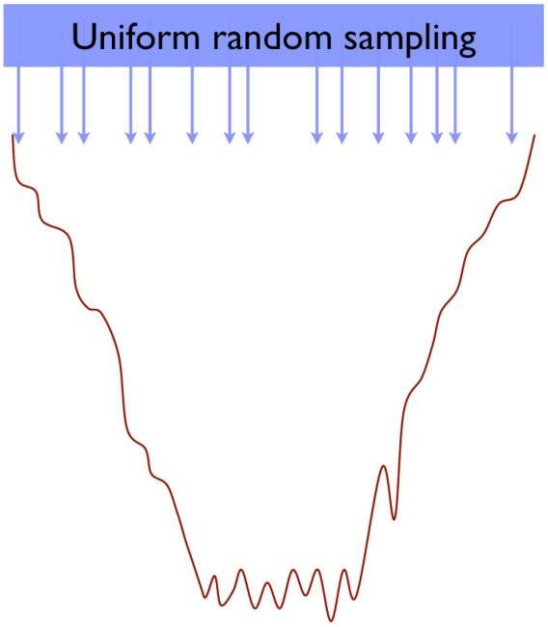

Structure searching (AIRSS)

- input: pressure, volume, number of atoms

The recipe

1. Make a random unit cell
2. Throw a given number of atoms, of given type into the unit cell
3. Relax carefully under quantum-mechanical forces and stress
4. Repeat
5. Look for the lowest energy or more “interesting” structures

Structure searching (AIRSS)

Example: Silicon

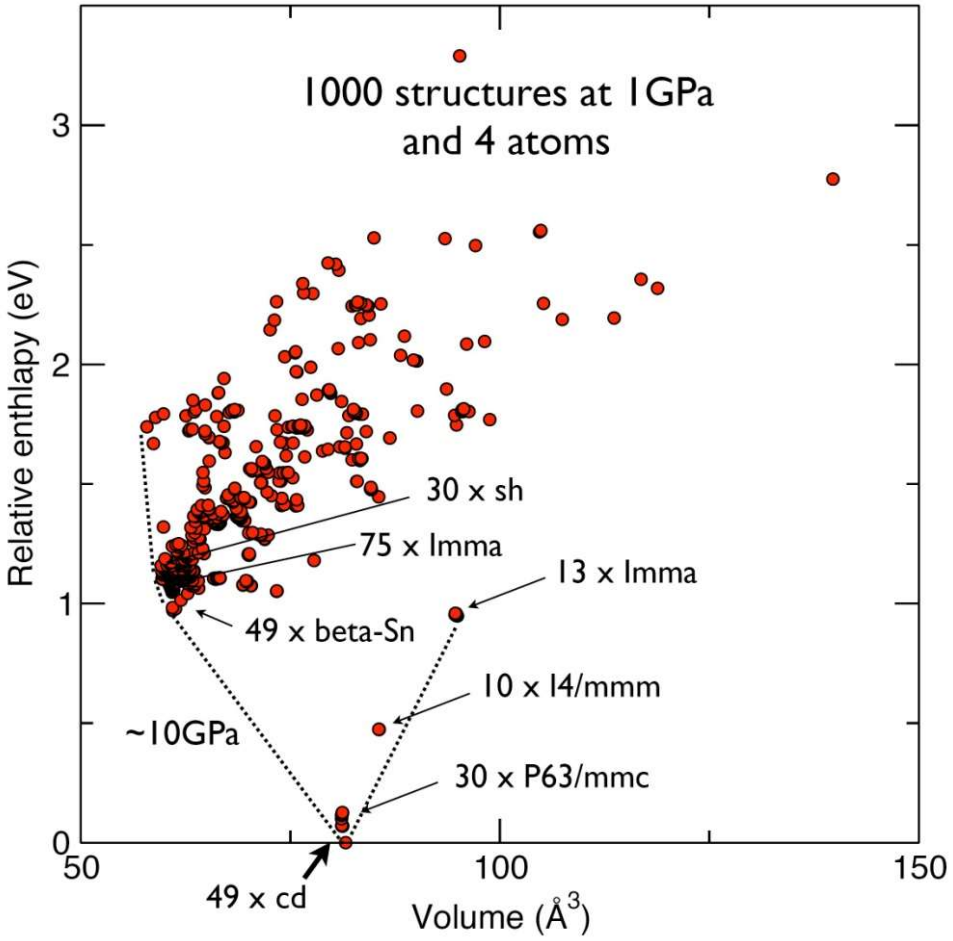

Structure searching (AIRSS)

Problem: Exponential wall

- The number of metastable states is expected to increase exponentially with the system size

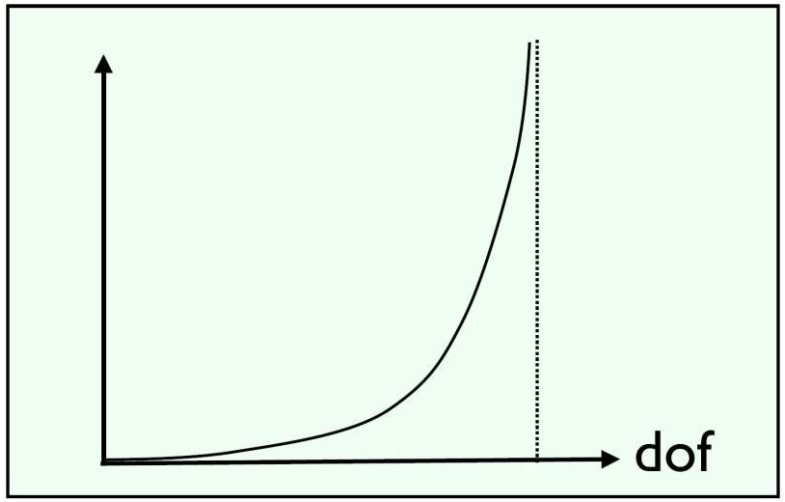

Solution: Use of constraints

- Based on: chemical ideas, symmetry, experimental data.

Evolutionary algorithms

- Inspired by natural evolution of a population where offspring resemble parents & procreation is a reward for success.
- Different computational codes: XtalOpt, GASP, USPEX….
- Initial (random) population of structures. Constraints: estimated volume, minima d_s, symmetry, lattice parameters, seeding with plausible structure, using building blocks…..
- After relaxing structures, a fingerprint & fitness are assigned to each structure.
- Identical structures are eliminated to prevent cancer growth.
- Select lowest-energy structures as parents for new generation.
- Standard variation operators: heredity, lattice mutation, permutation, atomic mutations.
- The best structure survives into the next generation & random structures also added to preserve diversity.

Evolutionary algorithms

Procedure repeated until lowest E structure does not change.

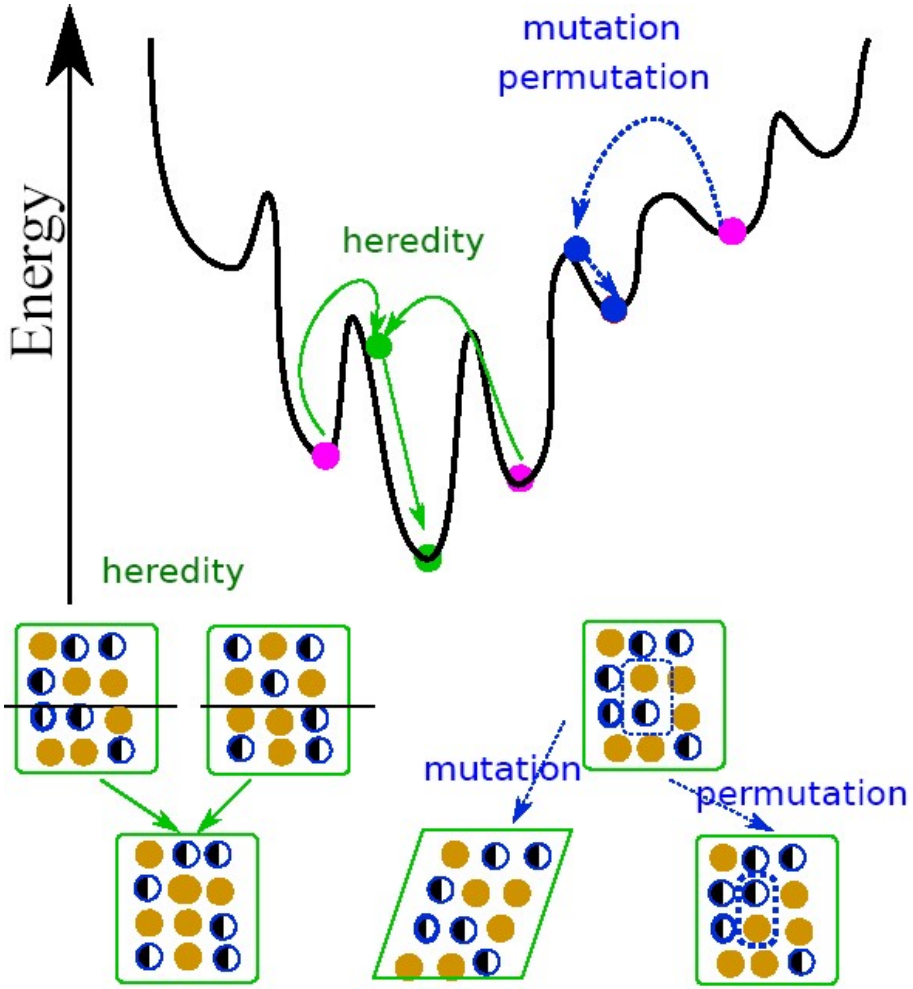

Particle swarm optimization

- Swarm intelligence: information exchanges between individual particles, self-improving evolution, evolution guided by optimal particle.

Particle swarm optimization

- Similar to evolutionary methods, but no evolution operators such as heredity or mutation.
- First population (swarm) randomly generated with constraints.
- Local optimization & discarding of identical structures.
- A fraction of the lowest E structures used to produce 60% of the structures in the new generation. (40% random).
- Movement of the particles influenced by their individual past experience ($pbest^t$, v^t) and that of the swarm ($gbest^t$).
- As the evolutionary methods, it learns from history and zooms in the most promising region of the configurational space.

Particle swarm optimization

Algorithm

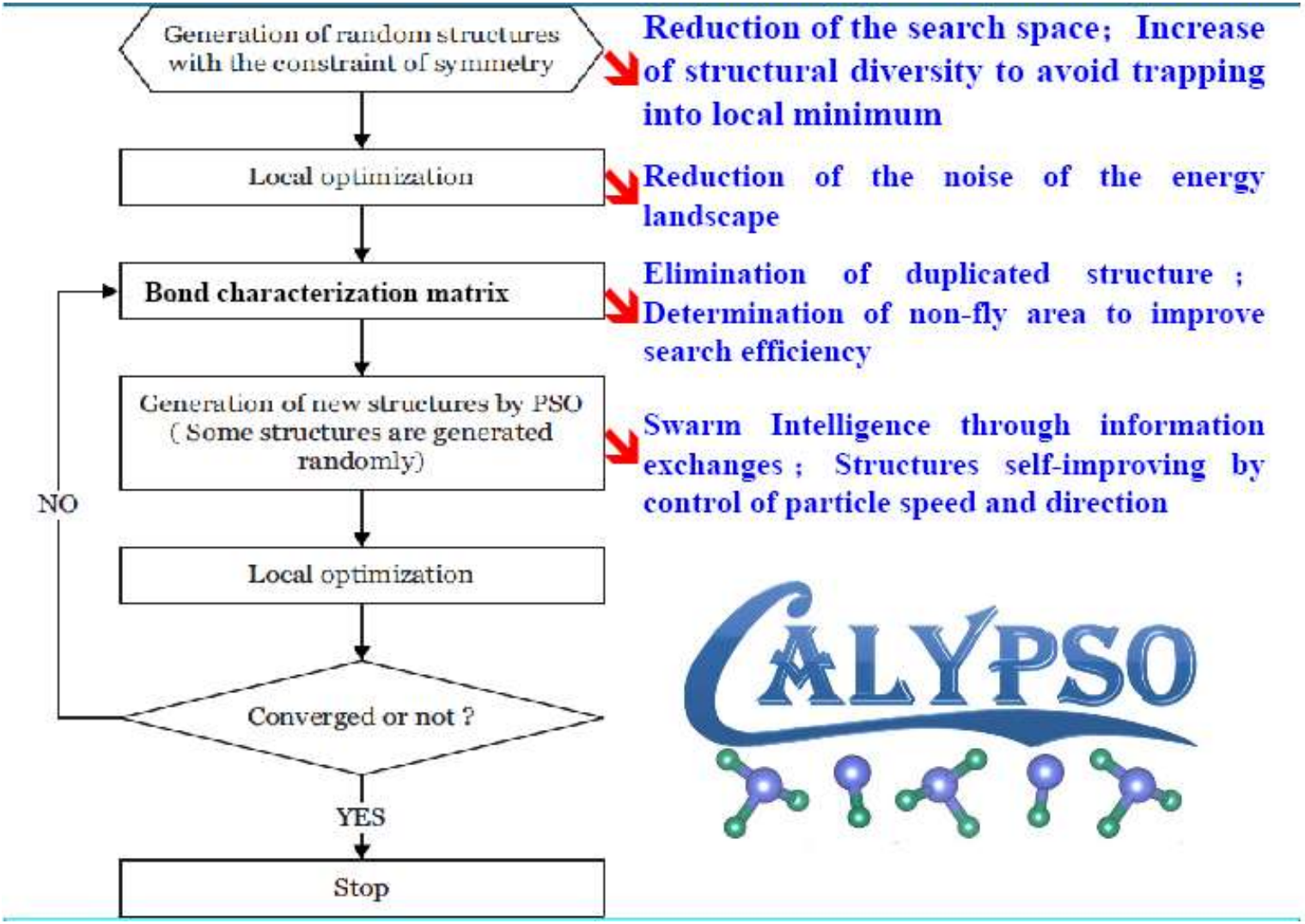

Particle swarm optimization

Algorithm

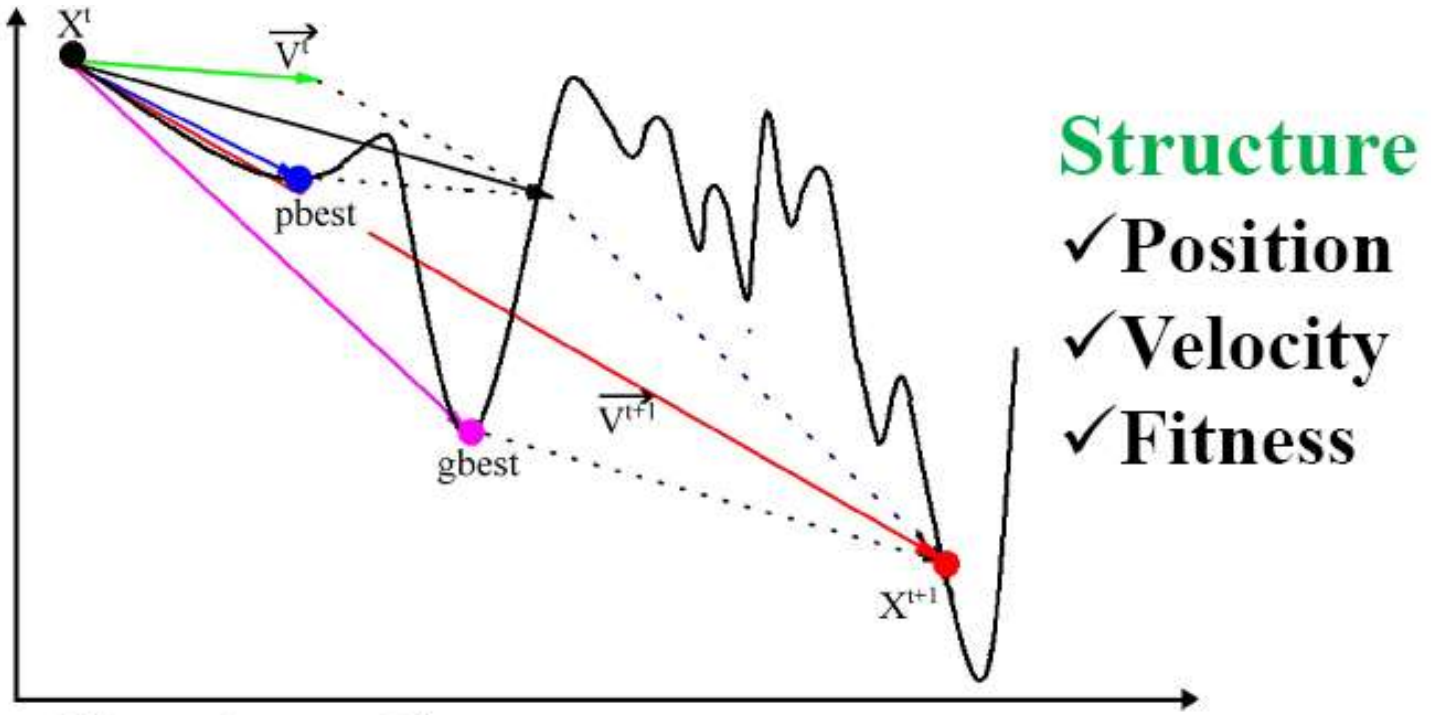

Structure

- ✓**Position**
- ✓**Velocity**
- ✓**Fitness**

$$x_{i,j}^{t+1} = x_{i,j}^{t} + v_{i,j}^{t+1}$$

$$v_{i,j}^{t+1} = \omega v_{i,j}^{t} + c_1 r_1 (pbest_{i,j}^{t} - x_{i,j}^{t}) + c_2 r_2 (gbest_{i,j}^{t} - x_{i,j}^{t})$$

Convex hull and stability

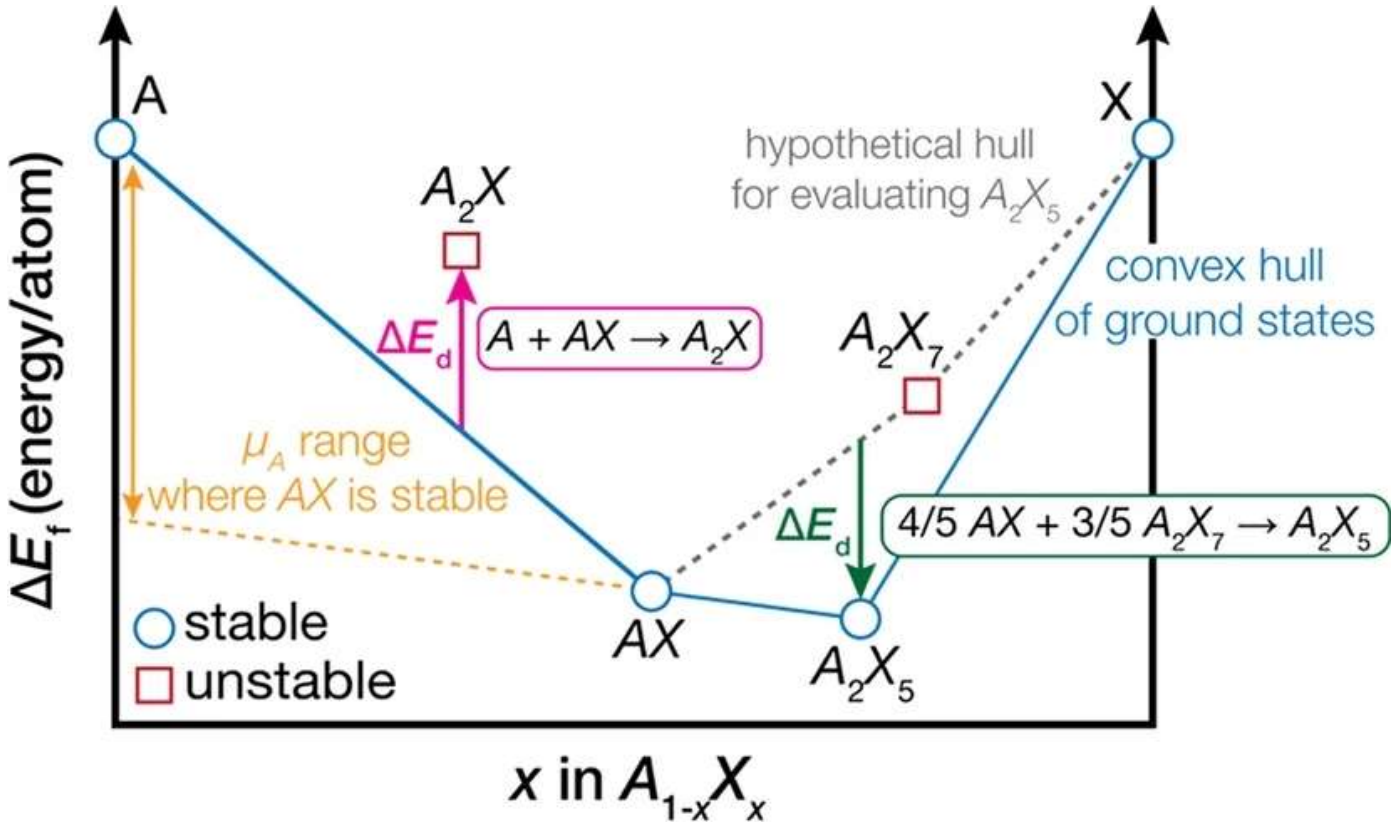

Convex hull and stability

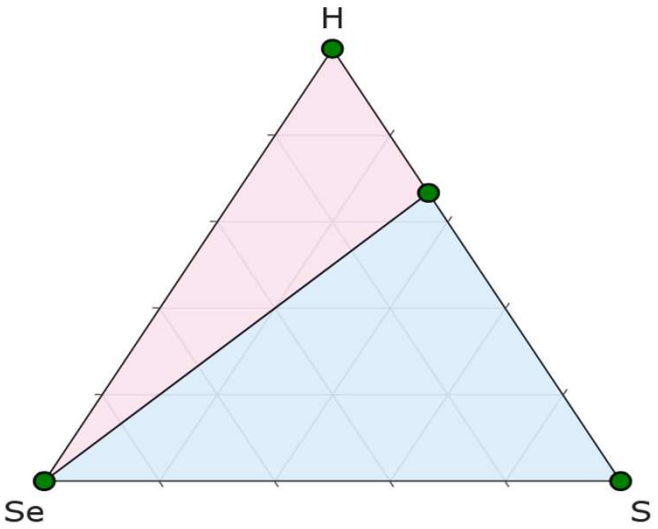

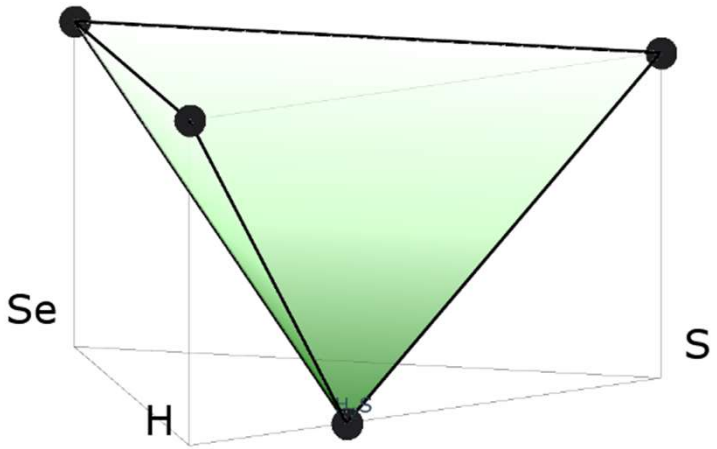

2D 3D

- H_2, S, Se, H_2S (H:2/3,Se:0, Se:1/3) estables
- Phase diagrams in Materials Project, choice of: elements, máximum energy above hull, exchange-correlation…..at 0 GPa

Convex hull and stability

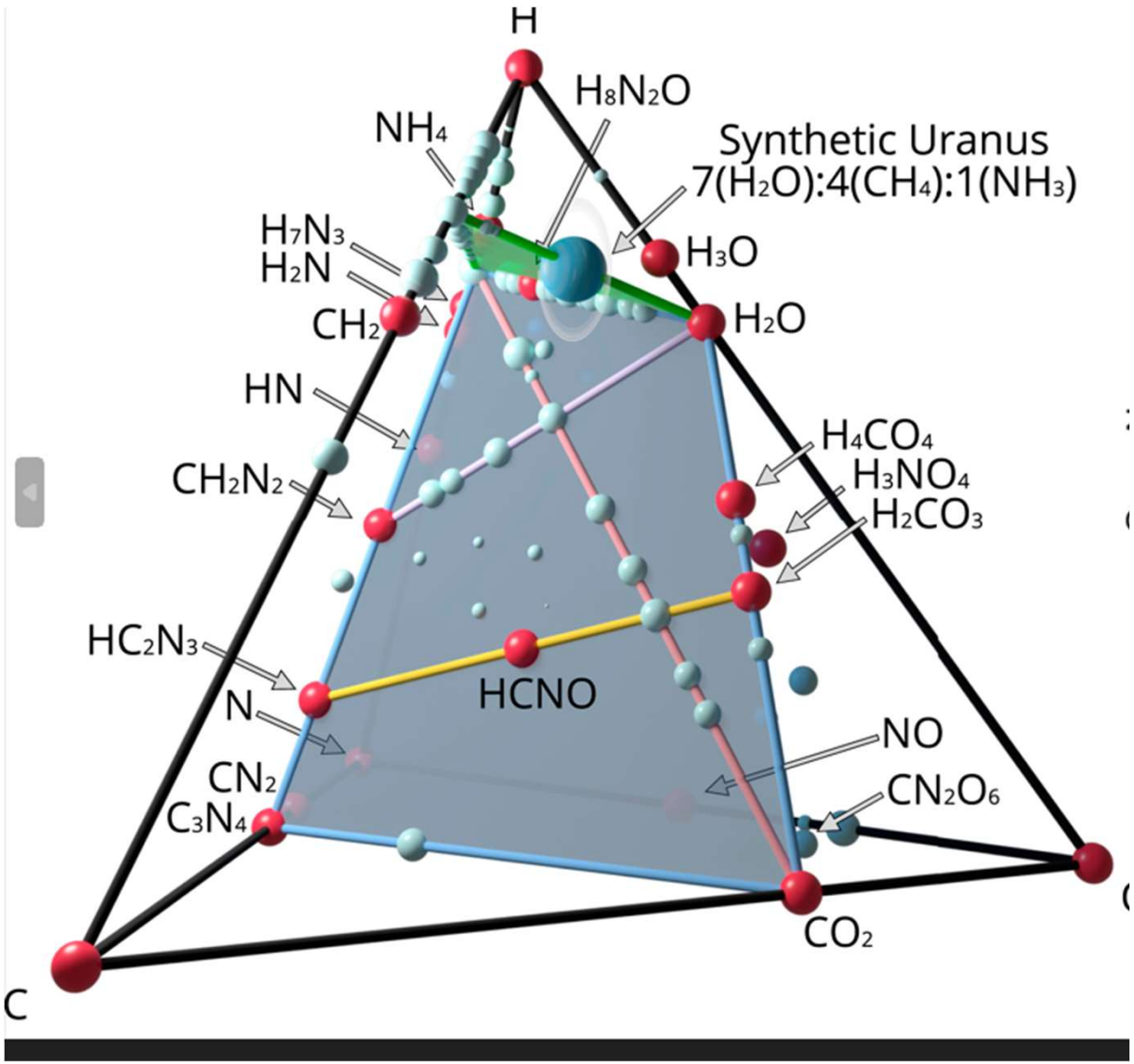

AIRSS calculations
100, 300, 700 Ga
400.000 structures

HCNO: stable
regla del octeto
Isoelectrónicos a diamante
Deficientes en hidrógeno

L. J. Conway *PNAS* 2021

The Electron Localization Function

Reconciliation of chemistry and quantum chemistry

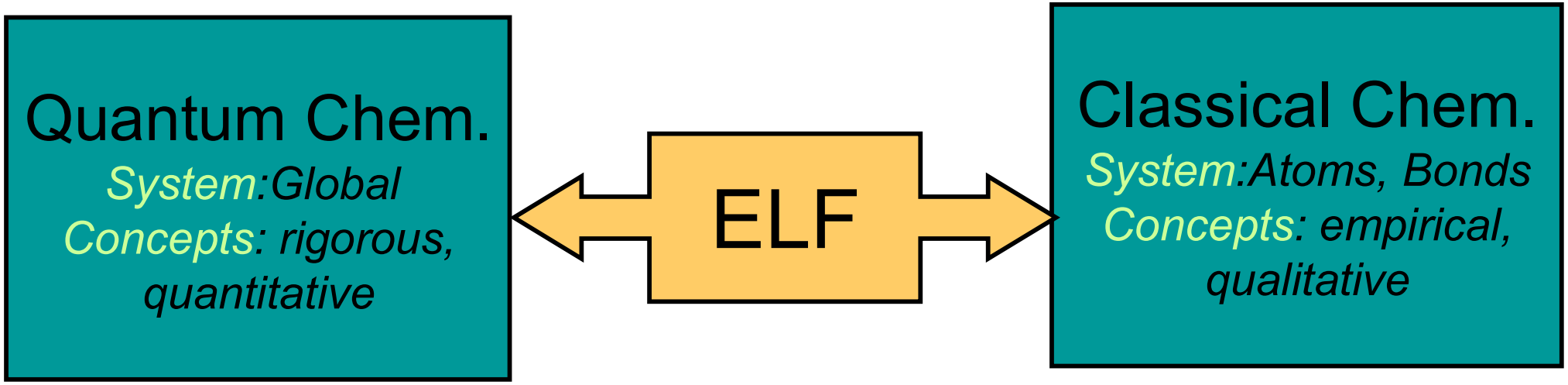

Mathematical definition of bond
Quantitative bond properties (q,v)

The Electron Localization Function

- In an attempt to better understand electron localization from a theoretical standpoint, Becke and Edgecombe developed in 1990 the electron localization function (ELF).
- It can be interpreted in terms of an excess of local kinetic energy due to the Pauli repulsion.

Pauli repulsion

$$t_P(\vec{r}) = t(\vec{r}) - \frac{1}{8}\frac{|\nabla\rho(\vec{r})|^2}{\rho(\vec{r})}$$

$$\chi(\vec{r}) = \frac{t_P(\vec{r})}{c_F\rho(\vec{r})^{5/3}} \qquad ELF = \frac{1}{1+\chi^2(\vec{r})}$$

The Electron Localization Function

What does it look like?

ELF is maximal in Lewis entities

- Bonds
- Lone pairs
- Shells

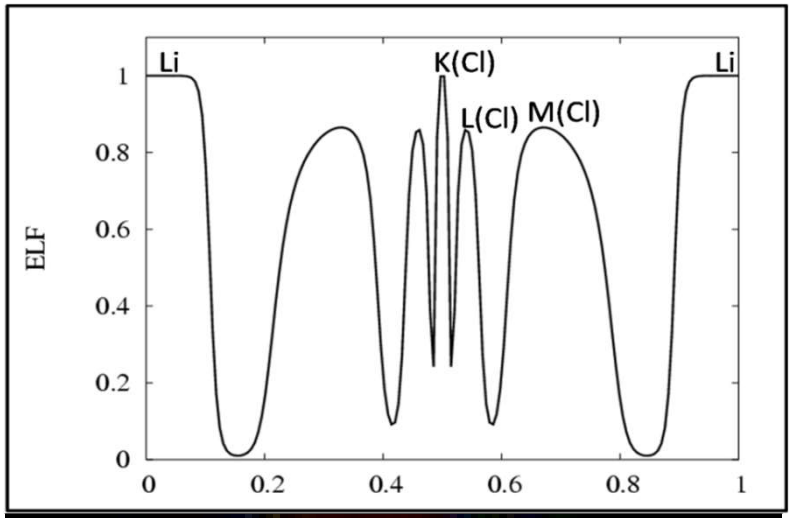

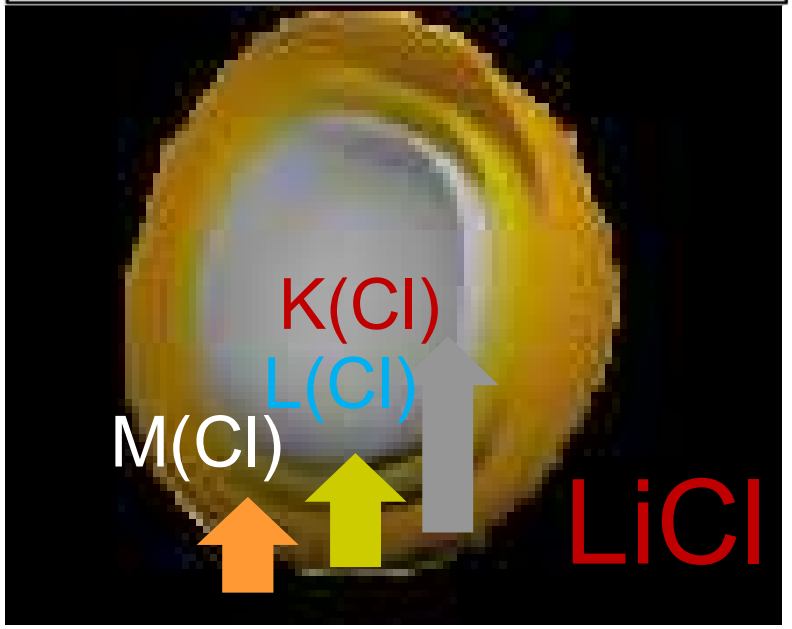

The Electron Localization Function

- Each bond, lone pair=maximum of ELF
- Each maximum has an associated region of space (basin)
  - Non overlapping
  - They fill up the volume
- Each region has its own properties, which
  - are additive
  - recover the crystal value

  E.g. volume, charge associated to a bond.

- Number, position and type of critical points (maxima, minima,etc) determine the topological features.
- The saddle point that connects two basins is called the Bond Interaction Point (*bip*).

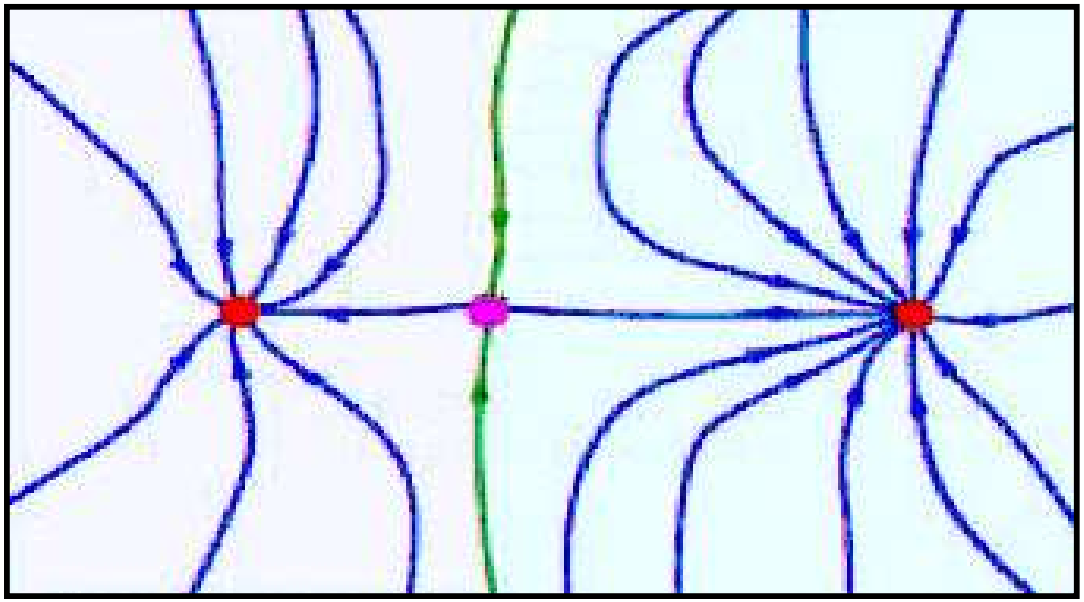

Alkali metals at HP

- It is becoming strikingly clear that the free-electron model of simple metals is not applicable when metals are compressed at intermediate pressures.

- New structures appear: open, incommensurate structures

- Unusual properties: decreased conductivity and melting points, superconductivity

- This challenging state of matter has been explained in terms of FSBZ interactions, s→p or s→d electronic transitions, and more recently related to an increase of valence electron density in interstitial regions.

Alkali metals: structural transformations under pressure

Li	bcc $\xrightarrow{7.5}$ fcc $\xrightarrow{39}$ $hR1$ $\xrightarrow{42}$ $cI16$ $\xrightarrow{60}$ $oC88$ $\xrightarrow{65}$ $oC40$ $\xrightarrow{95}$ $oC24$
Na	bcc $\xrightarrow{65}$ fcc $\xrightarrow{104}$ $cI16$ $\xrightarrow{117}$ $oP8$ $\xrightarrow{125}$ **h-g** $\xrightarrow{180}$ $hP4$
K	bcc $\xrightarrow{11.6}$ fcc $\xrightarrow{20}$ **h-g** $\xrightarrow{54}$ $oP8$ $\xrightarrow{90}$ $tI4$ $\xrightarrow{96}$ $oC16$ $\xrightarrow{25}$ $hP4$ $\xrightarrow{35}$
Rb	bcc $\xrightarrow{7}$ fcc $\xrightarrow{13}$ $oC52$ $\xrightarrow{17}$ **h-g** $\xrightarrow{20}$ $tI4$ $\xrightarrow{48}$ $oC16$
Cs	bcc $\xrightarrow{2.4}$ fcc $\xrightarrow{4.2}$ $oC84$ $\xrightarrow{4.3}$ $tI4$ $\xrightarrow{12}$ $oC16$ $\xrightarrow{72}$ dhcp

K: hP4 phase

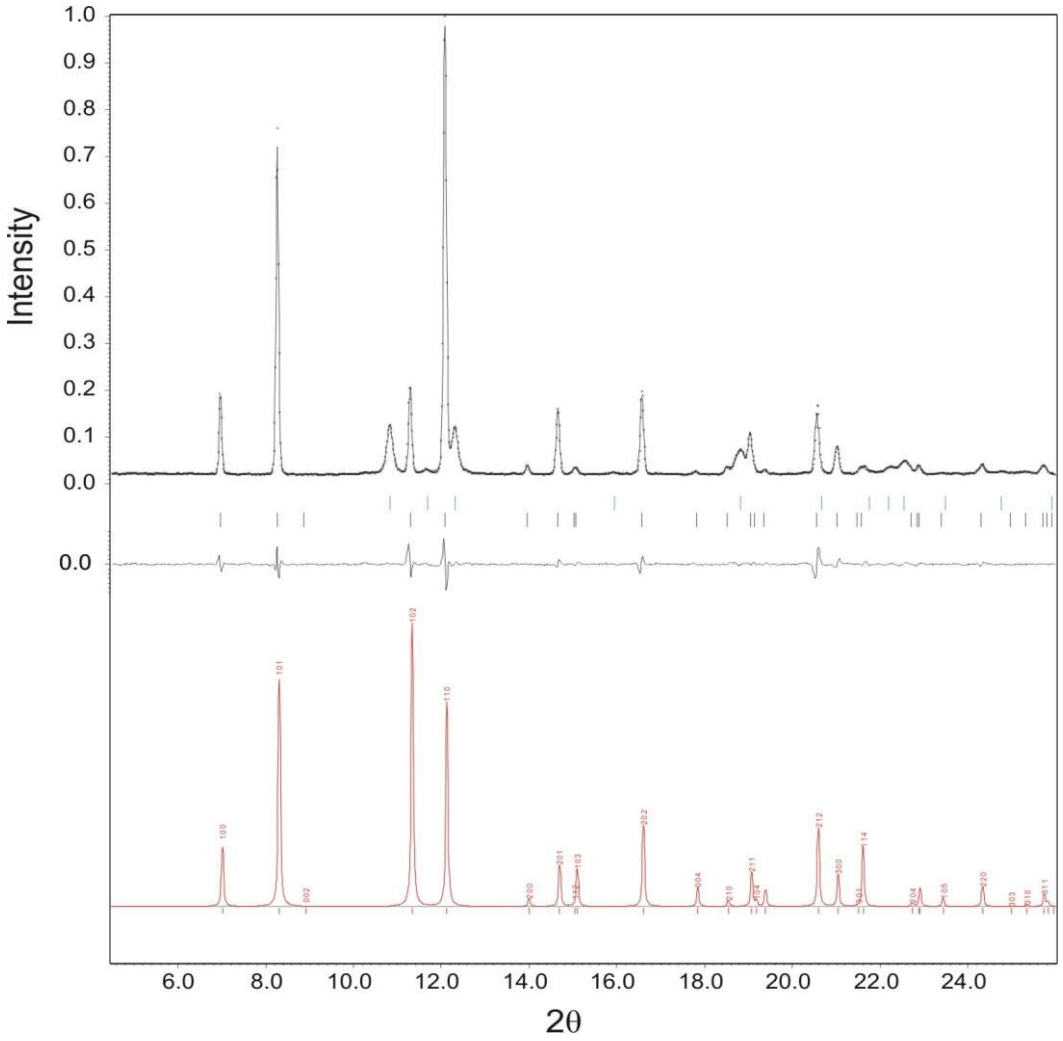

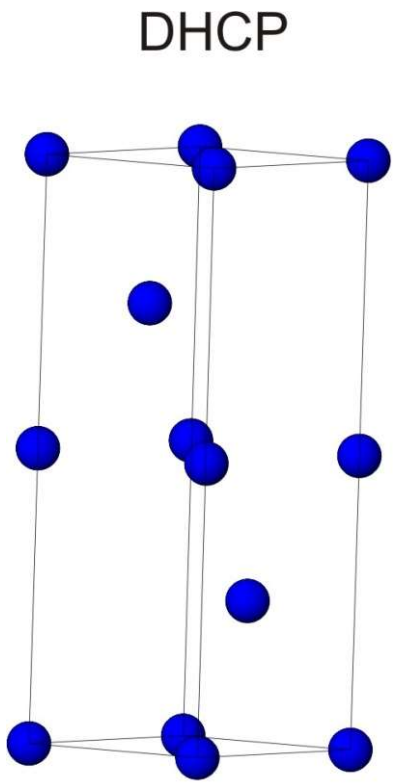

c/a=3.266

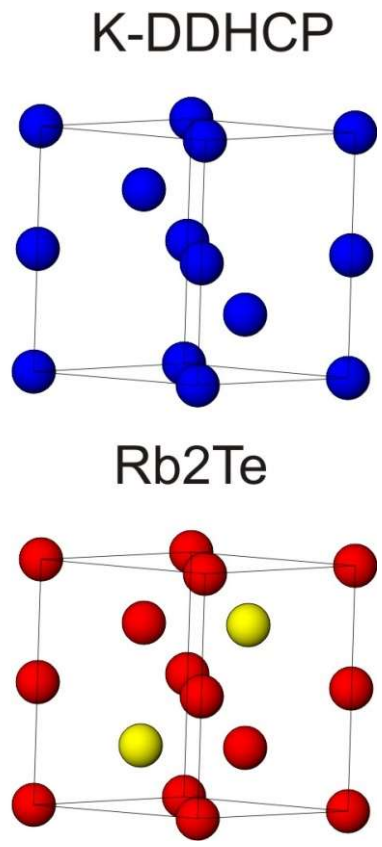

c/a=1.36

Crystal structure: hexagonal, SG $P6_3/mmc$, two different sites (Wyckoff 2*a* (0,0,0) and 2*c* (1/3,2/3,1/4))

K: hP4 phase

Localization regions in interstitial voids
Core-like topology
Same structure as A_2X compounds!
Electrons in same position as anions!
Close packing preserved if are considered!

COMPOUND→IONIC-LIKE

ELECTRONS→PSEUDOANIONS

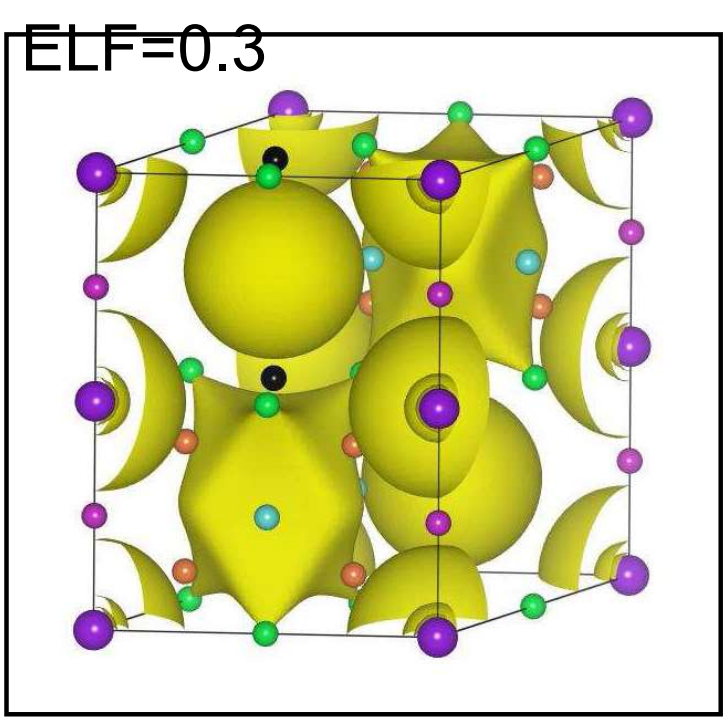

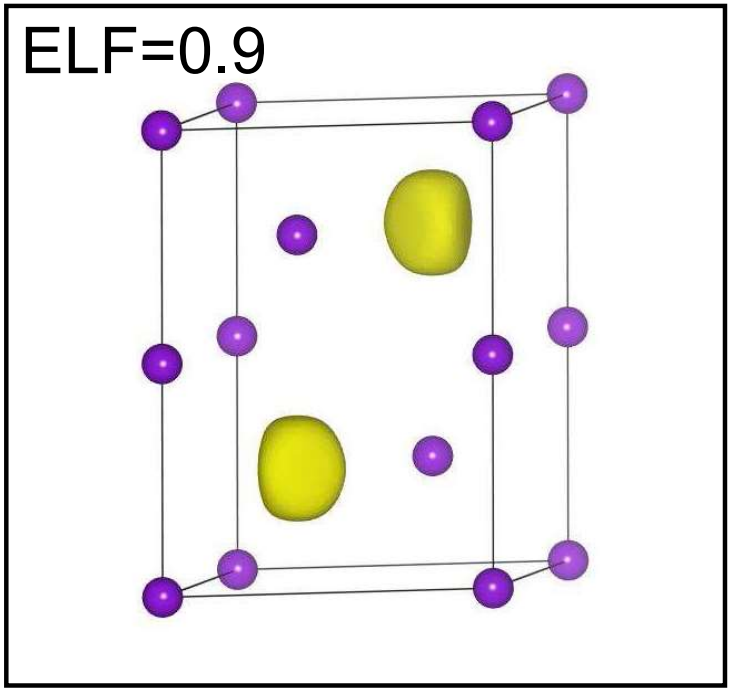

Experimental potassium at P=27 GPa

K at 58 GPa?

- tI4 structure predicted by variable-cell simulations
- behaviour of alkali-metal chalcogenides?

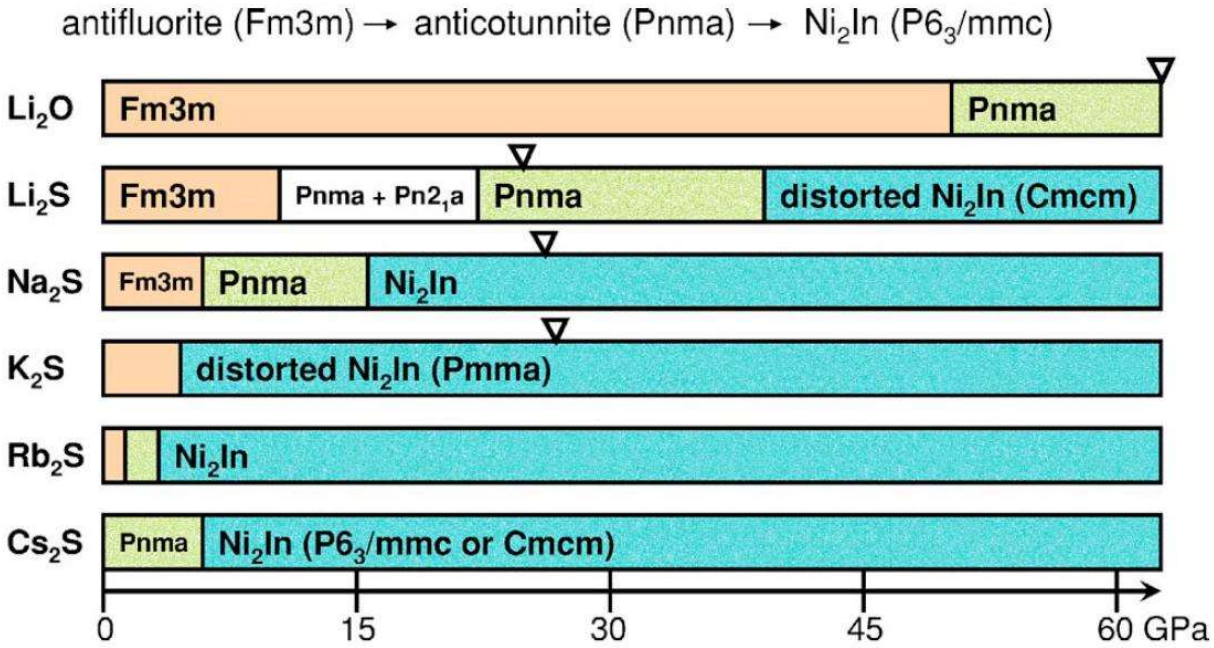

- cation sublattice of anticotunnite structure:

SG: *Pnma,* Pearson oP8, K1 and K2 atoms locate on 4*c* sites . subgroup of the Ni2In-type structure

K: oP8 phase

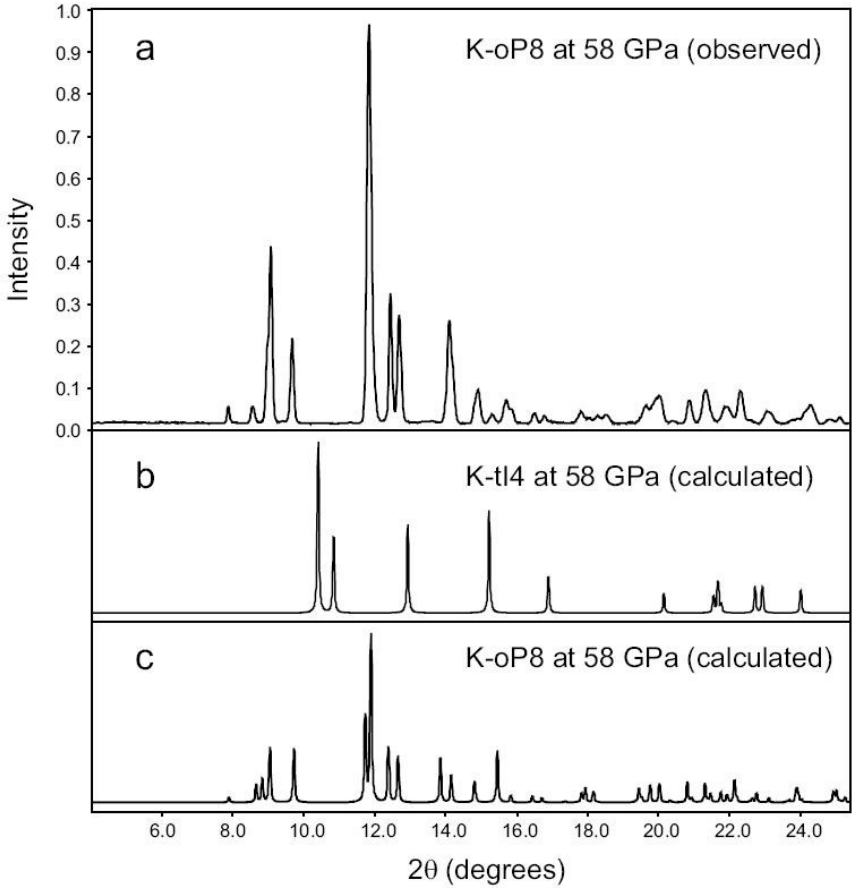

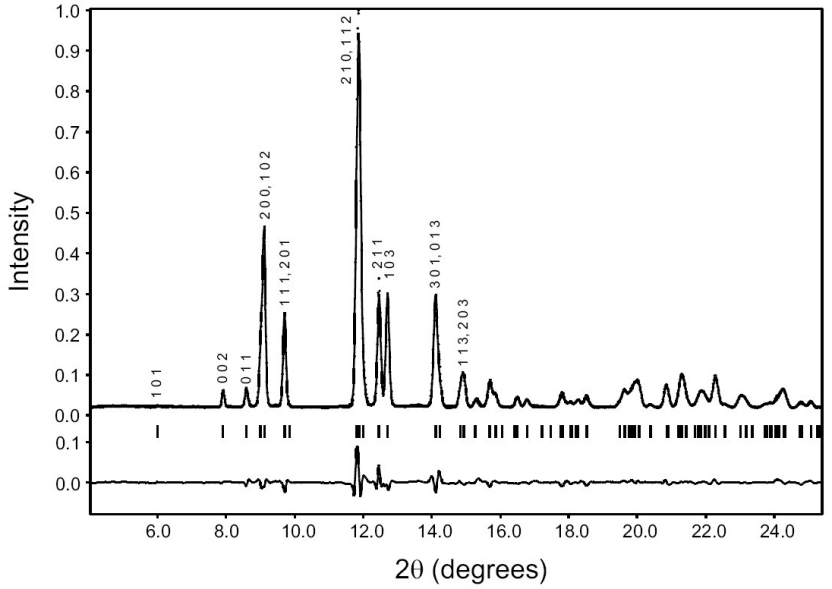

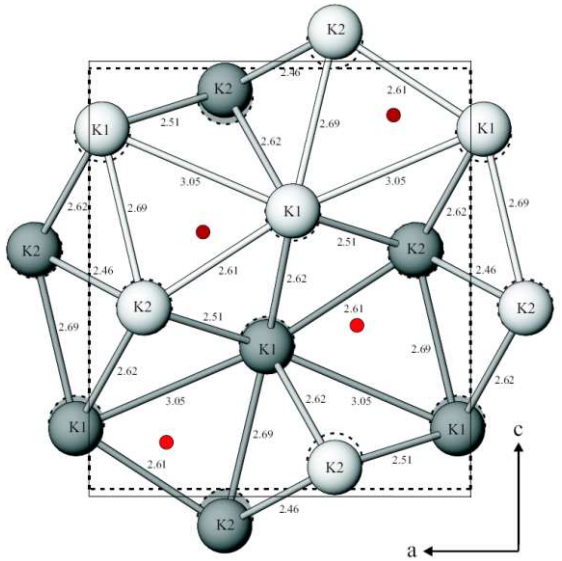

- Similar calculated oP8 and experimental diffraction pattern. Excellent Rietveld refinement.

K: electride phases

K→Alkali chalcogenide

Same structure as A_2X (Ni_2In)

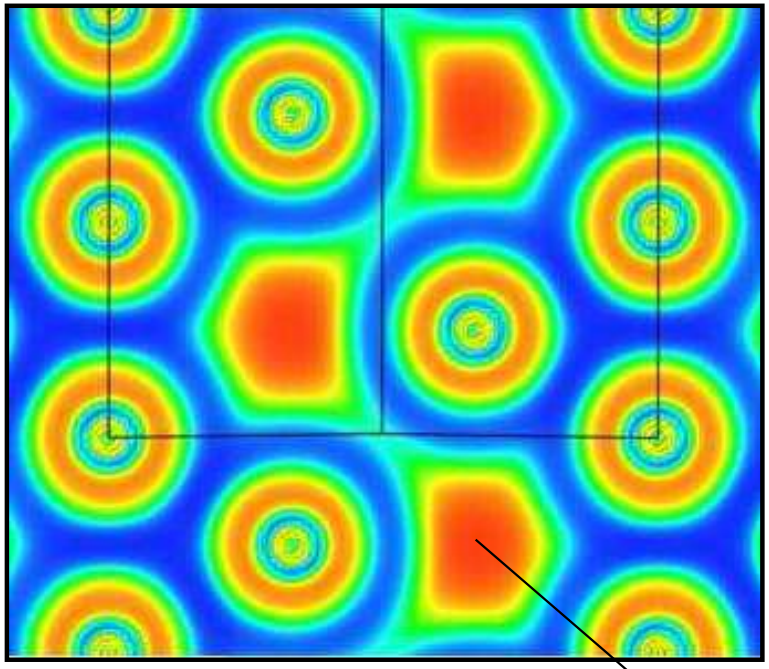

25 GPa
(ELF ≈ 0.95)
hP4 phase of K.

Chalcogenide position

Same structure as A_2X (anticotunnite)

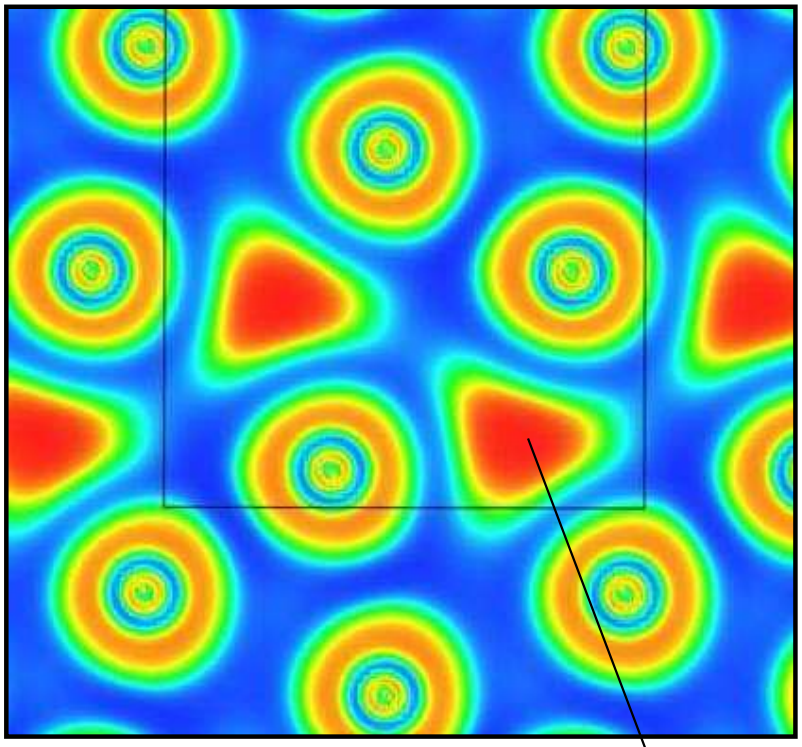

57 GPa
(ELF ≈ 0.95)
oP8 phase of K.

Chalcogenide position

K: origin of phase transitions

DRIVING FORCE OF DISTORTIONS AT INTERMEDIATE PRESSURES?
GREATER LOCALIZATION

c/a collapse
3.2→1.35

10 GPa:
Normal
metal.

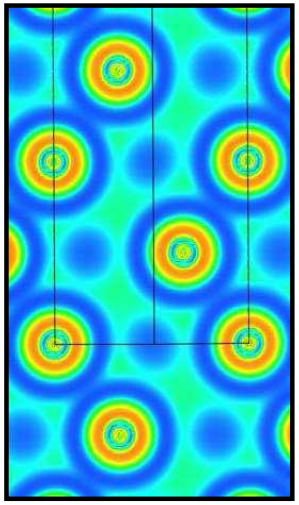

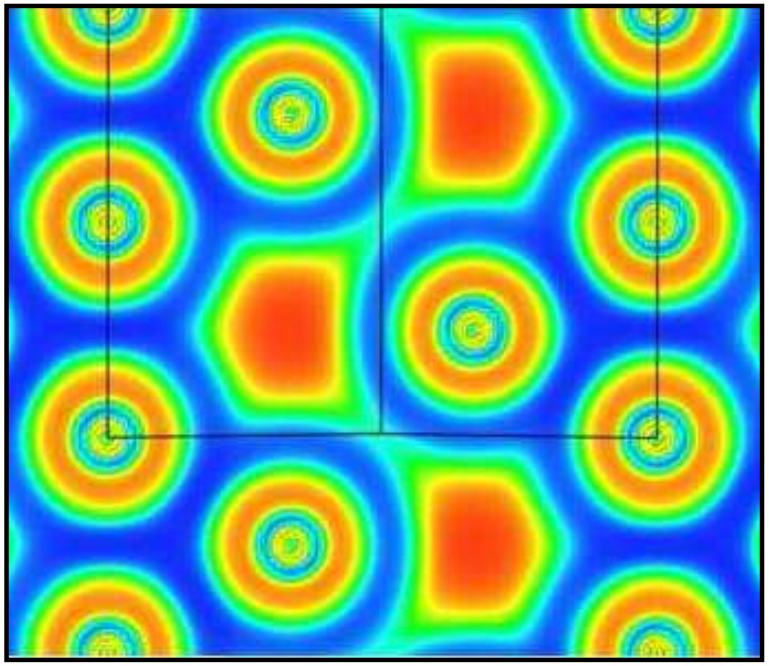

25 GPa: phase transition towards strong interstitial localization (ELF=0.95)

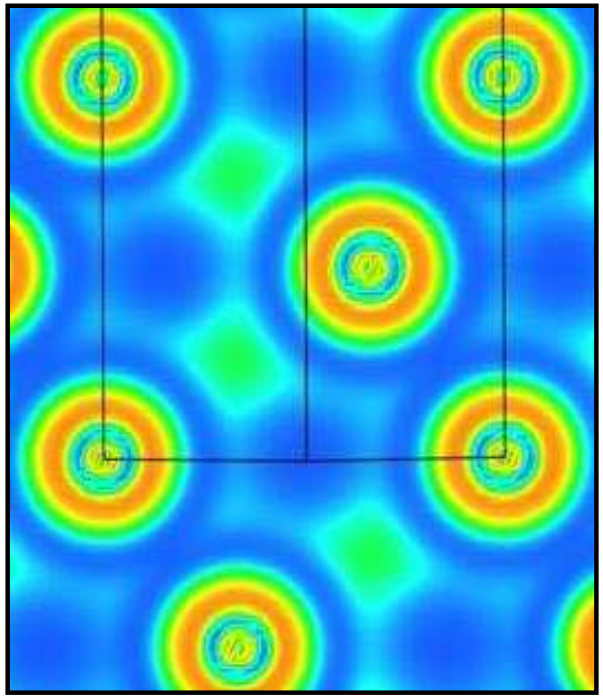

25 GPa. If no transition took place, localization would be a lot weaker

K: origin of phase transitions

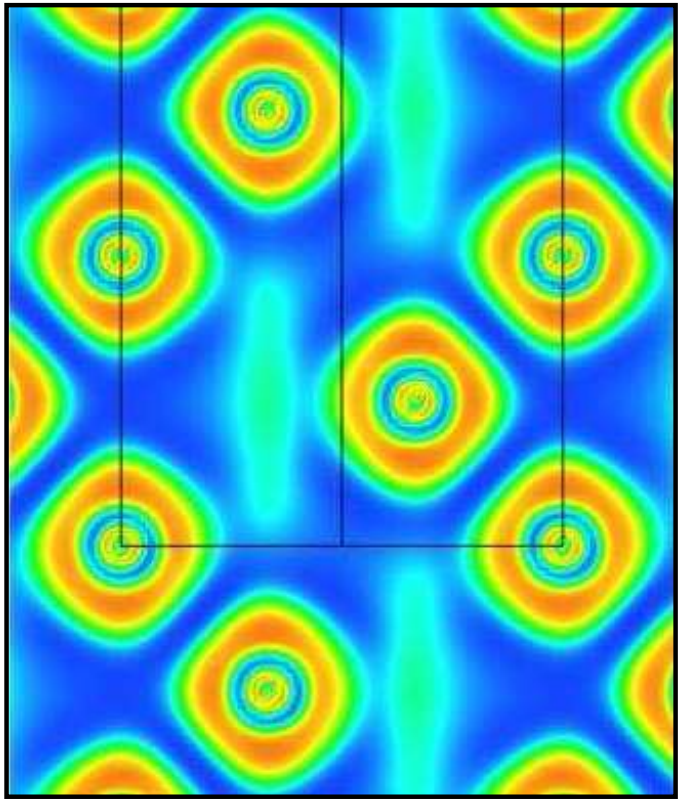

57 GPa: Elongated basins appear showing a flow of electronic localization towards other sites and instability of the phase vs distortion

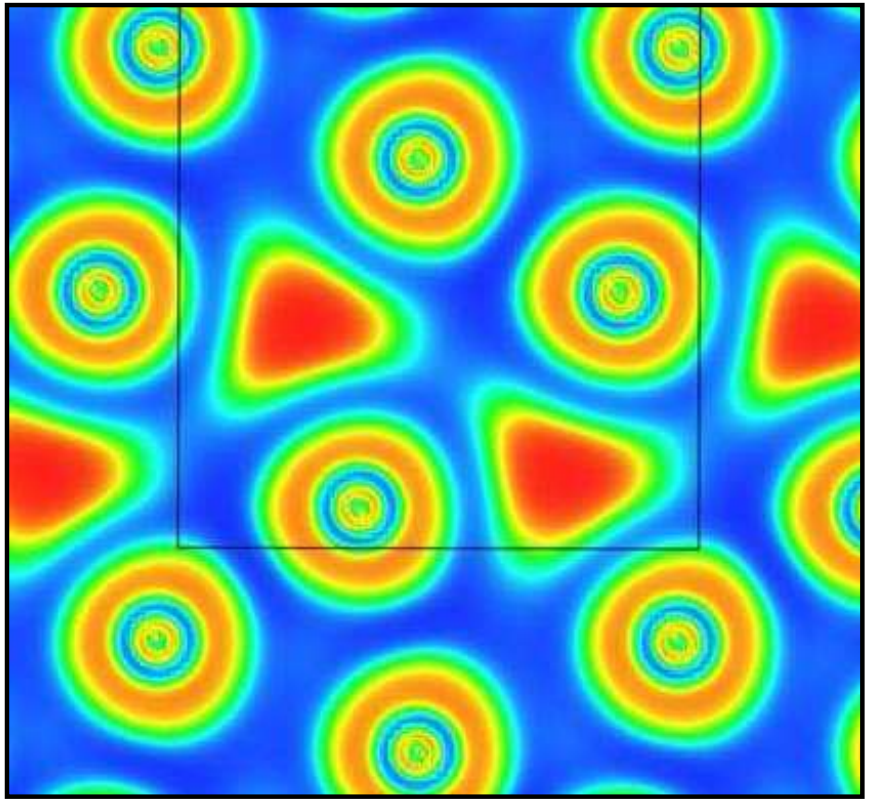

57 GPa with oP8 distortion. Distorted phase favors strong localization (ELF value close to 0.95)

oP8 distortion

K at higher pressures?

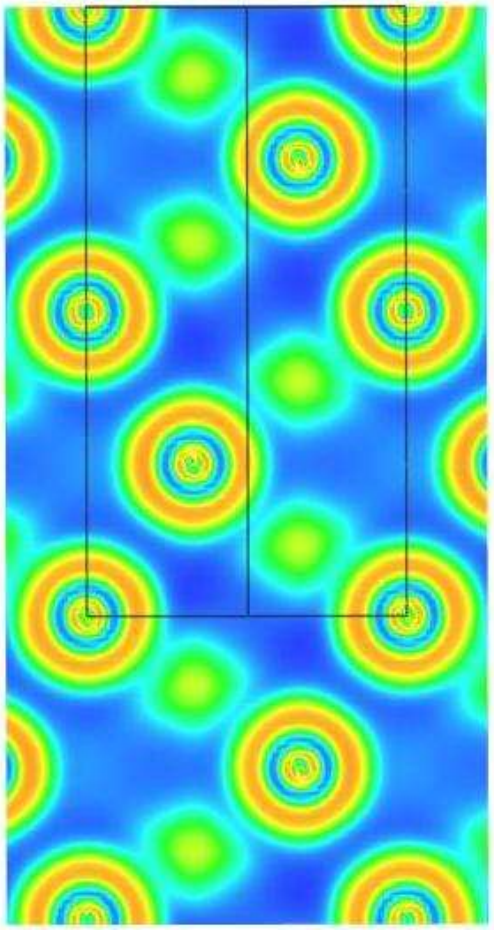

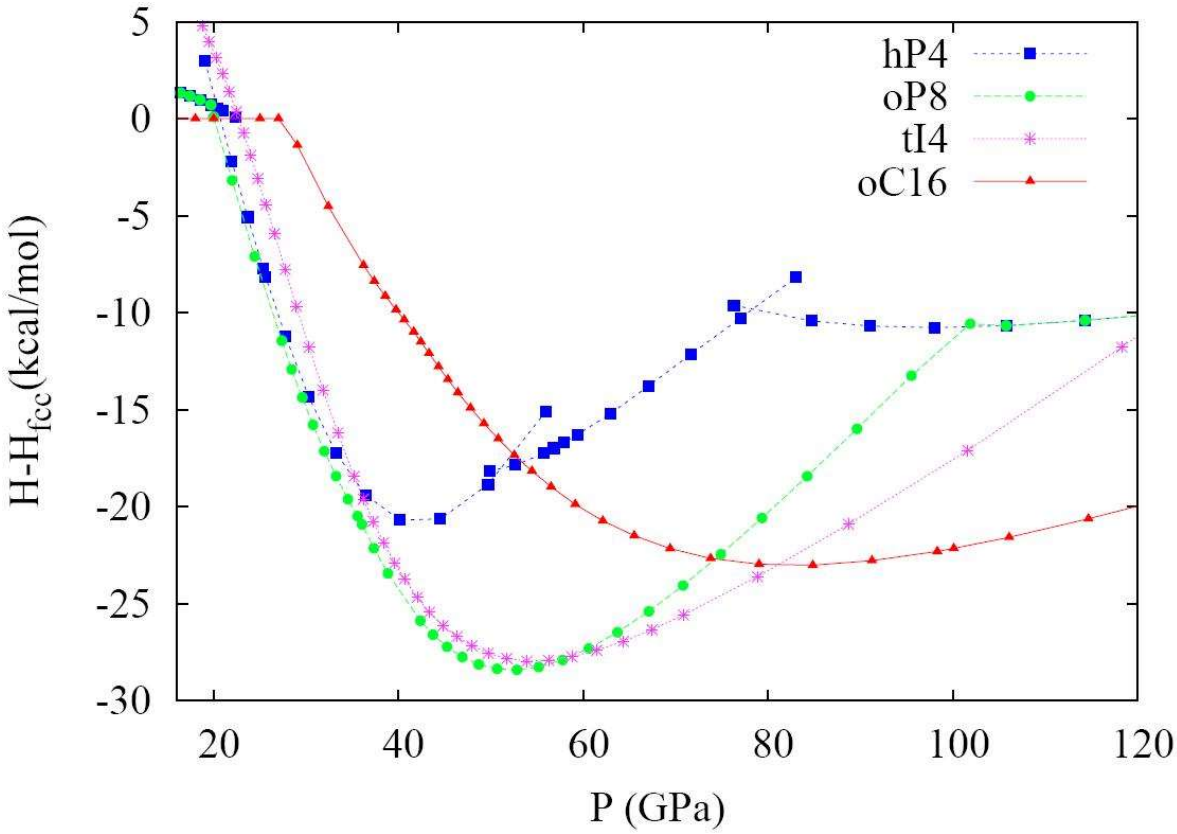

- Above 85 GPa, the electronic flow completes, metallic ELF maxima.
- Predicted transitions to tI4 and oC16 structures.
- Recovery of the dhcp arrangement above 250 GPa.

Li at high pressures

Our experiments:

- x-ray diffraction studies (P= 5-130 GPa, T=77-300K)
  - Extremely difficult: chemical reaction/Li penetration into diamonds

cI16 $\xrightarrow{60\ \text{GPa}}$ Li-VI $\xrightarrow{65\ \text{GPa}}$ Li-VII $\xrightarrow{95\ \text{GPa}}$ Li-VIII

- Structures of Li-VI, Li-VII and Li-VIII (first time observed)?
  - Proposed as oC88, oC40 and oC24.

After refinement:

- oC24 has the Cmca-24 structure proposed previously.
- oC40: cell parameters and Cmca space group
- oC88: cell parameters and Cmma space group. oC92?

*oC*40 Li

Our calculations:

- AIRSS approach (random structure searching + DFT calculations)

❖ CASTEP code, PBE PP, cutoff energy: 350 eV……..

❖ Stringent reoptimization of the lowest-enthalpy structures

*oC*40 structure:

❖ 20-atom primitive cells, initial expt. lattice parameters

❖ Using the experimental symmetry as a constraint

❖ Searches within *P21/c* (subgroup of *Cmca*), *Pc*, randomly-selected space groups with 4 and 2 symmetry operations and no symmetry (*P1*).

*o*C40 Li

Initial structures

Lowest enthalpy structure

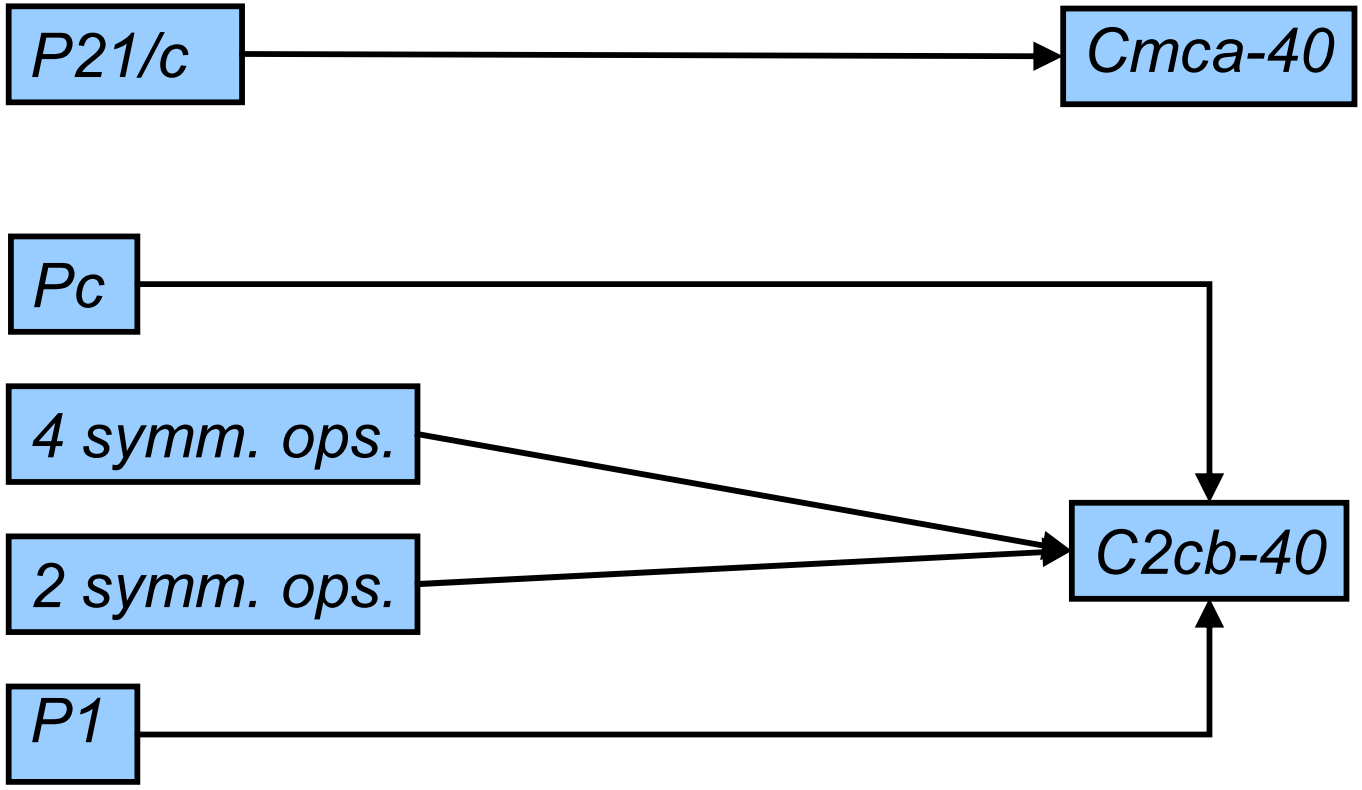

- C2cb-40 struct. is a subgroup of Cmca-40 struct.

*oC*40 Li

From H-P curves:

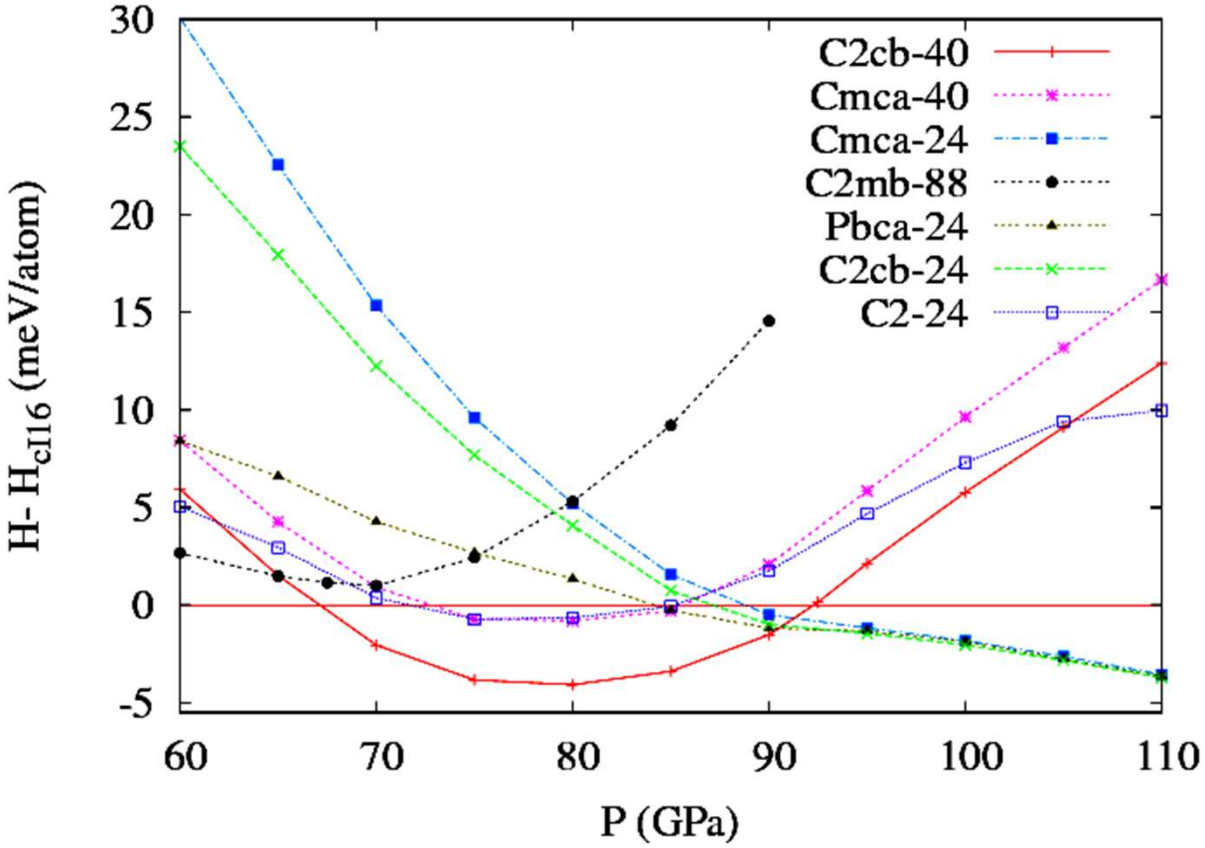

C2cb-40 is the most stable phase between 67-90.5 GPa.

Hypothetically:

C2cb-40 $\xrightarrow{91\text{GPa}}$ *Cmca*-24

- *C2cb*-40 $\xrightarrow{90.5\text{ GPa}}$ *Pbca*-24 $\xrightarrow{94\text{ GPa}}$ *C2cb*-24 $\xrightarrow{110\text{GPa}}$ *Cmca*-24

*oC*40 Li

Dynamical stability?

- Phonon calculations with the Quantum-ESPRESSO code.
- Imaginary frequency for a B_{3u} mode of the *Cmca*-40 struct.

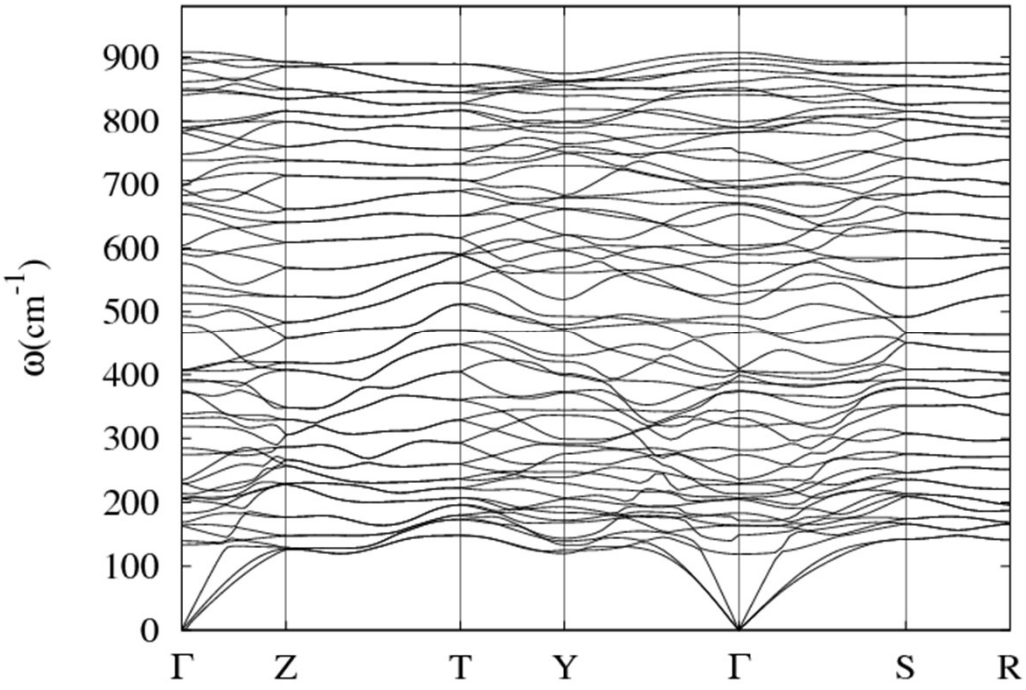

Phonon dispersion curves of the *C2cb*-40 structure: dynamically stable

*o*C40 Li

Semiconductor?

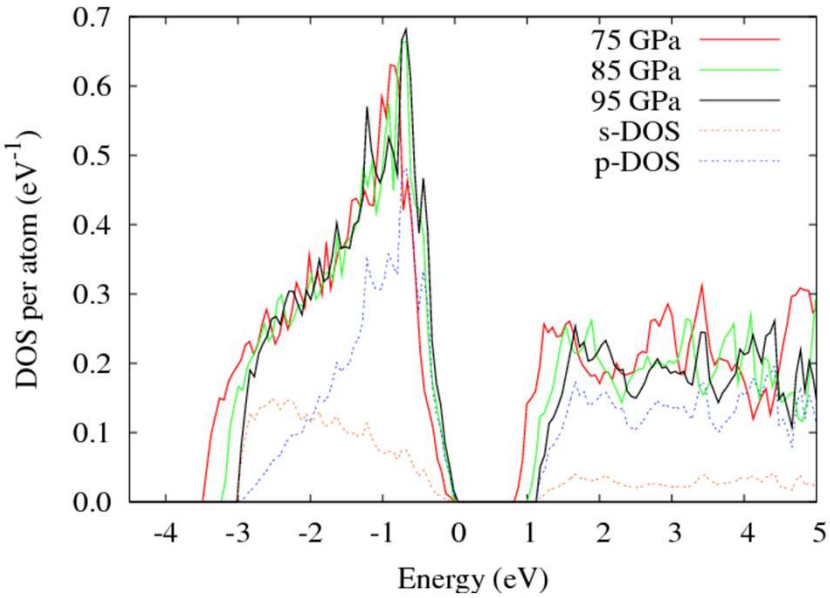

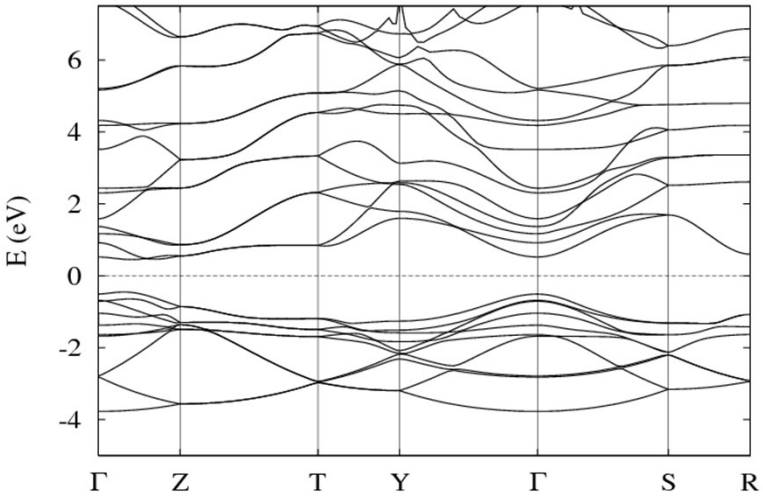

- Indirect band gap along ΓZ similar to the Γ-direct band gap
- Gap increases with pressure, 1.15 eV at 95 GPa
- Larger gap than the other structures (0.276 eV for the *C*2-24)

*o*C40 Li

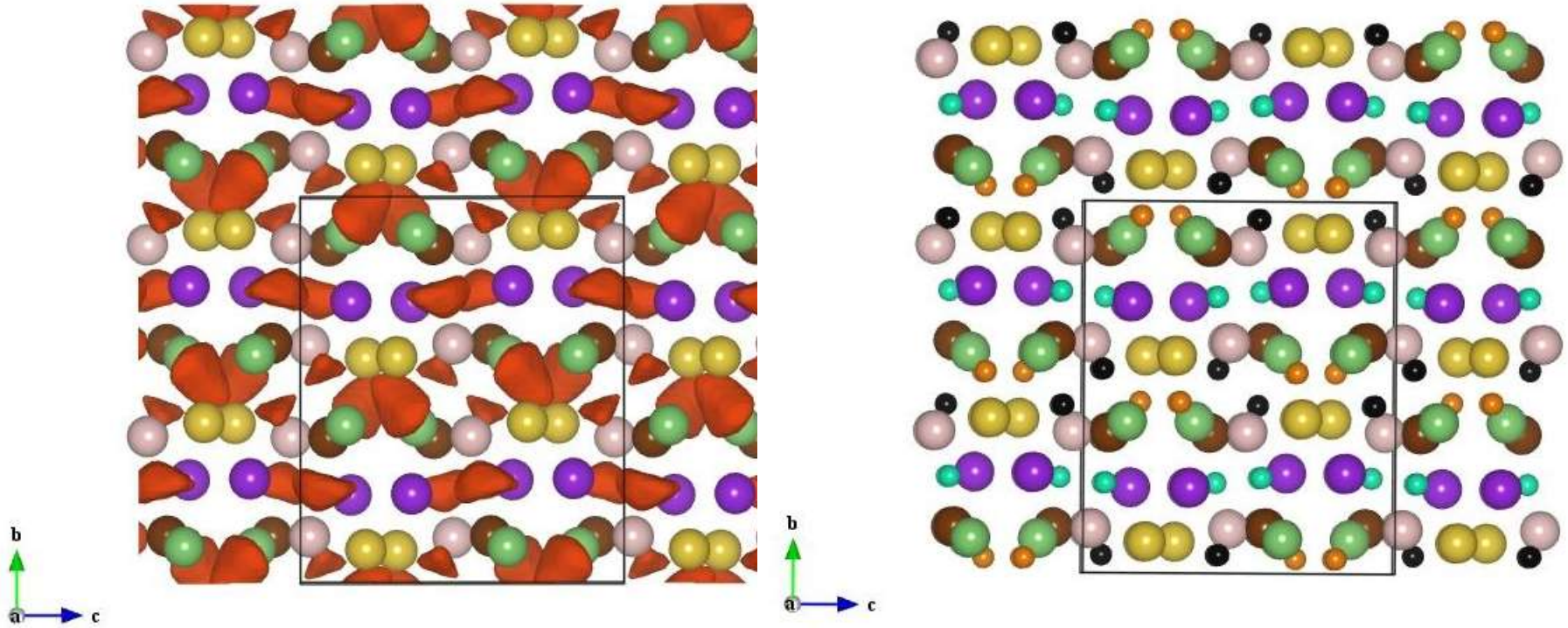

- Modulated layers. 5 neq. Li atoms, 3 ELF attractors.
- M1: 2 e^-_s, M2: 2 e^-_s, M3: 1e^- → Li_5ABC.
- New elemental structure, not found previously.

*o*C88 Li

*o*C88 structure

- 44-atom primitive cells, initial expt. lattice parameters.
- Searches within the *P2/c, Pc, C2* space groups and randomly selected space groups with 2 symmetry ops.
- Additional searches in oC92 and oC84 structures

Lowest enthalpy structure: *C2mb* space group.

- More stable than the rest of the phases (except *cI*16) in its experimental range of existence
- Stabilized by dynamical effects? Metastable?
- Reasonable agreement with diffraction data

*o*C88 Li

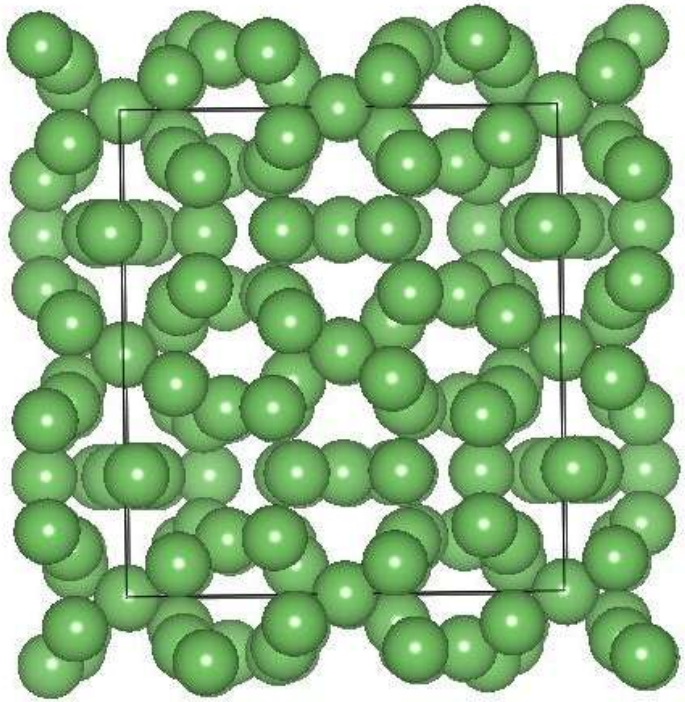

- Complicated structure.
- low DOS at E_{FERMI}, but no band gap.

Vibrational effects on Li

Raman

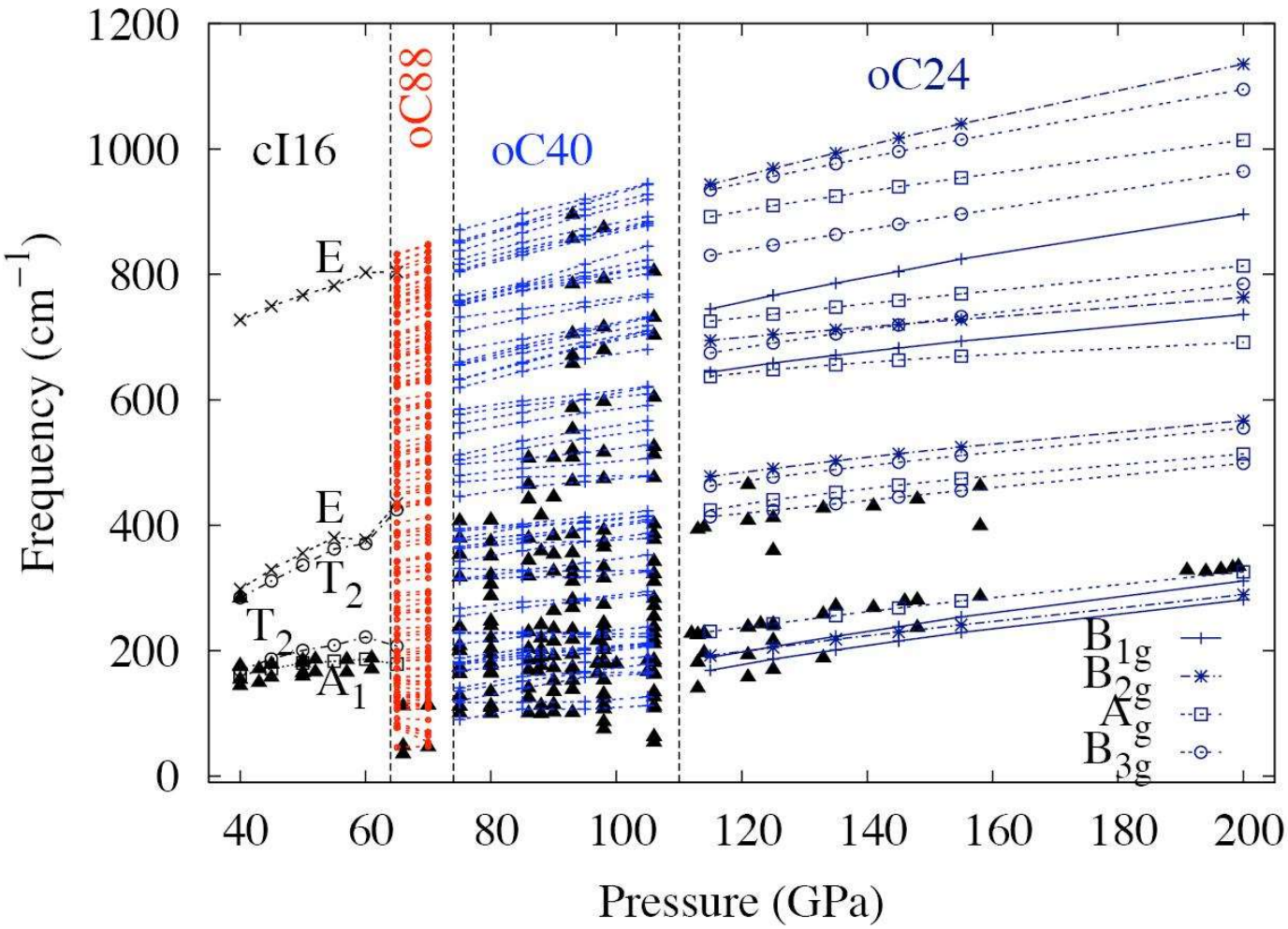

- Very low frequency modes in oC88.
- Intense and rich spectrum in oC40 and intense mode in oC24.

Vibrational effects on Li

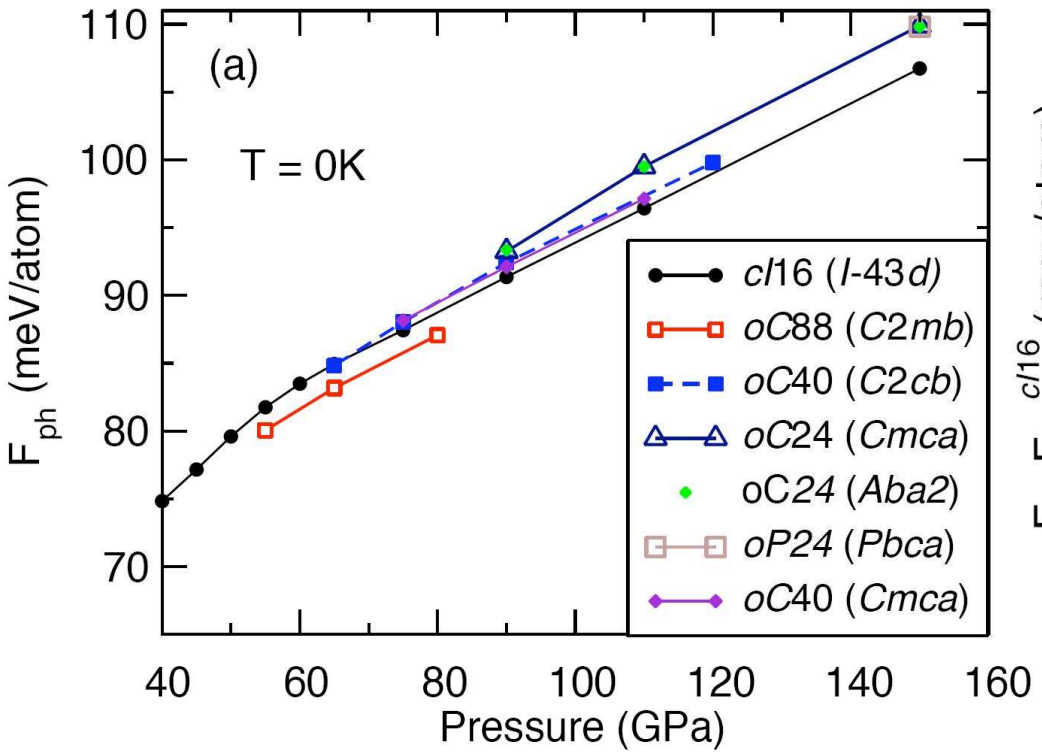

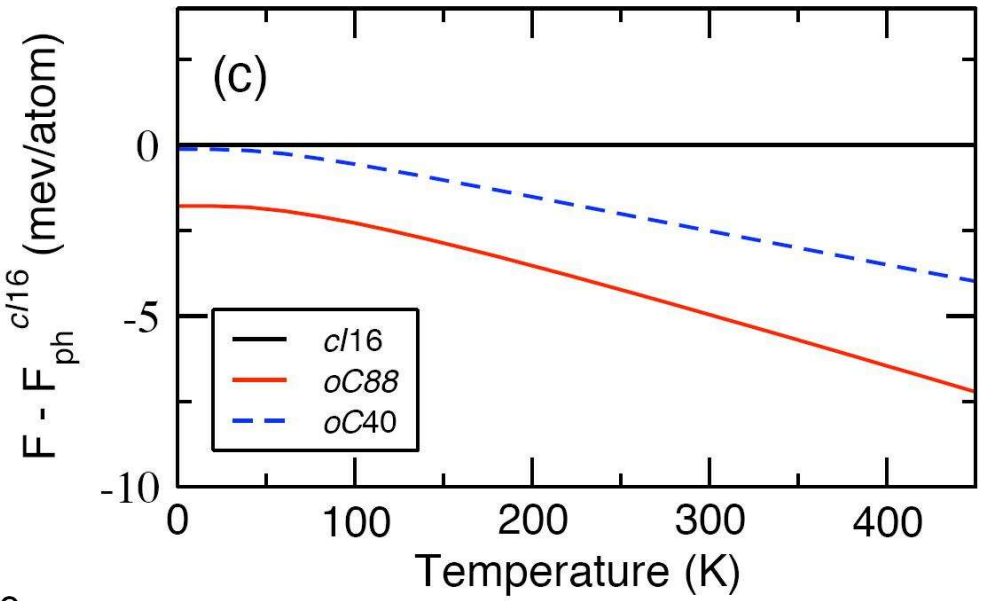

- Gibbs free energies calculated using QHA approx.
- $G = U + PV + k_B T \int g(\omega) \ln[2\sinh(\hbar\omega/2k_B T)] d\omega$.

Vibrational effects on Li

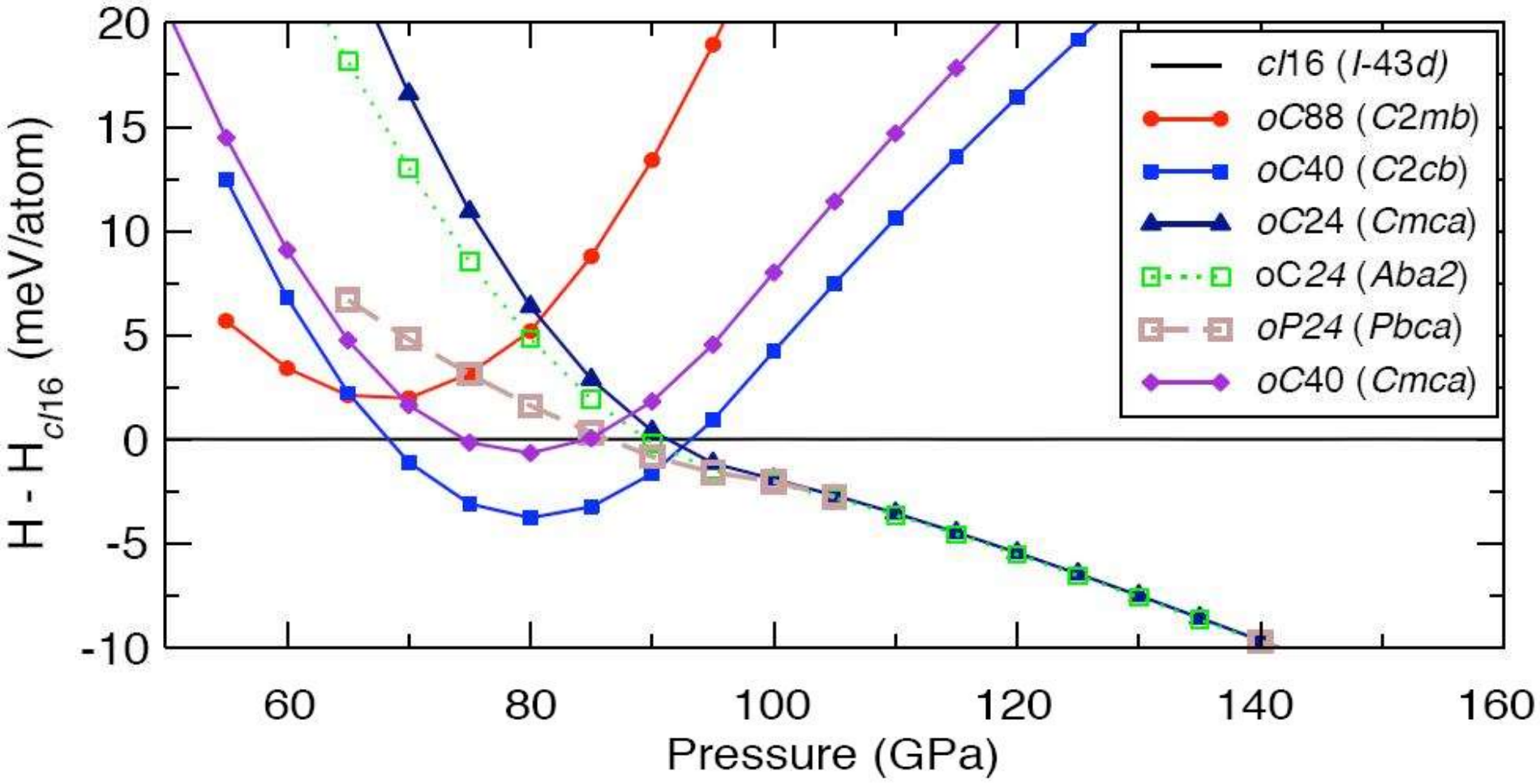

Neglecting ZPE at OK

Vibrational effects on Li

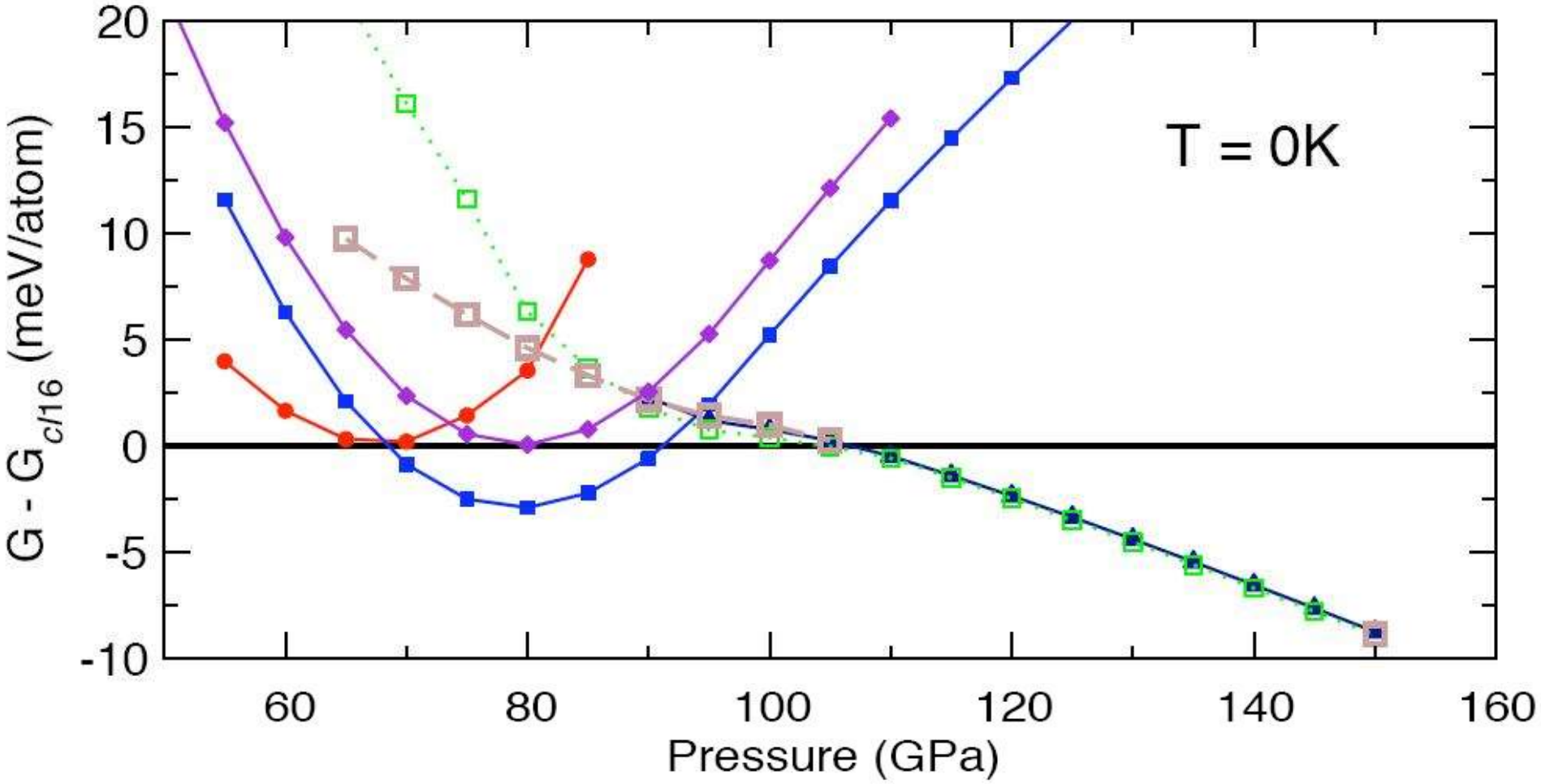

With ZPE at OK

Vibrational effects on Li

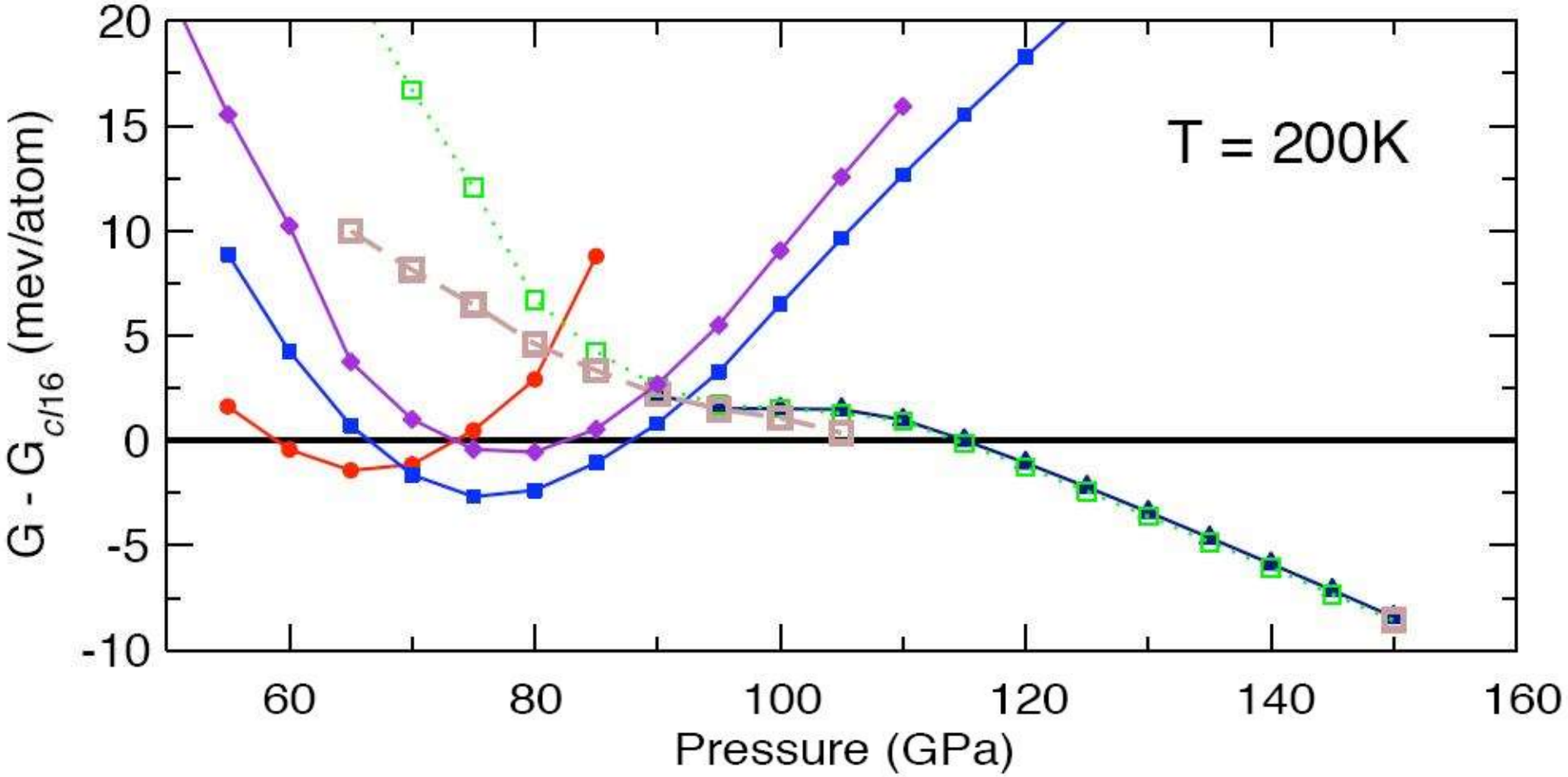

oC88 becomes stable at finite T

Incommensurate structures

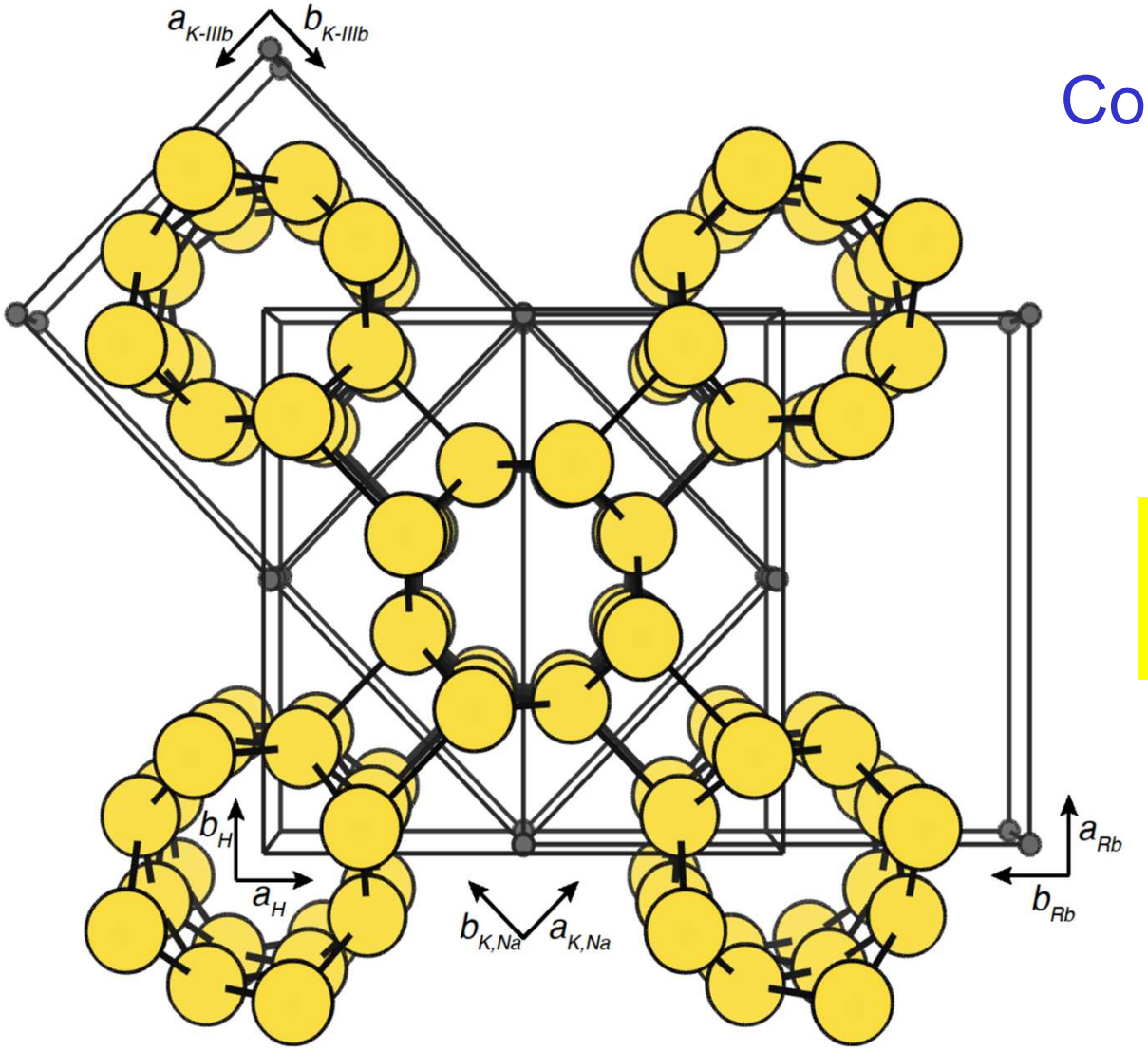

Common host structure

Tetragonal *I4/mcm*
16 atoms

Incommensurate structures

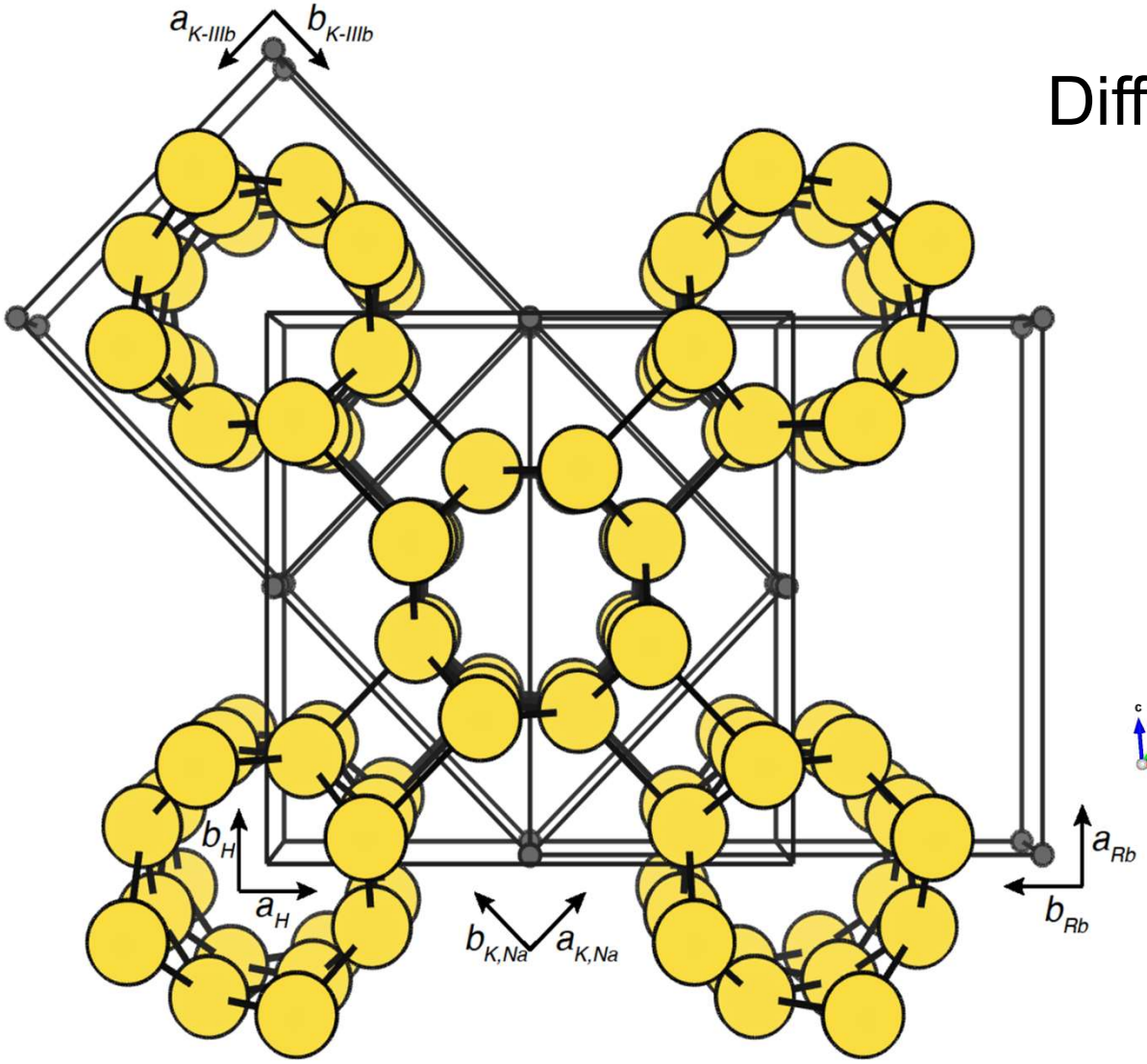

Different guest structures

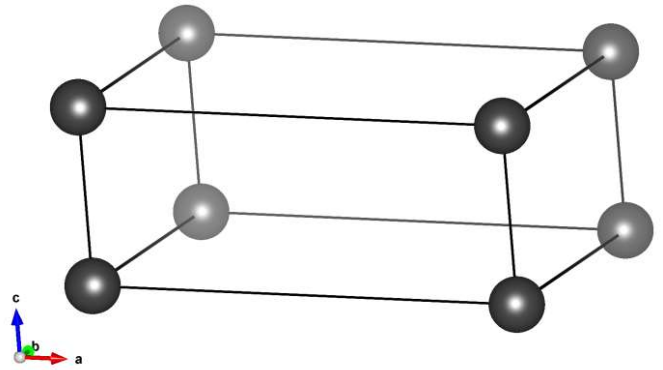

Na-V: *P2/m*, 1a (0,0,0)

$a_{guest} \sim b_{guest} = a_{host}/\sqrt{2}$

β=94.7, c_{host}/c_{guest}=1.66

(at 147 GPa)

Incommensurate structures

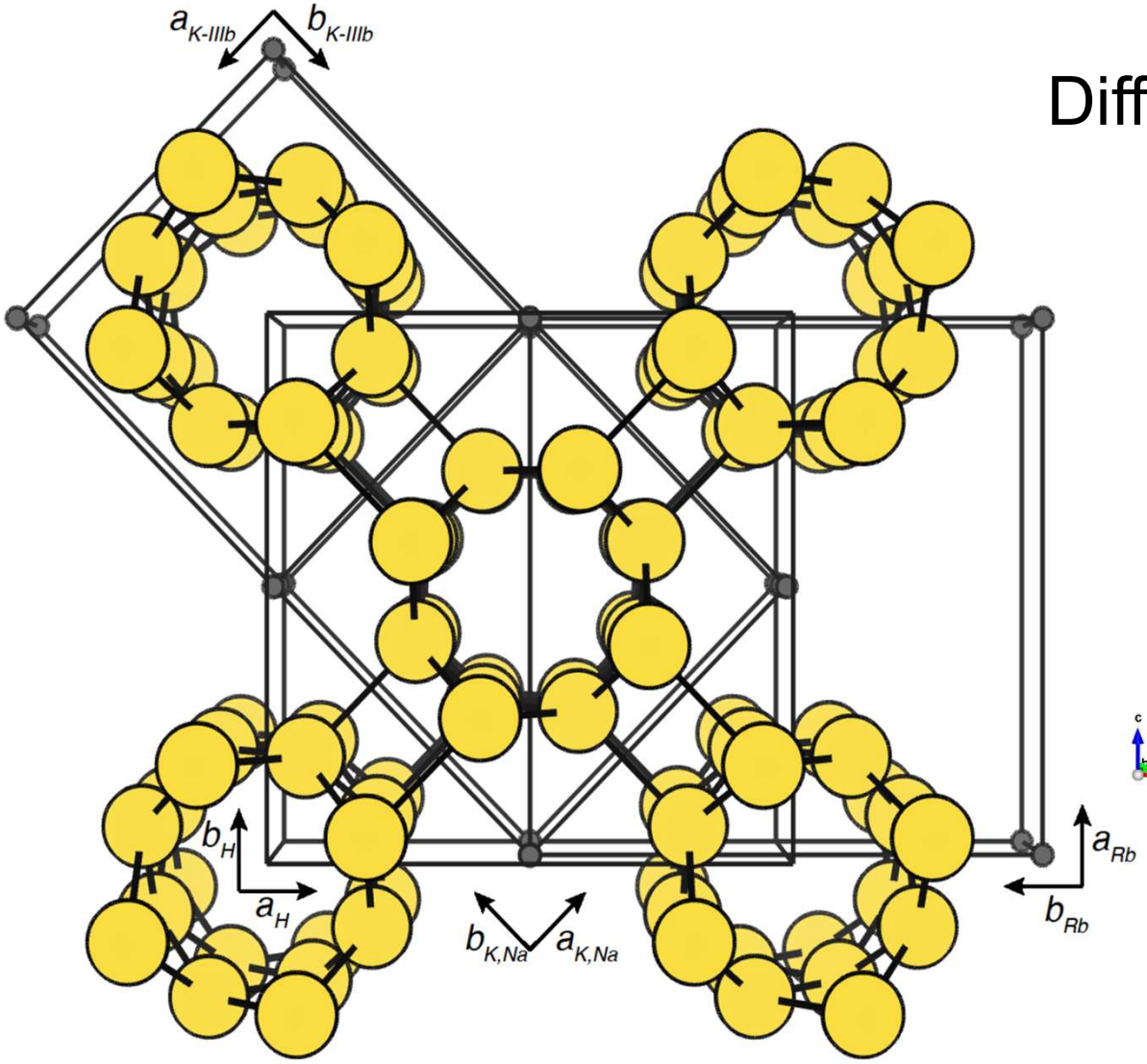

Different guest structures

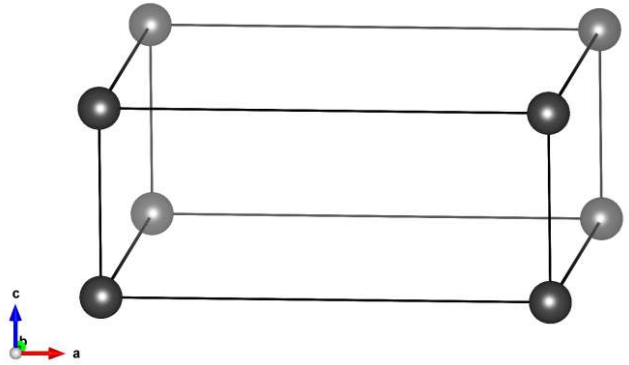

K-IIIa: *P4/mmm,* 1a (0,0,0)

$a_{guest} = b_{guest} = a_{host}/\sqrt{2}$

$c_{host}/_{guest} = 1.6\text{-}1.66$

Incommensurate structures

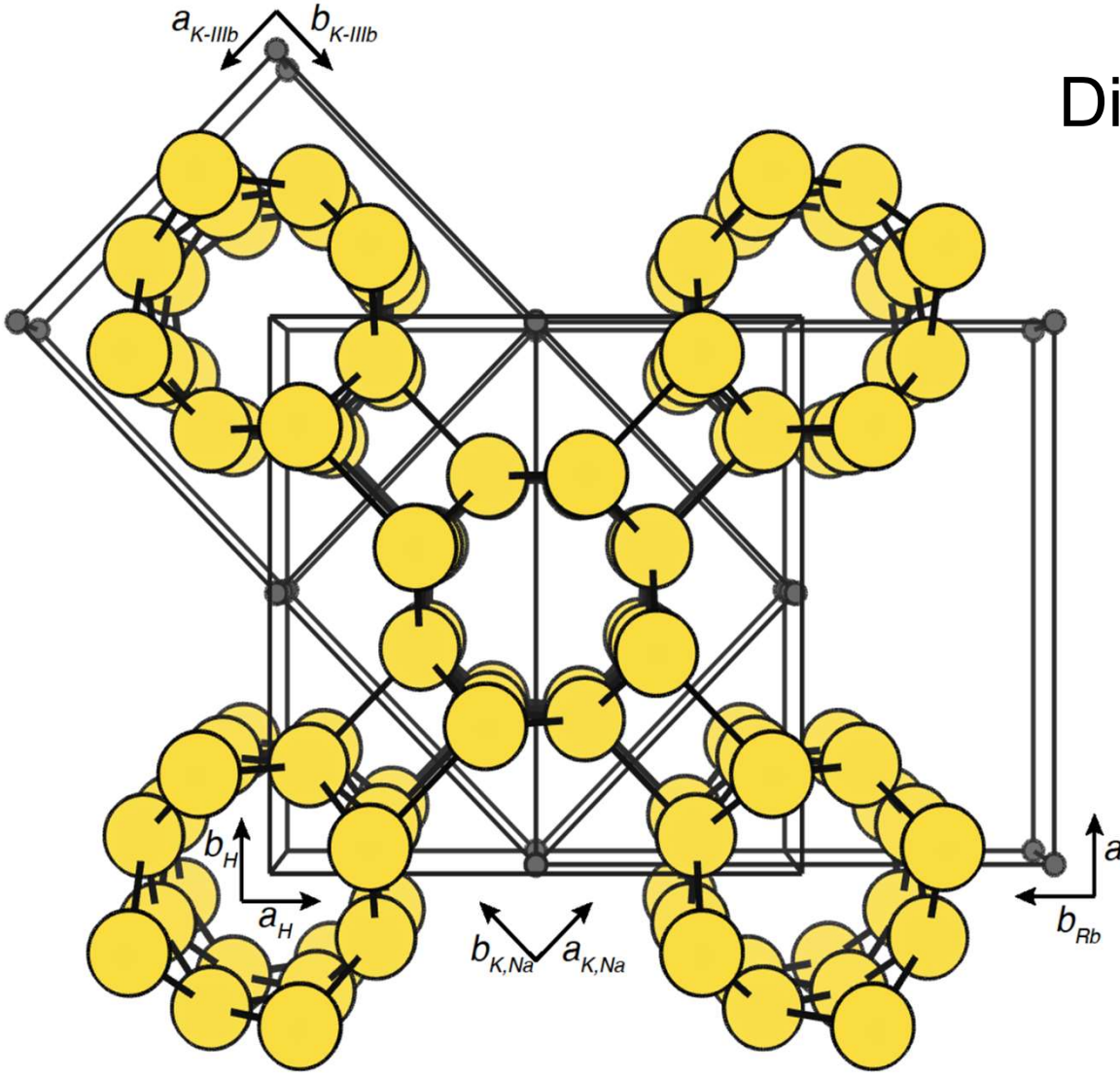

Different guest structures

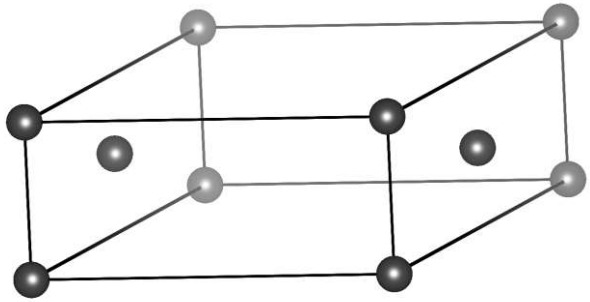

K-IIIb: A*mmm*, 2a (0,0,0)

$a_{guest} = a_{host}/\sqrt{2}$

$b_{guest} = \sqrt{2} b_{host}$

$c_{host}/c_{guest} = 1.58\text{-}1.60$

Incommensurate structures

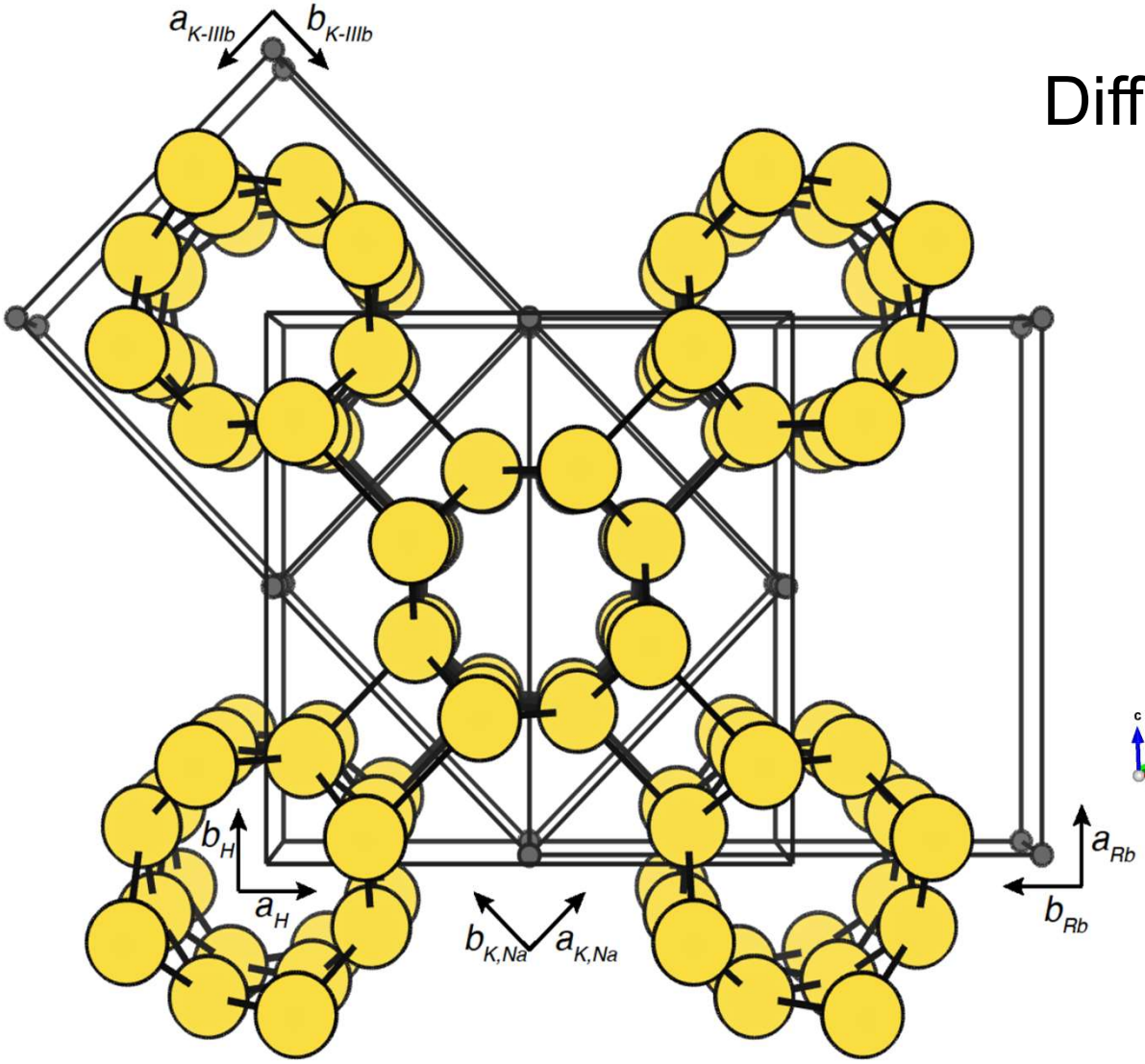

Different guest structures

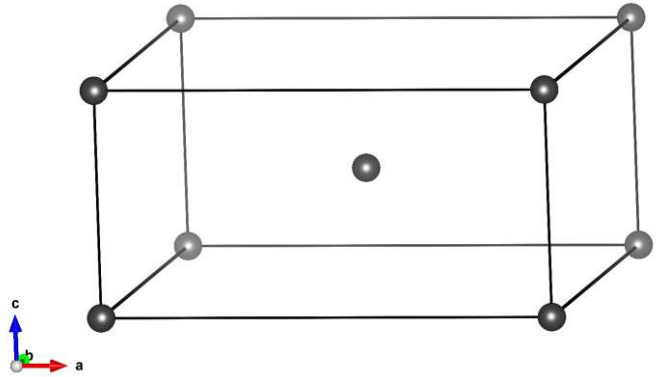

Rb-IV: I4/*mmm*, 2a (0,0,0)

$a_{guest} = a_{host}$

$c_{host}/_{guest} = 1.631$

Computational approach

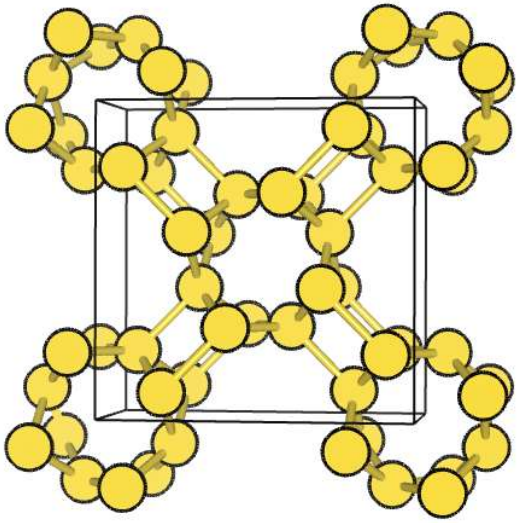

Empty tI19 host lattice

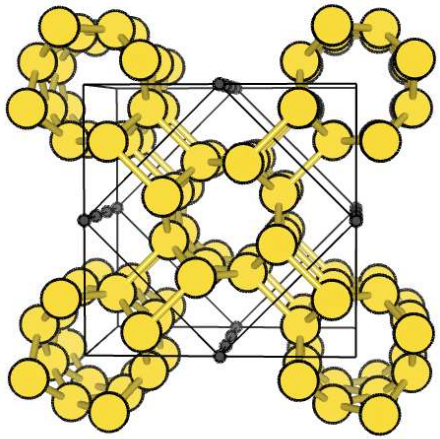

3g/2h approx.

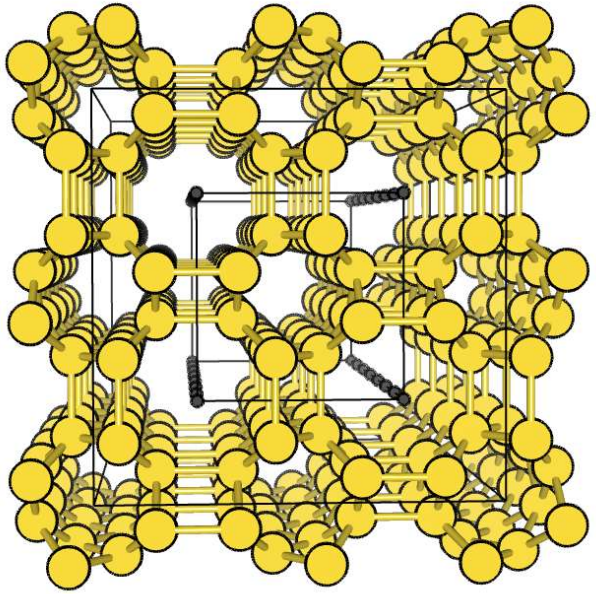

7g/4h approx ($\sqrt{2}\sqrt{2}$)

- c_H/c_G chosen to cover the respective experimental range
- 4g/3h (56 atoms), 3g/2h (38 atoms), 8g/5h (96 atoms), 5g/3h (58 atoms), 7g/4h (78 atoms), 9g/5h (98 atoms), 2g/1h (20 atoms)
- Unit cells for K-IIIb are twice as large
- c_H/c_G: 1.3333, 1.5, 1.6, 1.6666, 1.75, 1.8, 2
- Na-V approximants with tetragonal guest lattices

Potassium

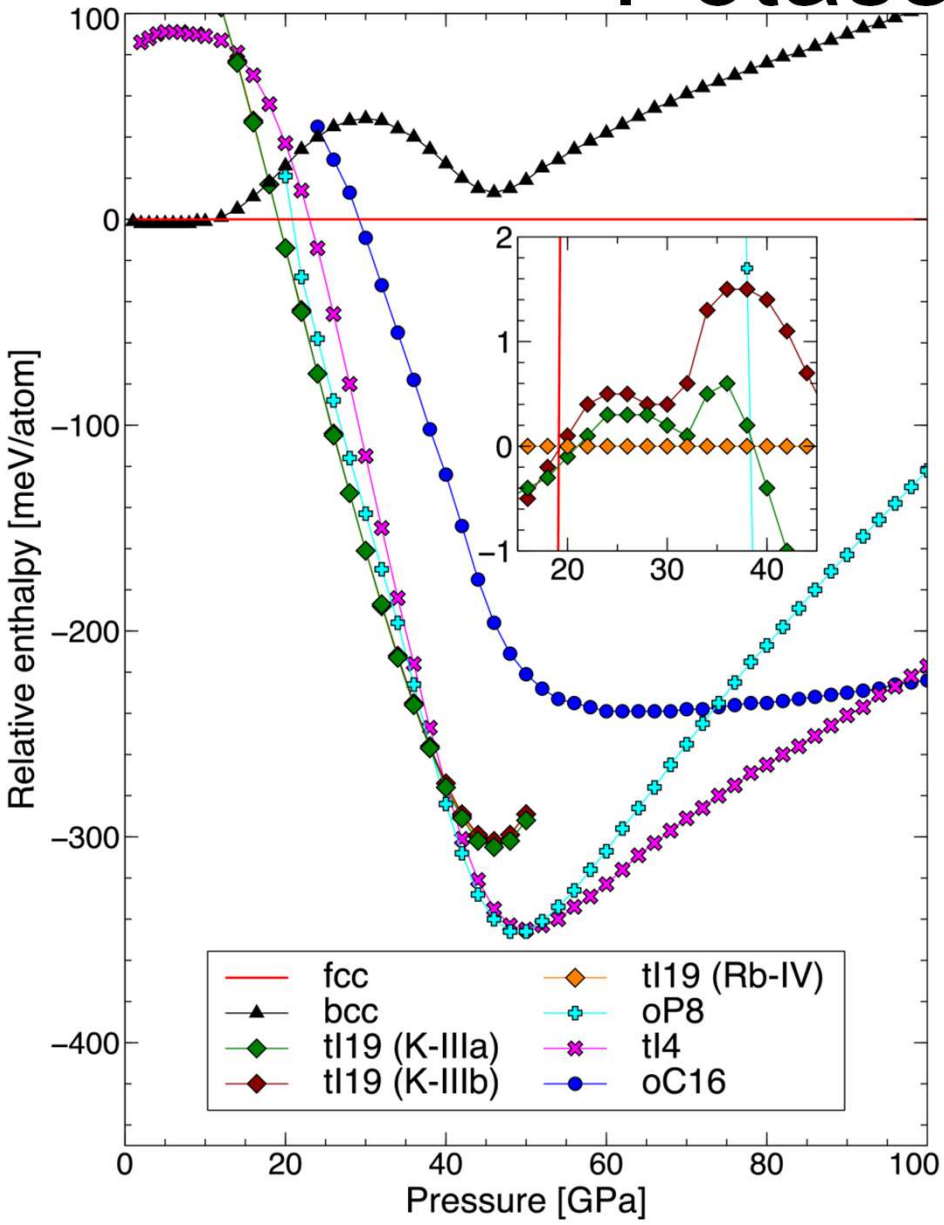

- bcc → fcc at 11 GPa
- 17.5 GPa < tI19 < 39 GPa
- oP8 → tI4 at 51 GPa
- tI4 → oC16 at 96 GPa

K-IIIa < 23 GPa
23 GPa < Rb-IV > 38 GPa
K-IIIa > 38 GPa

Potassium

Approximants with c_H/c_G from 1.5 (3g/2h structure) to 1.8 (9g/5h structure)

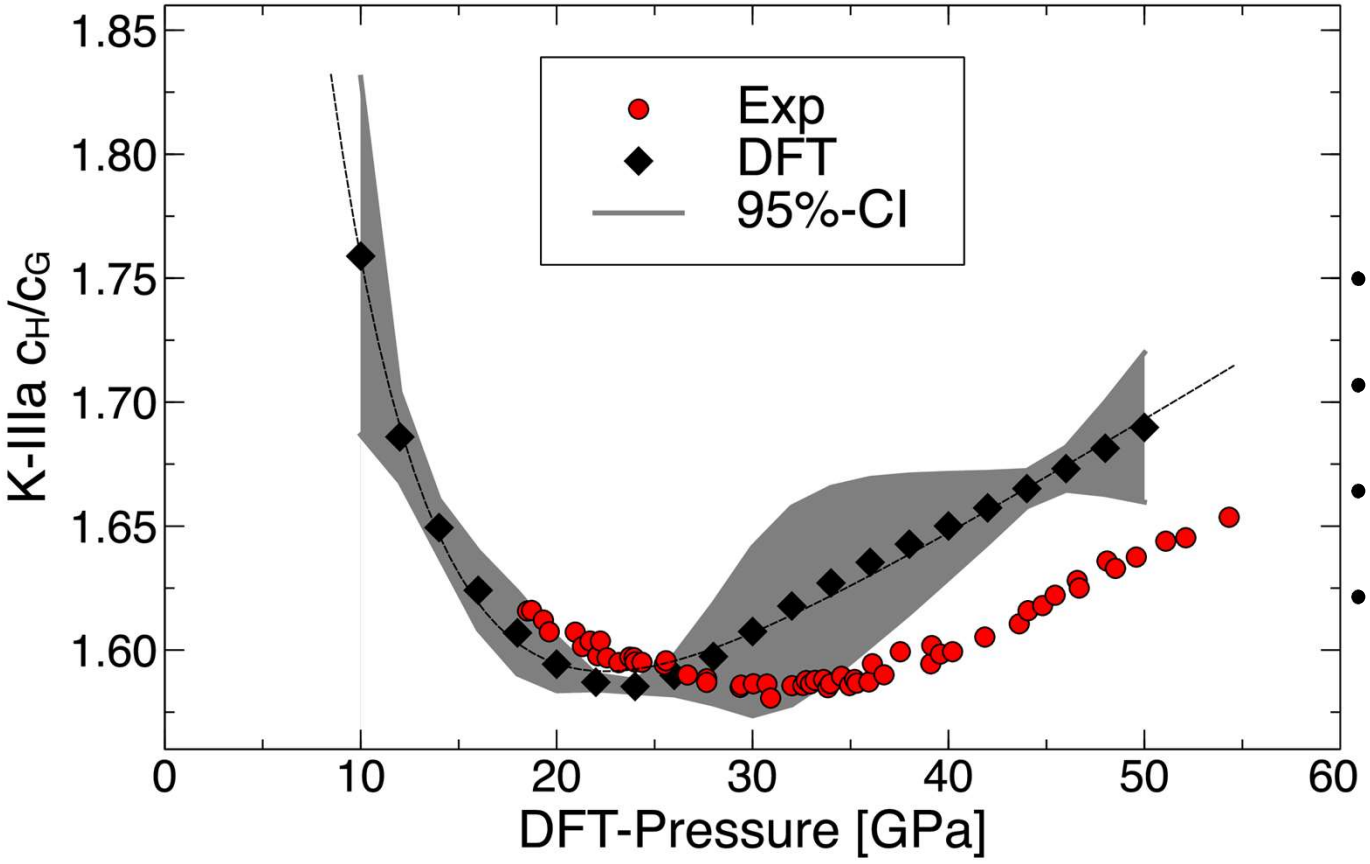

- Optimal c_H/c_G at each P
- Parabollic fits H--c_H/c_G
- Minimum c_H/c_G (24 GPa)
- c_H/c_G = 1.5---1.66

- 6-8 GPa offset calculated vs measured c_H/c_G curves

Na-V structure (ELF)

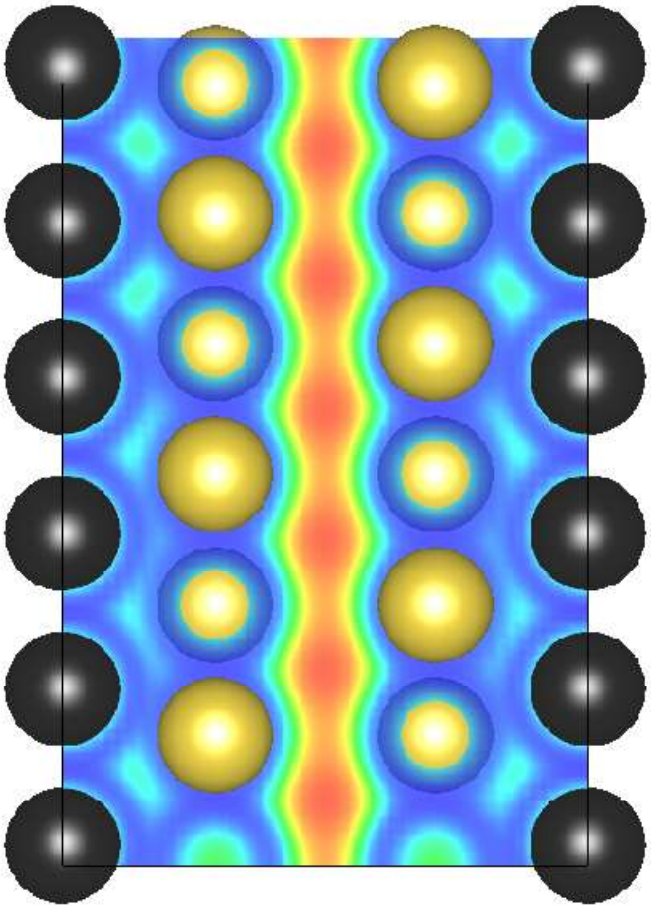

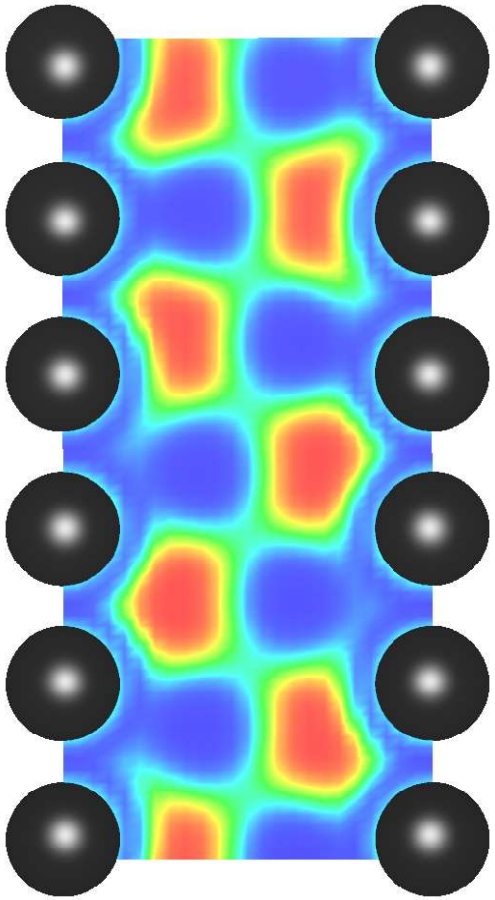

Guest ELF maxima
ELF(bip)=0.85
1.058 e^-/max
0.02961 e^-/bohr^3

Host ELF maxima
ELF(bip)=0.35
1.695 e^-/max
0.02994 e^-/bohr^3

Guest ELF maxima
ELF_{av}=0.94

Host ELF maxima
ELF_{av}=0.965

At 160 GPa

K-IIIa (ELF)

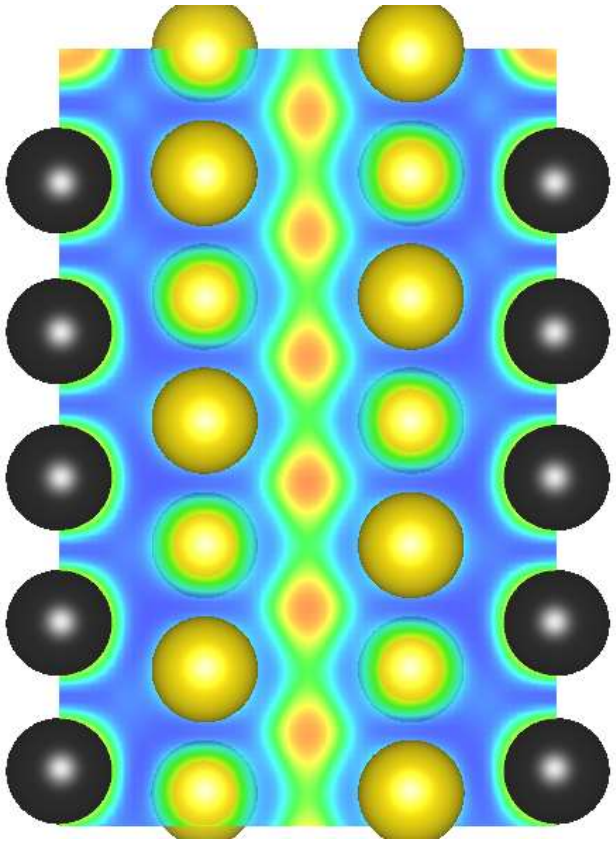

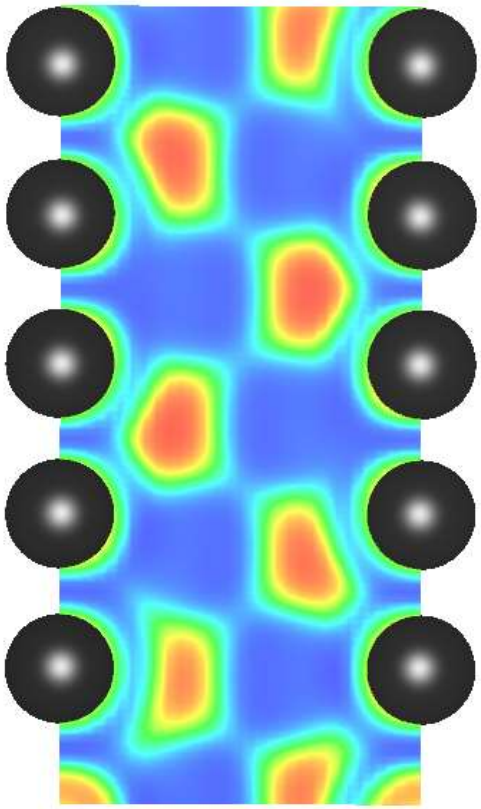

Guest ELF maxima
ELF(bip)=0.49
0.721 e^-/max
0.01826 e/bohr^3

Host ELF maxima
ELF(bip)=0.15
1.165 e^-/max
0.01680 e/bohr^3

Guest ELF maxima
ELF_{av}=0.89

Host ELF maxima
ELF_{av}=0.95

Silicon carbonate phase formed from carbon dioxide and silica under pressure

Mario Santoro[a,b,1], Federico Gorelli[a,b], Julien Haines[c], Olivier Cambon[c], Claire Levelut[d], and Gaston Garbarino[e]

[a]European Laboratory for Nonlinear Spectroscopy, Via Nello Carrara 1, 50019 Sesto Fiorentino, Italy; [b]Istituto per i Processi Chimico-Fisici–Consiglio Nazionale delle Ricerche, Unità Organizzativa di Supporto di Roma, Piazzale Aldo Moro 2,00185 Rome, Italy; [c]Institut Charles Gerhardt Montpellier, Equipe Chimie et Cristallochimie des Matériaux, Unité Mixte de Recherche 5253, Centre National de la Recherche Scientifique, Université Montpellier 2, Place Eugène Bataillon, cc1504, 34095 Montpellier Cedex 5, France; [d]Laboratoire Charles Coulomb, Unité Mixte de Recherche 5221, Centre National de la Recherche Scientifique, Université Montpellier 2, Place Eugène Bataillon, cc026, 34095 Montpellier Cedex 5, France; and [e]European Synchrotron Radiation Facility, 38343 Grenoble, France

Edited by Russell J. Hemley, Carnegie Institution of Washington, Washington, DC, and approved March 31, 2011 (received for review December 30, 2010)

The discovery of nonmolecular carbon dioxide under high-pressure conditions shows that there are remarkable analogies between this important substance and other group IV oxides. A natural and long-standing question is whether compounds between CO_2 and SiO_2 are possible. Under ambient conditions, CO_2 and SiO_2 are thermodynamically stable and do not react with each other. We show that reactions occur at high pressures indicating that silica can behave in a manner similar to ionic metal oxides that form carbonates at room pressure. A silicon carbonate phase was synthesized by reacting silicalite, a microporous SiO_2 zeolite, and molecular CO_2 that fills the pores, in diamond anvil cells at 18–26 GPa and 600–980 K; the compound was then temperature quenched. The material was characterized by Raman and IR spectroscopy, and synchrotron X-ray diffraction. The experiments reveal unique oxide chemistry at high pressures and the potential for synthesis of a class of previously uncharacterized materials. There are also potential implications for CO_2 segregation in planetary interiors and for CO_2 storage.

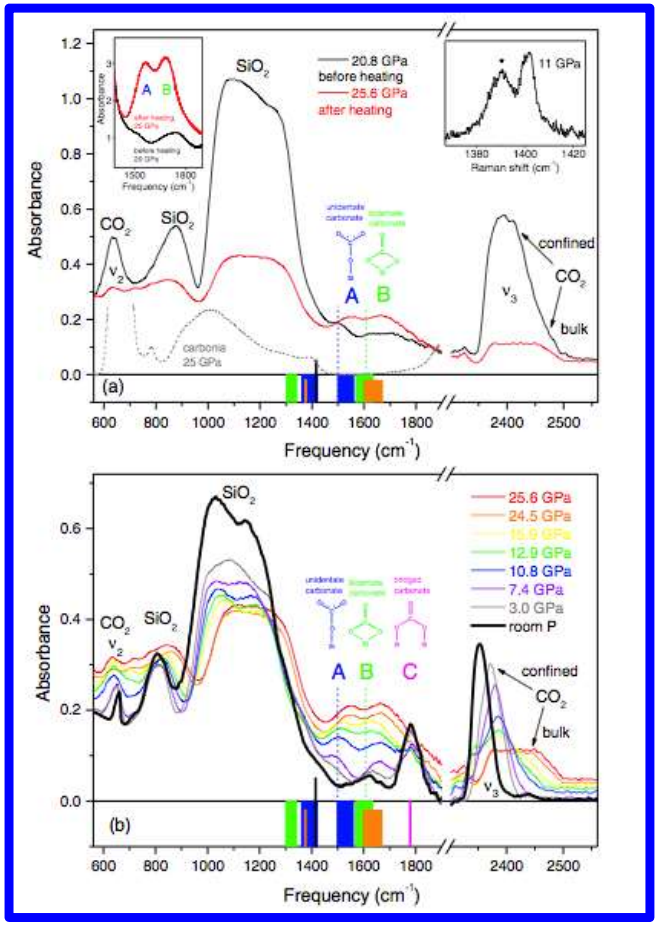

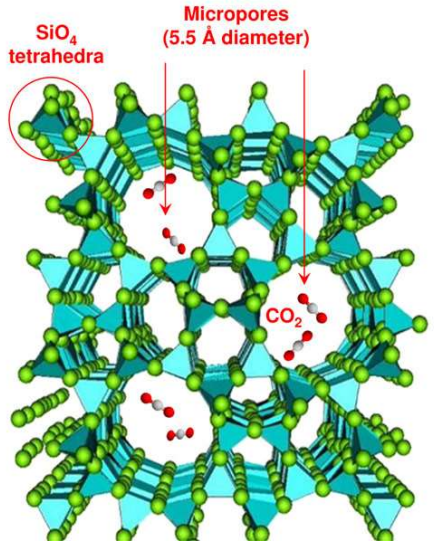

$xSiO_2 + yCO_2 \rightarrow Si_xC_yO_{2x+2y}$
18-26 GPa & 296-980 K

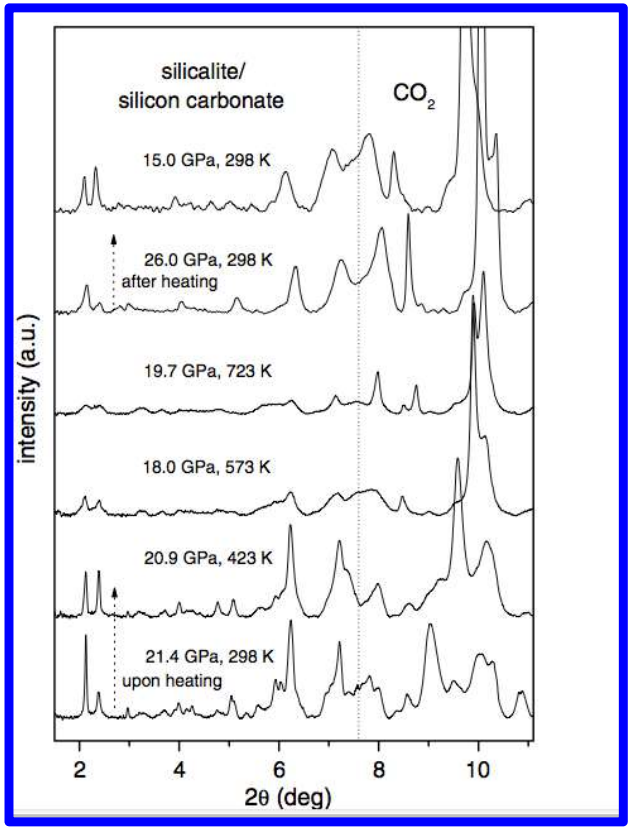

Is there any SiCO compound?

From database analysis

- Candidate structure UB_2O_6 & (*C2/c*, Z=4)
- Correct $Si_{1-x}C_xO_2$ stoichiometry & BO_3 units

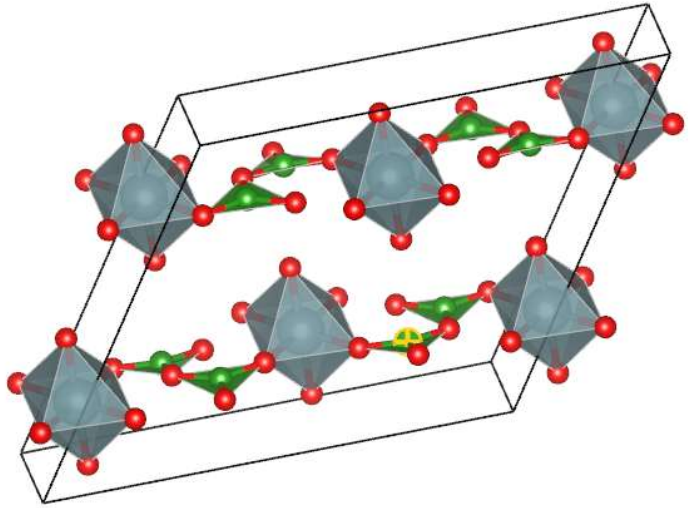

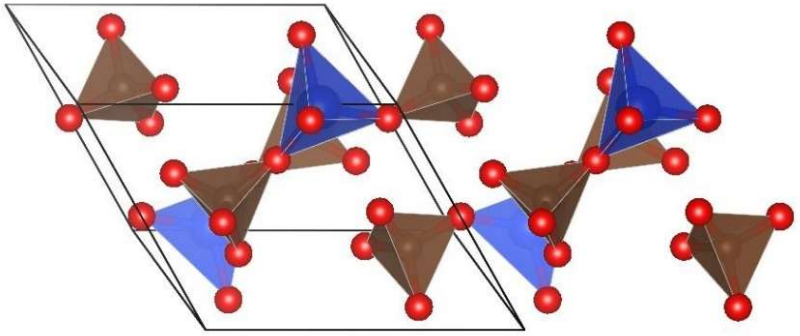

After optimization…

•Distorted CO_4 + SiO_6 units

•unstable vs decomposition into CO_2-III and SiO_2-stishovite

Global $Si_xC_yO_{2(x+y)}$ searches

Our calculations:

- Searches with the USPEX code + DFT calculation
- VASP code, PBE PP, cutoff energy: 600 eV...
- Stringent reoptimization of the lowest-enthalpy structures
- x,y =1-3; *Z* = 1-4. Selected pressures from 0 to 100 GPa
- Initial population:
  random + $C(Si)O_2$-derived + CO_4, SiO_4, CO_3, SiO_6 units
- Generations with 40Z structures (heredity & random)
- Convergence reached on 30-60 generations.

Global $Si_xC_yO_{2(x+y)}$ searches

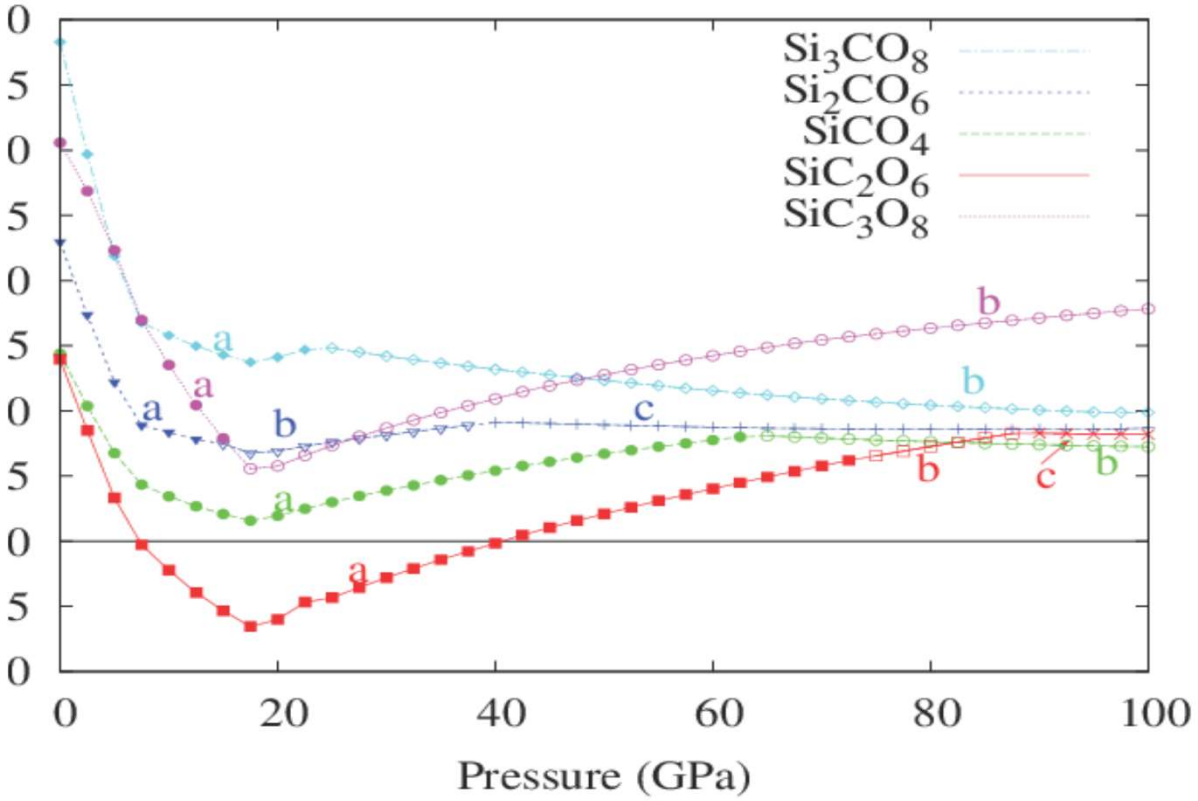

$\Delta H < 0$

↓

Stable $Si_xC_yO_{2(x+y)}$

$\Delta H = H(Si_xC_yO_{2(x+y)}) - xH(SiO_2) - yH(CO_2)$

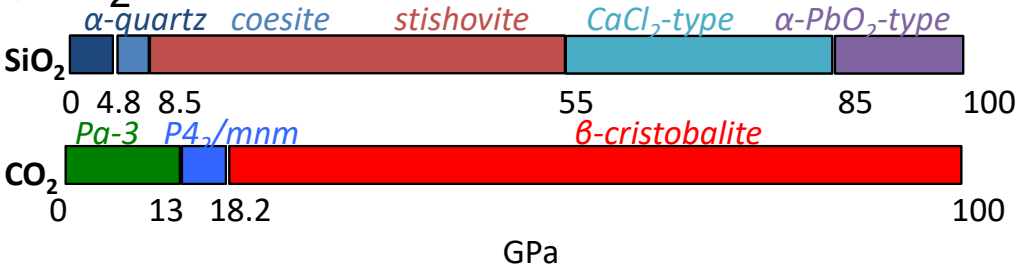

Global $Si_xC_yO_{2(x+y)}$ searches

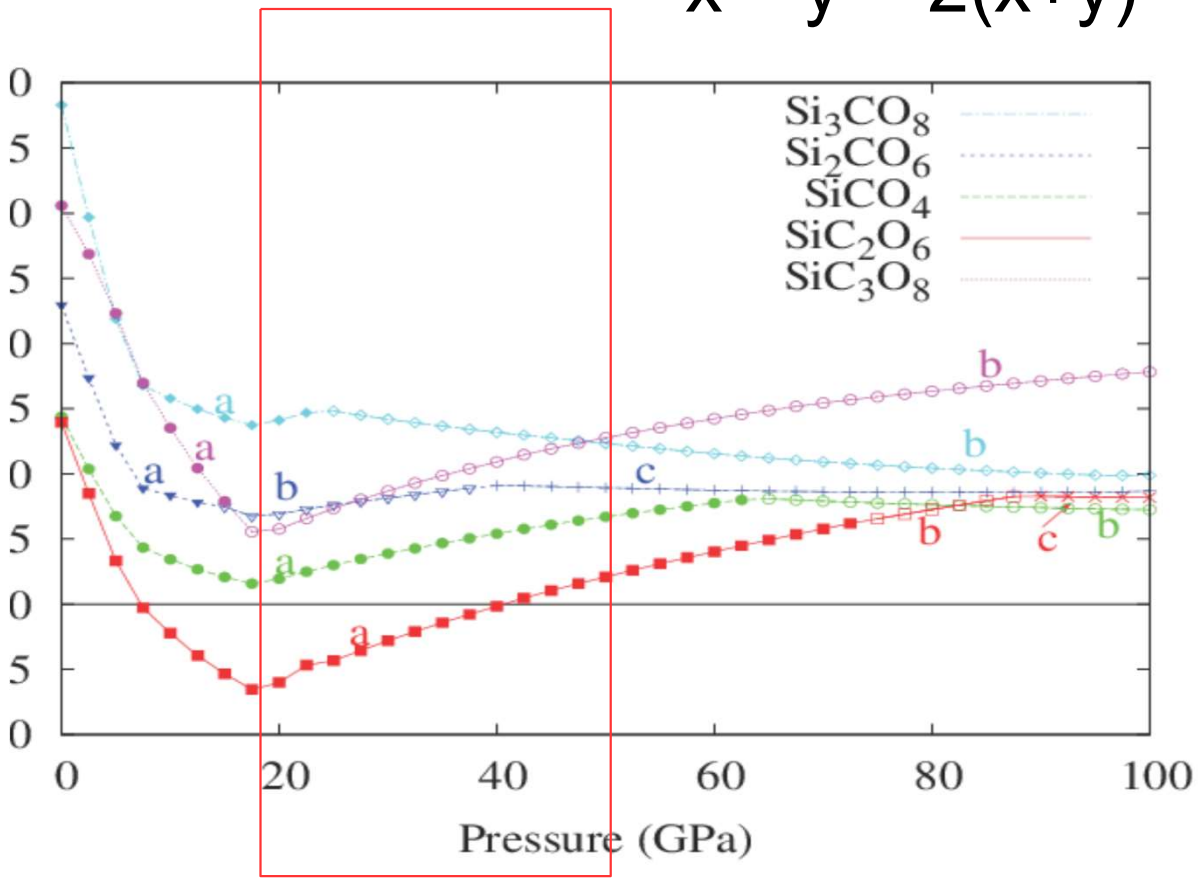

SiC_2O_6,

- Thermodynamically stable

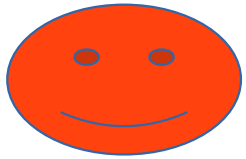

- *P2₁/c* structure, *Z*=2

On pressure increase,

- Minima ΔH region in the experimental range of stability.
- Lowest H structures consisting of SiO_6 and CO_3 units.

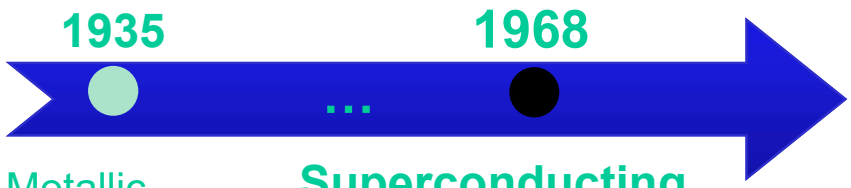

R. Howie et al. 2020

VOLUME 21, NUMBER 26 PHYSICAL REVIEW LETTERS 23 DECEMBER 1968

METALLIC HYDROGEN: A HIGH-TEMPERATURE SUPERCONDUCTOR?

N. W. Ashcroft
Laboratory of Atomic and Solid State Physics, Cornell University, Ithaca, New York 14850
(Received 3 May 1968)

Low pressure

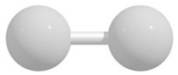

$rH-H(H_2) \approx 0.74$ Å

- Molecular Insulating

High pressure

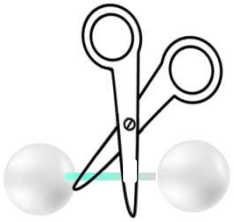

rH−H ≈0.9 -1-1.2 Å

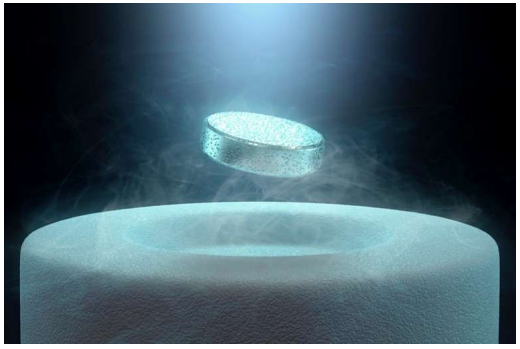

- Metallic
- High temperature superconductor

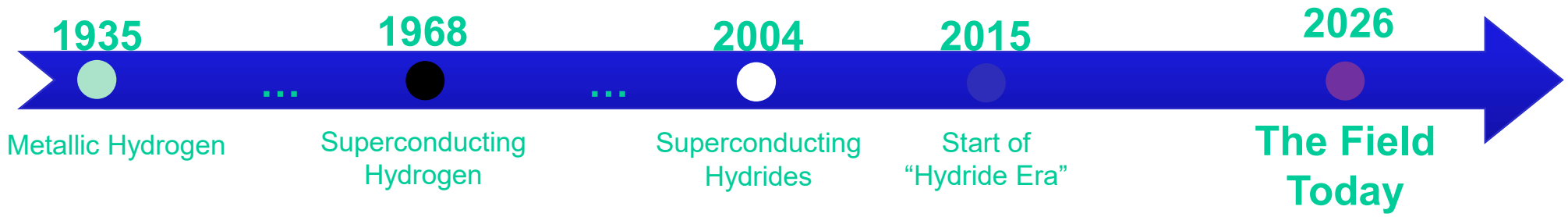

REVIEW

National Science Review
11: nwad270, 2024
https://doi.org/10.1093/nsr/nwad270
Advance access publication 31 October 2023

PHYSICS

Special Topic: Challenges to Achieving Room Temperature Superconductivity in Superhydrides under Pressure

Clathrate metal superhydrides under high-pressure conditions: enroute to room-temperature superconductivity

Ying Sun[1,2], Xin Zhong[1,2,*], Hanyu Liu[1,2,3,*] and Yanming Ma[1,2,3,*]

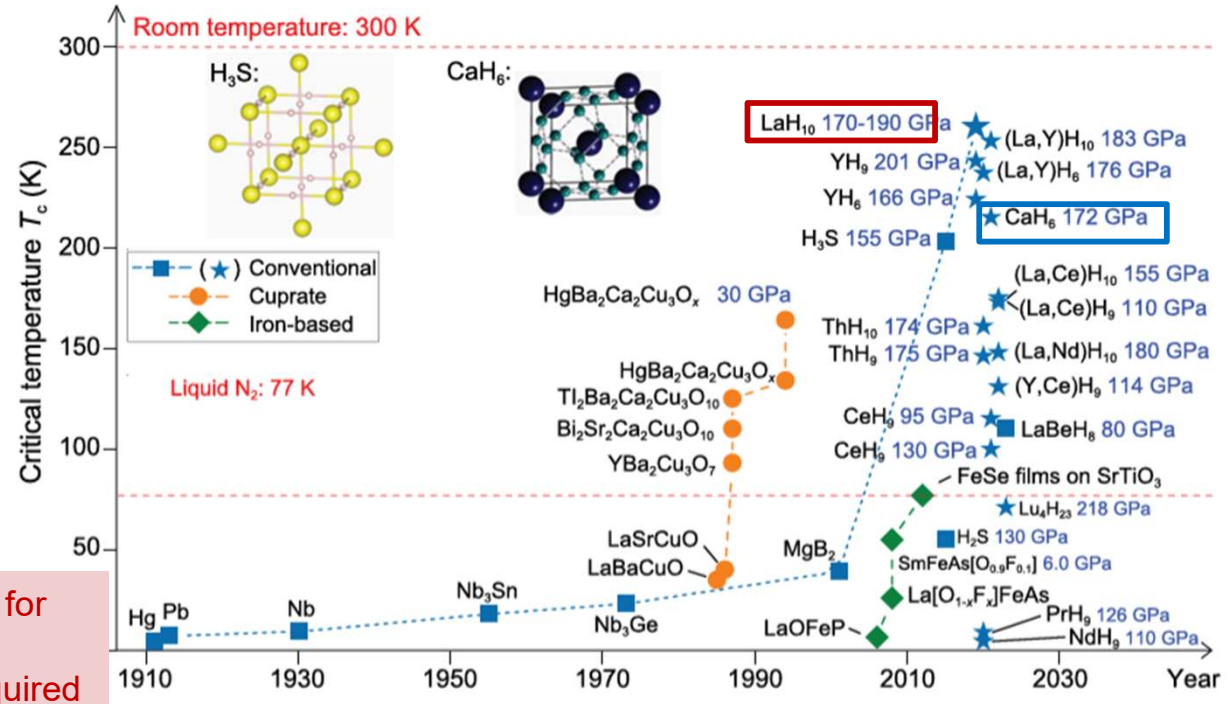

- All hydrides still require pressures 80-200 GPa for high Tc
- Understand how Tc can be promoted whilst required pressure is decreased

Chemical pre-compression: Group 2 tetrahydrides

DFT predicted structures

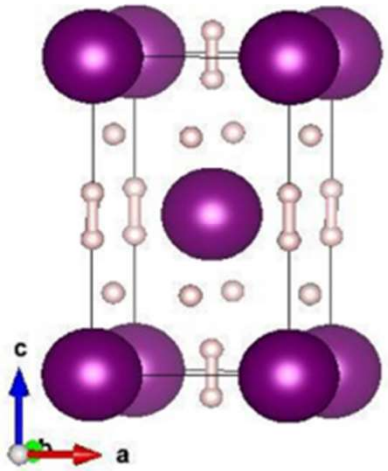

I4/mmm CaH_4

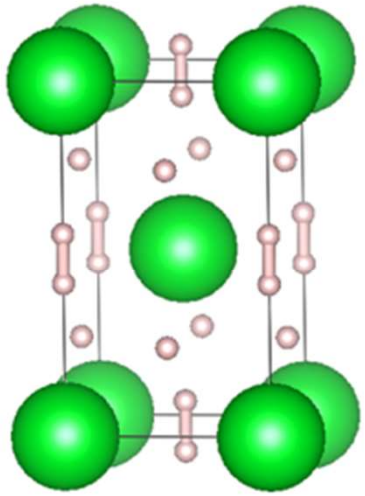

I4/mmm SrH_4

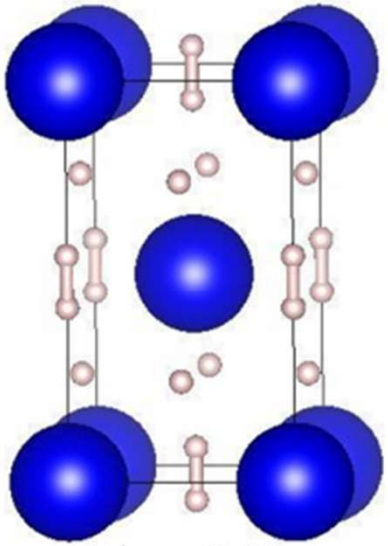

I4/mmm BaH_4

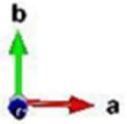

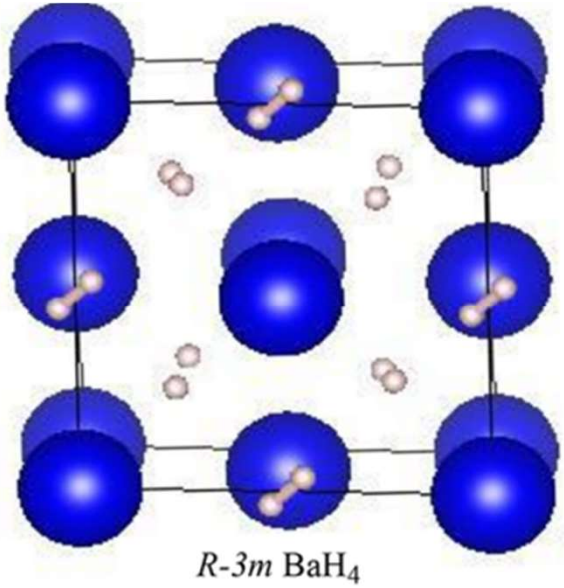

R-3m BaH_4

Fm-3m in theory symmetry breaks to R-3m

Quasi-molecular hydrogen units within octahedral interstices
H- in tetrahedra interstices

La IA revoluciona la búsqueda de estructuras cristalinas

Nature (2023) · Google DeepMind – GNoME

"Scaling deep learning for materials discovery"

2,2 millones de nuevos compuestos predichos; 380.000 estables (~10× lo conocido).

Nature (2025) · Microsoft Research – MatterGen

"A generative model for inorganic materials design"

IA generativa que diseña estructuras con propiedades a medida.

Nature (2023) · A-Lab, Berkeley – Síntesis autónoma

"An autonomous laboratory for the accelerated synthesis of novel materials"

- **41 de 58 compuestos** nuevos sintetizados en 17 días.
- Más de 700 materiales de GNoME ya validados experimentalmente.

Estructuras cristalinas descubiertas (acumulado)

Eje Y: nº de estructuras · Eje X: periodo (cifras aproximadas)

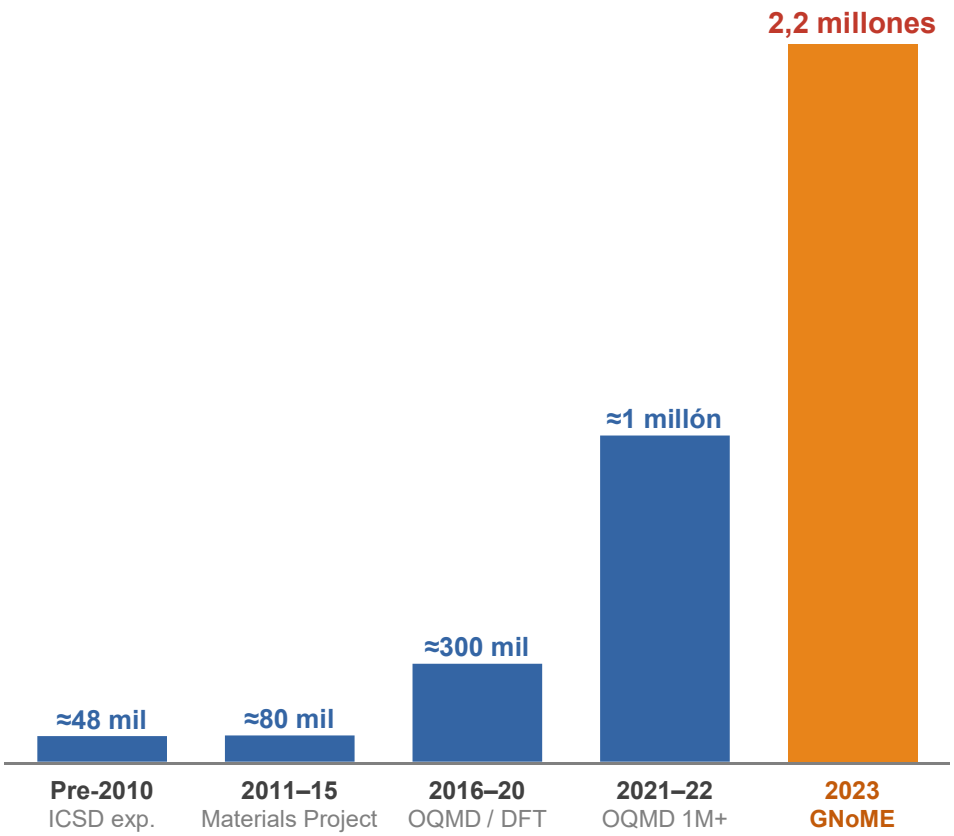

Fuentes: Merchant et al., Nature (2023) – GNoME; Szymanski et al., Nature (2023) – A-Lab; Zeni et al., Nature (2025) – MatterGen. Cifras del histograma aproximadas/acumuladas.

¿Cómo funciona GNoME?

1. Generar candidatos
Sustituir en estructuras conocidas + composiciones nuevas

→

2. Red neuronal de grafos
Predice energía y estabilidad de cada candidato

→

3. Filtrar por estabilidad
Se conservan los cercanos a la convex hull

→

4. Verificar con DFT
Cálculo cuántico confirma los más prometedores

→

5. Resultado
2,2 M predichas · 380 k estables

← **Aprendizaje activo:** los resultados de DFT reentrenan la red en cada ronda → eficiencia ~10×

¿Qué es una red neuronal de grafos (GNN)?

- Cada cristal se representa como un grafo: los átomos son nodos y los enlaces, aristas.
- Por "paso de mensajes" cada átomo aprende de su entorno y la red capta la geometría 3D.
- Así predice la energía de formación en milisegundos, sin resolver la mecánica cuántica (DFT) en cada caso.

Claves del método

- Solo los candidatos prometedores pasan a la costosa verificación con DFT.
- **Hallazgos:** ~528 posibles conductores de litio y ~52.000 materiales en capas.

NaCl: grafo real (coordinación 6)

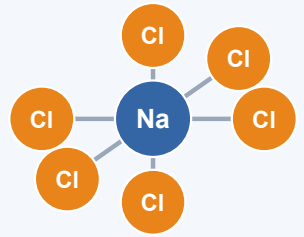

cada Na ↔ 6 Cl (octaédrica)

Red neuronal asociada

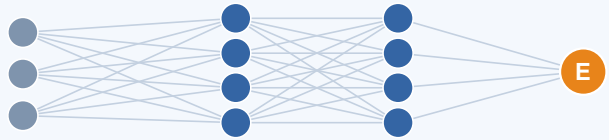

NaCl (tipo sal de roca): cada Na^+ se rodea de 6 Cl^-. La GNN procesa el grafo y predice la energía de formación.

Fuente: Merchant et al., "Scaling deep learning for materials discovery", Nature (2023). Esquema simplificado.

¿Cómo funciona MatterGen?

1. Ruido inicial
Átomos, posiciones y celda generados al azar

2. Difusión inversa
Una red elimina el ruido paso a paso (denoising)

3. Generar cristal
Aparece una estructura nueva y ordenada

4. Guiar por propiedades
Ajuste fino: banda, módulo, magnetismo

5. Resultado
Material nuevo, estable y sintetizable

Generación condicional: en vez de cribar millones de candidatos, MatterGen diseña directamente materiales con las propiedades deseadas.

¿Qué es un modelo de difusión?

- Parte de ruido aleatorio y aprende a revertirlo hasta formar un cristal coherente.
- Genera a la vez los tipos de átomo, sus posiciones y los parámetros de red.
- Con ajuste fino orienta la generación hacia una propiedad objetivo.

Claves del método

- Generativo, no solo de cribado: crea estructuras desde cero.
- **Hallazgos:** ~2× más probables de ser nuevas y estables y ~15× más cerca del mínimo de energía (DFT) que modelos previos.

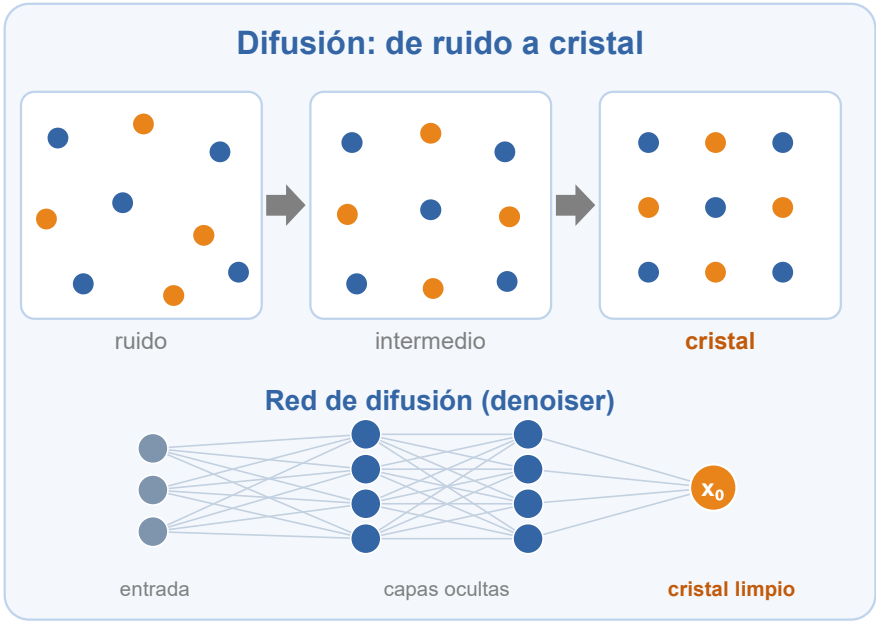

La red de difusión revierte el ruido paso a paso hasta obtener un cristal ordenado (esquema simplificado).

Fuente: Zeni et al., "A generative model for inorganic materials design", Nature (2025), Microsoft Research. Esquema simplificado.

¿Cómo funcionan los potenciales efímeros (EDDP)?

1. Estructuras al azar
Se generan al azar muchas estructuras: átomos, posiciones y celda

2. DFT en una muestra
Calculamos con DFT la energía de unas pocas de ellas

3. Potencial efímero
Con esos datos entrenamos un potencial rápido, a medida del sistema

4. Relajar
Ese potencial relaja y descarta miles de estructuras a bajo coste

5. Validar e iterar
Confirmamos las mejores con DFT y reentrenamos el potencial

La idea clave: el potencial se entrena para una búsqueda concreta y luego se descarta, así se acelera la búsqueda aleatoria sin perder la fiabilidad del DFT.

¿Qué es un potencial efímero?

- Es un potencial interatómico aprendido: estima la energía de una estructura mucho más rápido que el DFT.
- Se entrena a medida para el sistema que estudias; no sirve como modelo general.
- Como es tan barato de entrenar y usar, se crea para la búsqueda y luego se descarta (de ahí, "efímero").

Claves del método

- Combina dos ideas: la exploración al azar de AIRSS y la rapidez de un potencial aprendido, y así llega a sistemas más grandes.
- **Aprendizaje activo:** se van alternando DFT y potencial, que mejora en cada vuelta.

Ciclo de búsqueda acelerada

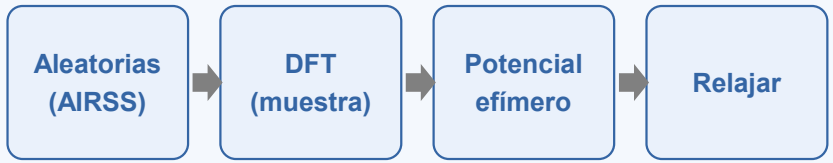

Aprendizaje activo: DFT ↔ potencial, se reentrena cada ciclo

Potencial efímero: ensemble de redes pequeñas

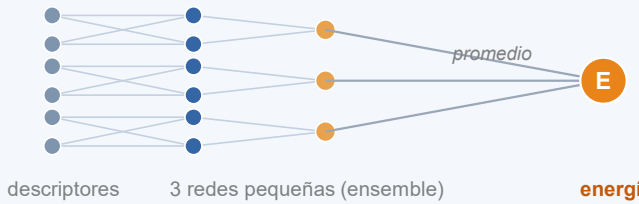

El potencial solo aprende energías; las fuerzas para relajar salen de derivarlo (esquema simplificado).

Fuente: C. J. Pickard, "Ephemeral data derived potentials for random structure search", Phys. Rev. B 106, 014102 (2022). Esquema simplificado.

Conclusiones

- DFT calculations provide an accurate description of the structural and energetic properties of materials, serving as a reliable framework for assessing the stability of the predicted crystal phases.
- Crystal structure prediction methods are effective tools for exploring the configurational space and identifying stable or metastable structures.
- The combination of global structure search algorithms with DFT calculations is a powerful approach for materials Discovery.
- Experimental-theoretical collaboration to interpret results, understand involved mechanism…..
- Artificial intelligence is revolutionizing crystal structure prediction by accelerating the exploration of the configurational space, reducing computational costs.